## NOTICE

The quality of this microform is heavily dependent upon the quality of the original thesis submitted for microfilming. Every effort has been made to ensure the highest quality of reproduction possible.

If pages are missing, contact the university which granted the degree.

Some pages may have indistinct print especially if the original pages were typed with a poor typewriter ribbon or if the university sent us an inferior photocopy.

Reproduction in full or in part of this microform is governed by the Canadian Copyright Act, R.S.C. 1970, c. C-30, and subsequent amendments.

## AVIS

La qualité de cette microforme dépend grandement de la qualité de la thèse soumise au microfilmage. Nous avons tout fait pour assurer une qualité supérieure de reproduction.

S'il manque des pages, veuillez communiquer avec l'université qui a conféré le grade.

La qualité d'impression de certaines pages peut laisser à désirer, surtout si les pages originales ont été dactylographiées à l'aide d'un ruban usé ou si l'université nous a fait parvenir une photocopie de qualité inférieure.

La reproduction, même partielle, de cette microforme est soumise à la Loi canadienne sur le droit d'auteur, SRC 1970, c. C-30, et ses amendements subséquents.

# STUDY ON REVERSE OSMOSIS MEMBRANE SEPARATION OF BINARY ORGANIC LIQUID MIXTURES

by

QING-HUA ZHOU

A Thesis
Presented to the University of Ottawa
in Fulfillment of the Thesis
Requirement for the Degree of
MASTER OF APPLIED SCIENCE
in
Chemical Engineering

ISBN 0-315-59992-8

UNIVERSITÉ D'OTTAWA
UNIVERSITY OF OTTAWA

# Abstract

There is an increasing interest for the separation of organic liquid mixtures with reverse osmosis primarily due to its great promise in industrial applications.

Based on Surface Force–Pore Flow model (SFPF) developed by Matsuura and Sourirajan, the study was conducted with the aid of a computer program, for the separation of organic liquid mixtures by reverse osmosis for the purpose of design and prediction of membrane performance. The results show that for a given separation system the pore size on the membrane surface and the interaction force between the membrane material and solute are two important factors which govern the effectiveness of the membrane separation of organic liquid mixtures.

# Acknowledgments

The author would like to express her sincere gratitude to Dr. Matsuura and Dr. Sourirajan for their advice, guidance and patience during this work. The author is grateful to ESSO Petroleum Canada for partial support for her work. The author also thanks all her colleagues for their assistance in this work. Finally, the author wishes to thank her parents for their encouragement during her studies.

# Nomenclature

| | |
|---|---|
| $A$ | Pure solvent permeability constant, $mol/m^2 \cdot s \cdot kPa$ |
| $A_P$ | Surface area of polymer powder in the chromatography column, $m^2$ |
| $a_A$, $a_B$, $a_w$ | Activity of the component A , that of the component B and that of water, respectively |
| $B$ | Constant characterizing the Van der Waals attraction force, $m^3$ |
| $b_A$ | Frictional function of the component A defined by Eq.(3.62) |
| $B_{AA}$, $B_{BB}$ | Second virial coefficient for component A and for component B, respectively |
| $B_{AB}$ | Second cross virial coefficient |
| $C$ | Molar concentration, $mol/m^3$ |
| $C_A$ | Molar concentration of the component A in the binary mixtures, $mol/m^3$ |
| $\bar{C}_A$ | Average value of $C_A$ in the pore, $mol/m^3$ |
| $C_B$ | Molar concentration of the component B in the binary mixtures, $mol/m^3$ |
| $\bar{C}_B$ | Average value of $C_B$ in the pore, $mol/m^3$ |
| $C_{A,b}$, $C_{B,b}$ | $C_A$ and $C_B$ in the bulk solution, respectively, $mol/m^3$ |

| | |
|---|---|
| $C_{A,i}$ | $C_A$ in the interfacial solution, $mol/m^3$ |
| $C_{A,pure}$, $C_{B,pure}$ | Molar concentration of the pure liquid of the component A and the component B, respectively, $mol/m^3$ |
| $C_{s,ln}$ | Log mean of the solute concentration on either side membrane, $mol/m^3$ |
| $C_s$ | Concentration of solute (salt) in the membrane |
| $C_w$ | Concentration of solvent (water) in the membrane |
| $D_A, D_B$ | Stoke's law radius of the molecule of the component A and that of the component B, respectively |
| $D_{AB}$ | Diffusivity of the component A in solvent B |
| $D$ | Constant characterizing the steric repulsion at the interface, $m$ |
| d | Distance between polymer material surface and the center of the solute molecule, $m$ |
| $D_s$ | Diffusion coefficient of the solute (salt) in the membrane |
| $D_w$ | Diffusion coefficient of the solvent (water) in the membrane |
| $D_{AM}/K\delta$ | Solute transport parameter |
| $F_A$(r,z), $F_B$(r,z) | Diffusion force working on the component A and the component B, respectively, $N/mol$ |
| $F_{AB}$(r,z) | Friction force between component A and component B, $N/mol$ |
| $F_{AM}$(r,z) | Friction force between component A and pore wall, $N/mol$ |
| $J_A$, $J_B$ | Molar flux of the component A and the component B, respectively, $mol/m^2 \cdot s$ |

| | |
|---|---|
| $J_s$ | Flux of the solute (salt) due to the gradient of chemical potential with respect to membrane |
| $J_w$ | Flux of the solvent (water) due to the gradient of chemical potential with respect to membrane |
| $J_v$ | Volume flux; the sum of the diffusive solute and solvent fluxes due to the gradient of chemical potential |
| $k$ | Mass transfer coefficient, $m/s$ |
| $k_s$ | Distribution coefficient |
| $k_w$ | Water permeability |
| $L_p$ | Filtration coefficient (Kedem-Katchalsky model) |
| $M_A$, $M_B$ | Molecular weight of the component A and the component B, respectively |
| $N_A, N_B$ | Solute and Solvent water flux through membrane, respectively, $mol/m^2 \cdot s$ |
| $p$ | Total vapor pressure of component A and component B |
| $p_A, p_B$ | Vapor pressure of component A and that of component B, respectively |
| $P$ | Operating pressure, $kPa$ |
| $P_2$, $P_3$ | Pressure at the pore inlet and at the pore outlet, respectively, $kPa$ |
| $(PR)$ | Membrane permeated product rate for given area of membrane surface, $kg/h$ |
| $(PWP)$ | Pure water permeation rate for given area of membrane surface, $kg/h$ |
| $[PSP]_B$ | Pure solvent (of the component B) permeation rate for given area of membrane surface, $kg/h$ |
| $R_a$ | $R_b - D_A$, $m$ |

| | |
|---|---|
| $R_b$ | Membrane pore radius, $m$ |
| $R$ | Universal gas constant |
| $r$ | Radial distance in the cylindrical coordinate, $m$ |
| $S$ | Effective membrane area, $m^2$ |
| $T$ | Absolute temperature, $K$ |
| $u$ | Velocity of solution in the pore, $m/s$ |
| $u_A$ | Velocity of the component A in the pore, $m/s$ |
| $u_B$ | Velocity of the component B in the pore, $m/s$ |
| $[V_R']$ | Chromatography retention volume, $m^3$ |
| $\bar{V}_A, \bar{V}_B$ | Average molar volume of the component A and the component B, respectively, $m^3/mol$ |
| $V_w$ | Partial molar volume of water |
| $v_s$ | Permeation velocity of the product solution, $m/s$ |
| $X_A$, $X_B$ | Mole fraction of the component A and the component B, respectively |
| $\bar{X}_A$, $\bar{X}_B$ | Average $X_A$ and $X_B$ values in the pore, respectively |
| $x_A, x_B$ | Mole fraction of component A and component B in the liquid phase, respectively |
| $X_{A,b}$, $X_{B,b}$ | $X_A$ and $X_B$ in the bulk solution, respectively |
| $X_{A1}$, $X_{A2}$, $X_{A3}$ | $X_A$ in the bulk feed solution, concentrated boundary solution and the membrane permeated product solution, respectively |
| $y_A, y_B$ | Mole fraction of component A and component B in the vapor phase, respectively |
| $\Delta x$ | Total membrane thickness |
| $z$ | Axial distance in the cylindrical coordinate, $m$ |

## Greek Letters

| | |
|---|---|
| $\gamma_A$ | Activity coefficient in liquid phase of component A |
| $\gamma_B$ | Activity coefficient in liquid phase of component B |
| $\Gamma$ | Surface excess, $mol/m^2$ |
| $\Gamma_A$, $\Gamma_B$ | $\Gamma$ for the component A and for the component B, respectively, $mol/m^2$ |
| $\delta$ | Length of the cylindrical pore, $m$ |
| $\delta_{AB}$ | Defined by $2B_{AB} - B_{AA} - B_{BB}$ |
| $\eta$ | Solution viscosity, $Pa{\cdot}s$ |
| $\lambda_f$ | Dimensionless quantity defined by $D_A/R_b$ |
| $\mu_A$, $\mu_B$ | Chemical potential of the component A and the component B, respectively, $J/mol$ |
| $\mu_A^0$, $\mu_B^0$ | $\mu_A$ and $\mu_B$ corresponding to $a_A = 1$ and $a_B = 1$, respectively, $J/mol$ |
| $\mu_w$ | Chemical potential of water |
| $\pi_A, \pi_B$ | Osmotic pressure of the component A and the component B (nonaqueous solution), respectively, $Pa$ |
| $\pi(X_A)$ | Osmotic pressure of the solution correspond to $X_A$ (aqueous solution) |
| $\rho$ | density, $kg/m^3$ |
| $\rho_2$, $\rho_3$ | Quantities defined by Eq.(3.24) and Eq.(3.25), respectively, $kPa$ |
| $\phi$ | Potential function of interaction force exerted on the solute from the pore wall, $J/mol$ |
| $\Phi$ | $\phi/RT$ |

| | |
|---|---|
| $\chi_{AB}$ | Proportionality constant defined by $RT/D_{AB}$ $J \cdot s/m^2 \cdot mol$ |
| $\chi_{AM}$ | Proportionality constant defined by Eq.(3.61) $J \cdot s/m^2 \cdot mol$ |
| $\sigma$ | Staverman reflection coefficient (coulpling coefficient) |
| $\Omega$ | Solute flux at zero volume flux |

## Subscripts

| | |
|---|---|
| $A$ | Solute or the component A in the binary mixture |
| $B$ | Solvent or the component B in the binary mixture |
| $b$ | Bulk solution |
| 1 | Bulk feed solution on the high pressure side of membrane |
| 2 | Concentrated boundary solution on the high side of membrane or pore inlet outside the pore |
| 3 | Membrane permeated product solution on the atmospheric side of the membrane or pore outlet outside the pore |

## Superscripts

| | |
|---|---|
| $A$ | The component A used as chromatographic solvent |
| $B$ | The component B used as chromatographic solvent |
| $L$ | Liquid phase |
| $mixt$ | The binary mixture of A and B used as chromatographic solvent |

# Contents

# List of Tables

# List of Figures

# Chapter 1

# Introduction

The reverse osmosis process is a general and widely applicable technique for the separation, concentration, or fractionation of inorganic or organic substances in aqueous or nonaqueous solutions in the liquid or the gaseous phase. Because of its low energy requirements [1] compared with conventional separation processes such as distillation, extraction and crystallization, the reverse osmosis process is spreading rapidly for the industrial application. In the future, the reverse osmosis process will be a new type of unit operation which may replace a major part of the conventional separation processes.

For describing the reverse osmosis process, several approaches have been proposed [2]. They are the solution-diffusion approach, the irreversible thermodynamics approach and the preferential sorption-capillary flow approach. According to the solution-diffusion approach developed by Lonsdale et al., each permeant passes through the membrane which is treated as a single solid phase by diffusion in response to its gradient in chemical potential [3]. In irreversible thermodynamics approach, less information is required to set up this approach. Nonequilibrium or

irreversible thermodynamics is the main principle to separation process. The membrane is treated as a " black box " barrier separating two phases which are far from equilibrium [4]. In this work, the preferential sorption- capillary flow approach is used for analysis of reverse osmosis performance. The approach is based on the Gibbs' preferential adsorption effect and the porous nature of the membrane. For this reason the preferential sorption-capillary flow approach is thought to represent the reverse osmosis process most adequately.

On the basis of the preferential sorption-capillary flow mechanism, the first membrane from cellulose acetate material for industrial water desalination application was developed by Loeb and Sourirajan in 1960 [5]. This is the first breakthrough in the development of the science and technology of RO membranes. According to the preferential sorption-capillary flow mechanism (as Figure 1) [6], reverse osmosis is partly governed by a surface phenomenon and partly by the fluid transport under pressure through capillary pores. One of the components in the solution is preferentially absorbed at the membrane-solution interface and the fluid mixture at the membrane- solution interface is continually removed through membrane capillaries under pressure. It results in a product solution whose composition is different from that of the bulk feed solution. An appropriate chemical nature of the membrane surface in contact with the solution as well as the existence of pores of appropriate size and number on the area of the membrane at the interface together constitute the indispensable twin-requirement for the practical success of this separation process [7]. That is, RO membrane separation is governed by an equilibrium effect and a kinetic effect according to the PSCF mechanism. The equilibrium effect which is concerned with the details of preferential sorption in the vicinity of the membrane surface is governed by repulsive and attractive potential gradients in the vicinity of the membrane surface. The kinetic effect is concerned

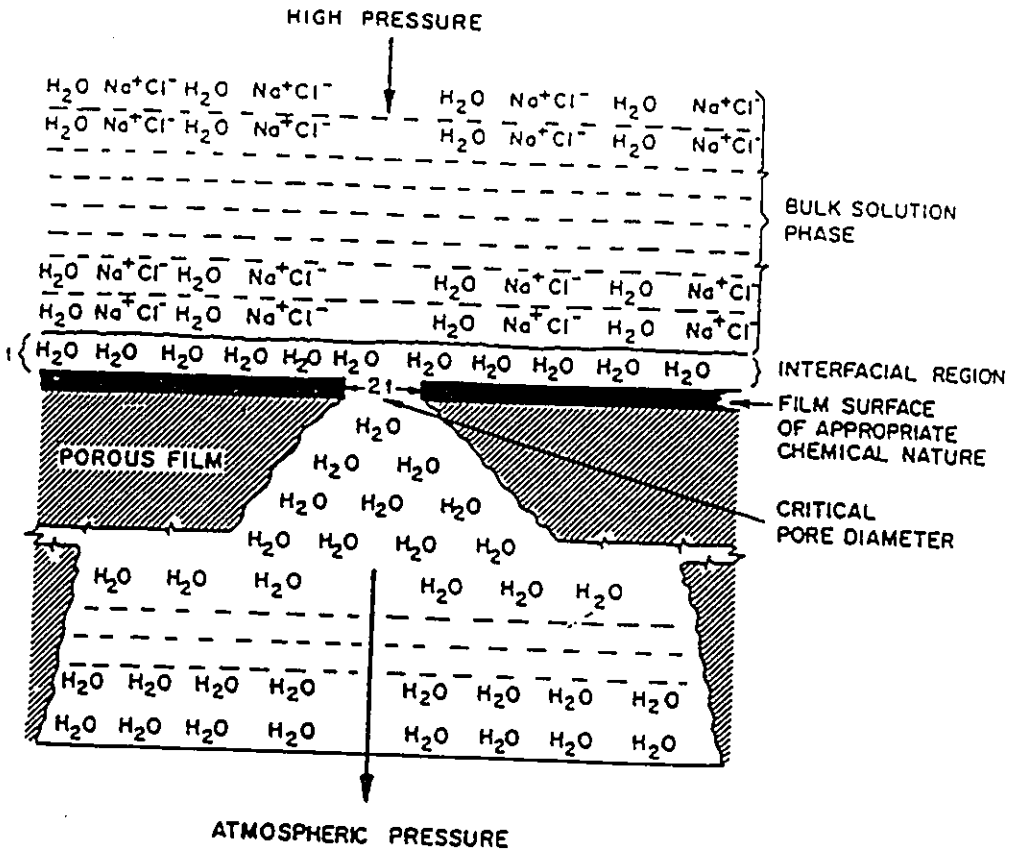


Figure 1: Schematic of Preferential Sorption –Capillary Flow Mechanism for Reverse Osmosis Separation of Sodium Chloride from Aqueous Solutions

with the mobilities of solute and solvent through membrane pore. The mobilitiy effect is governed both by the equilibrium and the steric effects associated with the structure and the size of molecules relative to that of the pores on the membrane surface.

In order to express quantitatively the preferential sorption- capillary flow mechanism, Matsuura and Sourirajan developed the surface force-pore flow model (SFPF) [8]. In this model, the concentration gradient of the solute at the solution-membrane material interface caused by the interaction force working between the solution components and the membrane surface and the flow of the an interfacial fluid through porous membranes can be expressed quantitatively.

The surface force-pore flow model states that the solute-solvent transport through the membrane pores is governed by interfacial surface forces. Consequently, the RO membrane separation process is controlled by kinetic, physical and thermodynamic effects. The transport equations based on the surface force-pore flow model are very useful for describing and predicting the behavior of membrane separation systems. Such description and prediction can help us to design the RO membrane and the membrane separation process.

In spite of the importance of the SFPF model, the development of transport equations for describing the SFPF model is still in its early stages of development and application. Though transport equations for treating aqueous solutions have been widely applied, the transport equations for describing the separation of organic liquid mixtures have not been developed. There is only one literature reference on the subject published by Matsuura et al. [9]. This is because organic liquid mixtures show more complicated physical nature than aqueous solutions in the RO membrane separation process. The most widely used method for the separation of organic

liquids is distillation, but problems arise when azeotropes are formed. It is required to develop alternative methods which demand less energy than the phase change methods such as distillation. The RO membrane separation has obvious advantages in the separation of organic liquid mixtures because of its low energy requirements. It is expected that the separation of organic liquid mixtures by reverse osmosis will grow industrially in the future. Then, an appropriate transport model will be required for the design of membrane and the membrane separation process. The objective of this work is to extend the SFPF model to separation of binary organic liquid mixtures. On the basis of the SFPF model, a set of transport equations is derived for the RO membrane separation of binary organic liquid mixtures, and their applications are illustrated through parametric and analytical studies.

# Chapter 2

# Literature Survey

## 2.1 Introduction

Two main methods exist for separating mixtures of organic liquids by using membranes. They are pervaporation in which the product phase is vapor, and reverse osmosis in which feed and product phases are both liquid. The published literature for the membrane separation of organic liquid mixtures by pervaporation is extensive. However, the literature shows that the membrane separation of organic liquid mixtures by reverse osmosis remains largely unexplored at the present time. This work is mainly concerned with the membrane separation of organic liquids by reverse osmosis.

Reverse osmosis process has changed from a simple laboratory technique into important industrial unit operations. To date however, membrane separation processes are restricted mainly to aqueous solutions. The applicability for the separation of organic liquid mixtures by reverse osmosis has not been known very well, though the great possibility of such an application was demonstrated experimen-

tally a long time ago [10,11]. Only a few published papers on the experiments of reverse osmosis separation of organic liquids are available in the literature. Particularly, there appears to be no published literature in the field of the analysis of the data on the separation of organic liquid mixtures by reverse osmosis . Therefore, it should be of great value to study this subject, because the analysis of the data on the separation of organic liquid mixtures by reverse osmosis is very useful to design membrane separation process and to extend the experimental technology to its fullest industrial applications. For this reason, the analysis of the data on the reverse osmosis separation of organic liquid mixtures is carried out by using computer model based on SFPF model.

### 2.1.1 Survey of RO Experiments of Organic Liquids

Hagerbaumer and Kammermeyer (1955) [10] investigated liquid phase separation of several hydrocarbon mixtures by pressure permeation through microporous glass having an average pore diameter of about 40 $\AA$. Only one type of membrane was investigated. Their study was concerned mainly with the question of whether liquid mixtures could be separated by permeation through a microporous membrane. Therefore, the experimental apparatus and the procedure were very simple. The reported results indicated the possibility of separation of organic liquids by reverse osmosis.

Sourirajan (1964) [11] studied reverse osmosis separation of hydrocarbon liquids by flow under pressure through porous membranes. He suggested that an appropriate chemical nature of the film surface in contact with the solution, together with the existence of pores of appropriate size on the area of the porous film at the interface, was an indispensable twin requirement for the success of this separa-

tion technique. Three different types of porous films, designated as S and S, CA and PE films, were used in the experiments. Experimental results illustrated the fact that the separation of hydrocarbon liquids by reverse osmosis was successful and demonstrated that porous cellulose acetate membranes developed in connection with saline water conversion could also be profitably used in separation of the mixtures of hydrocarbon liquids by reverse osmosis.

Kopecek and Sourirajan (1970) [12] extended the work of Sourirajan [11] to the reverse osmosis separation of binary mixtures of some organic liquids using the Loeb-Sourirajan type porous cellulose acetate membranes. Experimental results demonstrated that for the separation of some organic feed solutions, such as alcohol-hydrocarbon mixtures containing more than about 25 mole per cent alcohol, porous cellulose acetate membranes of the type used in the work were sufficiently good for consideration for industrial application. Hydrocarbons tend to collapse the porous structure of the cellulose acetate membranes used; hence, for feed mixtures containing hydrocarbons, some other type of membranes would have to be developed for reverse osmosis application. The experimental data also indicated that hydrogen bonding and solubility parameter might offer valid criteria of preferential sorption for nonelectolyte binary feed mixtures containing components whose solubilities are governed primarily by either polar or dispersion forces.

Strathmann (1977) [13] used asymmetric polyimide membranes for reverse osmosis separation of nonaqueous solutions. In his work, a range of asymmetric skin type ultrafiltration and reverse osmosis membranes was prepared from various monomers and by different preparation procedures. These membranes were used for filtration tests and chemical stability tests. The test results showed that these membranes had good filtration properties and excellent mechanical and thermal stability. However, in aqueous solutions, their stability was rather poor.

Nomura et al.(1978) [14] investigated the permselectivities of some aromatic compounds in organic medium through cellulose acetate membranes by reverse osmosis. Two kinds of experiments were carried out to examine the factors governing permeabilities of organic solutes through cellulose acetate membranes in reverse osmosis; one was the measurement of the diffusion coefficient in dialysis, and the other was the measurement of the partition coefficient between the membrane and the solution phases. The experimental data for a number of benzene derivatives showed that only phenol was rejected and the others were enriched. For the compounds with various substituent groups, the solute permeabilities had the following order; $OH < CH_3 < H < Cl < NH_2 < NO_2$. In the series of benzene, naphthalene, and anthracene, the permeability is related to the molar volume of solutes and varies as follows: benzene > naphthalene > anthracene.

Iwama and Kazuse (1982) [15] used the new polyimide membranes that could be made from 1,2,3,4–butane tetracarboxylic acid and an aromatic diamine to separate organic liquid mixtures by reverse osmosis. They found the membranes had excellent stability and high fluxes with most common organic solvents, even at elevated temperatures.

Aadm, Luke and Meares (1983) [16] studied the separation of mixture of organic liquids by reverse osmosis. They used toluene + n-heptane with an asymmetric polyacrylonitrile membrane and methanol + isobutanol with a uniform cellulose membrane to carry out experiments. The experimental results showed that the separation of organic liquid mixtures by reverse osmosis with dense polymer membranes appeared to be well described by a simple treatment of the solution-diffusion mechanism.

Farnand (1983) [17] investigated the separation of organic liquid mixtures by

reverse osmosis. He used ethanol-heptane binary organic liquid mixtures to perform a large number of experiments of reverse osmosis separation. Three membrane types were used in his work (PPPH 8273, cellulose acetate , and cellulose). The experimental results demonstrated that each membrane type showed different permeation rates and separation characteristics as well as properties attributable to the variation of porosity. The results showed that the preferential sorption-capillary flow mechanism could describe very well the RO separation process of organic liquid mixtures.

Farnand and Sawatzky (1986) [18] reported a study of reverse osmosis under static conditions to remove methanol from the etherification products. This involved both the selective rejection of methanol from the permeate by non-polar membranes and the selective passage of methanol by polar membranes. Both types of membranes gave significant separation factors for methanol.

Hazlett et al. (1986) [19] investigated the effects of normal alcohols and paraffins on polysulfone membrane at three operating temperatures. Surprisingly, alcohols were found to alter the membranes, enlarging the pore structure and shifting the characteristic per cent separation - molecular weight curve to higher molecular weight values. Paraffinic hydrocarbons contracted the pore structure and shifted the per cent separation curve towards lower molecular weights. The experimental results showed that the use of polysulfone ultrafiltration membranes for nonaqueous separations was a promising area for new developments in membrane technology.

Matsuura, Sourirajan, Farnand and Talbot (1987) [9] extended the surface force-pore flow model to separation of binary mixtures of organic liquids by reverse osmosis where the solution composition covered the mole fraction of one component of the mixture from zero to unity. The transport equations for the separation of

the binary mixture of organic liquids were used to calculate membrane performance data. The agreement between the calculated and experimental values was tested by reverse osmosis separation of the binary mixtures of ethyl alcohol-heptane. The results showed that the surface force-pore flow model could describe well experimental data. A computer simulation could demonstrate the effects of the interaction force, the size of component molecule and the operating pressure on the membrane performance.

Matsuura and Sourirajan (1989) [20] applied surface force-pore flow model to separation of binary mixtures of organic liquids in the entire mole fraction range of one of the component liquids. In their paper, they have treated the reverse osmosis separation processes which include the separation of solute and solvent and the separation of liquid mixtures, membrane gas separation and pervaporation as a uniform view of the preferential sorption-capillary flow mechanism. They indicated that the presence of an interfacial layer, the property of which is different from that of the bulk fluid, and the collection of such an interfacial layer through pores of molecular dimensions are the central theme of the preferential sorption - capillary flow mechanism.

Farnand (1989) [21] studied reverse osmosis fractionation of organic solutes in nonaqueous solutions. His work was concerned with the performance of reverse osmosis in nonaqueous solutions and demonstrated that the mechanism was independent of the solvent in the solution. The description of reverse osmosis performance in nonaqueous solutions could be described by the same physicochemical principles as in aqueous reverse osmosis, and this formed the basis for demonstrating that nonaqueous and aqueous reverse osmosis processes were controlled by the same mechanism.

### 2.1.2 Conclusions

The experiments of the above researchers illustrate the general applicability of the reverse osmosis process for the separation of organic liquid mixtures. However, the literature does not reveal evidence of anyone's having carried out the analysis of experimental data of separation of organic liquid mixtures by reverse osmosis. There is a great need for a valid analysis of experimental data, because it is very useful to understand well reverse osmosis separation process of organic liquids and design new membrane separation processes of organic liquid mixtures.

## 2.2 Survey of Membrane Separation Approaches

There are several approaches available in the literature to describe transport phenomena in the reverse osmosis separation. They are irreversible thermodynamics approach, solution- diffusion approach and preferential sorption-capillary flow approach. Based on the above approaches, it is possible to understand the mechanism of membrane separation processes and to predict membrane separation performance. A brief summary for these approaches is given in the following sections.

### 2.2.1 Irreversible Thermodynamics Approach

Kedem and Katchalsky (1958) [22] developed the first practical irreversible thermodynamics approach. According to this approach, a system can be divided into small subsystems in which " local equilibrium " exists, therefore they could be described by thermodynamic parameters. Membrane is treated as a black box in which relatively slow processes are taking place near equilibrium. No information

is needed on the mechanism of transport. For isothermal non-electrolyte systems, the Kedem-Katchalsky Model could be described by following equations:

$$J_v = L_p(dp - \sigma d\pi) \tag{2.1}$$

$$J_s = (1 - \sigma)C_{s,ln}J_v + \Omega d\pi \tag{2.2}$$

In which $J_v$ is the total volume flux, $J_s$ is the molar solute flux, $L_p$ is filtration coefficient, $\sigma$ is Staverman reflection coefficient, $dp$ is permeation pressure, $d\pi$ is osmotic pressure difference, $\Omega$ is solute permeability at zero volume flux, $C_{s,ln}$ is log. mean of solute concentration on either side of the membrane.

### 2.2.2 Solution-Diffusion Approach

Lonsdale et al. (1965) [23] presented solution-diffusion approach. According to the approach, the reverse osmosis separation is governed by a solution-diffusion mechanism. Both solvent and solute dissolve in the homogenous nonporous surface layer of the membrane and permeate through the membrane by diffusion. Membrane with a completely nonporous surface layer ( perfect membrane ) can be described by this approach. A perfect membrane has high solubility and diffusivity for the solvent as compared with those of the solute.

Flux equations can be written as follows :

$$J_w = -D_w \frac{dC_w}{dx} \tag{2.3}$$

where $D_w$ is the diffusivity of water and $C_w$ is the concentration of water in the membrane. If the water-membrane solution obeys Henry's law, $d\mu_w = -RTdlnC_w = -RTdC_w/C_w$

Equation (2.3) becomes :

$$J_w = \frac{D_w C_w}{RT}\frac{d\mu_w}{dx} \approx \frac{D_w C_w}{RT}\frac{\Delta\mu_w}{\Delta x} \tag{2.4}$$

where $d\mu_w$ is gradient of chemical potential of water, $R$ is gas constant, $T$ is temperature and $\Delta x$ is membrane thickness. For isothermal systems, $d\mu_w$ can be expressed by

$$d\mu_w = RTdlna_w + V_w dP \tag{2.5}$$

where $a_w$, $P$ and $V_w$ are activity, pressure and partial molar volume of water, respectively.

Using Lewis'equation, the osmotic pressure could be expressed by

$$V_w d\pi = -RTdlna_w \tag{2.6}$$

Substituting Eqns. (2.5) and (2.6) into Eq(2.4), yields the solvent permeation equation of Lonsdale:

$$J_w = \frac{D_w C_w V_w}{RT}\frac{(dp - d\pi)}{dx} = k_w(dp - d\pi)/dx \tag{2.7}$$

where $k_w$ is solvent permeability, for the solute

$$J_s = -D_s k_s \frac{\Delta C_s}{\Delta x} \tag{2.8}$$

In which $D_s$ is the solute diffusivity, $k_s$ is the distribution coefficient.

In order to modify the solution-diffusion model, Sherwood, et al., (1967) proposed the " solution-diffusion-imperfection " model [24]. In the model, some imperfections on the membrane surface were suggested and the pore flow of solute and solvent in an undiluted form was allowed.

### 2.2.3 Preferential Sorption-Capillary Flow Approach

Loeb and Sourirajan (1960) [5] developed the preferential sorption-capillary flow approach. Dickson, et al., (1975, 1976) [25,26] described in detail this approach.

According to this approach, reverse osmosis separation is partly governed by surface phenomena and partly by fluid transport under pressure through capillary pores. The surface layer of a successful reverse osmosis membrane is considered microporous and heterogeneous at all levels of solute separation. The chemical nature of the membrane surface and the size and number of pores on the area of the membrane at the interface constitute the indispensable twin-requirement for the practical success of the separation process. If the surface of a porous membrane in contact with the solution is of such chemical nature that it has preferential sorption for solvent or preferential repulsion for the solute, then a multimolecular layer of preferentially sorbed fluid layer could exist at the membrane-solution interface. Consequently, the interfacial fluid layer is enriched in one of the constituents of the bulk solution. A continuous removal of this interfacial layer by flow under pressure through the membrane capillaries results in a product solution whose composition is different from that of the bulk feed solution.

A critical pore diameter for maximum separation and permeability is twice the thickness of the interfacial pure water layer, and it could be several times larger

than salt or water molecular diameters and still achieve reasonable separation.

The basic transport equations for the preferential sorption- capillary flow mechanism are given as follows [27] :

$$A = (PWP)/M_B \times S \times 3600 \times P \tag{2.9}$$

$$N_B = A[P - \pi(X_{A2}) + \pi(X_{A1})] \tag{2.10}$$

$$N_B = (D_{AM}/K\delta)((1 - X_{A3})/X_{A3})(C_2X_{A2} - C_3X_{A3}) \tag{2.11}$$

$$N_B = C_1k(1 - X_{A3})ln(X_{A2} - X_{A3})/(X_{A1} - X_{A3}) \tag{2.12}$$

where $A$ is pure water permeability constant, $P$ is operating pressure, $k$ is the mass transfer coefficient, $C_1$, $C_2$ and $C_3$ are molar density of the feed solution, the concentrated boundary solution, and the product solution, respectively, $(PWP)$ is pure water permeability through effective area of the membrane surface, $S$ is the effective membrane area, $X_{A1}$, $X_{A2}$ and $X_{A3}$ are the mole fraction of the feed solution, the concentrated boundary solution and the product solution, respectively, $\pi(X_A)$ is osmotic pressure of the solution corresponding to $X_A$, $D_{AM}/K\delta$ is solute transport parameter, $M_B$ is molecular weight of water, $N_B$ is solvent water flux through membrane.

Matsuura and Sourirajan (1981) developed the surface fore-pore flow model (SFPF) which expresses quantitatively the preferential sorption-capillary flow model. This has made great advance in the development of membrane separation transport theory which is introduced in the next section.

### 2.2.4 Conclusions

Literature shows that there are the three main types of approaches to describe the reverse osmosis separation process. Different approaches can be applied to membrane separation processes. All the above theories and equations were developed for the reverse osmosis separation of solute and solvent. They are not applicable, as they are, for the separation of organic liquid mixtures where solute and solvent cannot be easily defined. This work is to extend PSCF mechanism for the separation of organic liquid mixtures and to derive a set of new transport equations for the separation of organic liquid mixtures. It is very useful to use the transport equations to predict membrane performance and to design new membrane separation processes.

# Chapter 3

# Theory

## 3.1 Surface Force-Pore Flow Model (SFPF)

In this section, the surface force-pore flow model (SFPF), which was developed to express quantitatively the preferential sorption-capillary flow model is briefly introduced.

The surface force-pore flow model (SFPF) put emphasis on the major role of the interaction between solute, solvent and membrane pore wall in reverse osmosis separation. According to this model, reverse osmosis separation is the combined result of the preferential sorption of one of the constituents of the feed solution at the membrane-solution interface, and the mass transport by fluid permeation under pressure through the capillaries in the microporous membrane. Preferential sorption at the interface is a function of solute-solvent-membrane material interactions arising from polar (including ionic), steric, and nonpolar characters of each one of the components involved in the reverse osmosis systems. The interaction force results in the interfacial concentration distribution. This model states that

there are circular cylindrical pores on the membrane surface [28]. The model which expresses quantitatively the interfacial concentration distribution and the simultaneous velocity distribution permits an accurate prediction of membrane separation performance.

## 3.2 Transport Equations

This work is to extend the surface force-pore flow model to the separation of binary mixtures of organic liquid mixtures where the solution composition covers the mole fraction of one component of the mixture from zero to unity. As mentioned above, the model postulates that the pores on membrane surface are circular and cylindrical and the cylindrical coordinates (r, z) are set in the cylinders (as Figure 2). A force balance is established among diffusive force, viscous force and pressure force at the steady state of the organic liquid mixtures transporting through the membrane pore. Based on the above force balance, a set of new transport equations for the separation of organic liquid by the reverse osmosis is developed. These equations are proven to adequately represent the membrane performance by experimental results. It is possible to predict the membrane performance for the separation of organic liquid by the transport equations. The detailed derivation of the transport equations is given in the following:

To find an expression for the velocity profile in the radial direction in the cylindrical coordinate for the binary organic liquid mixture systems including the component A and component B (the size of component molecule A $<$ the size of component molecule B), let us begin by picturing a small ring-shaped space confined between

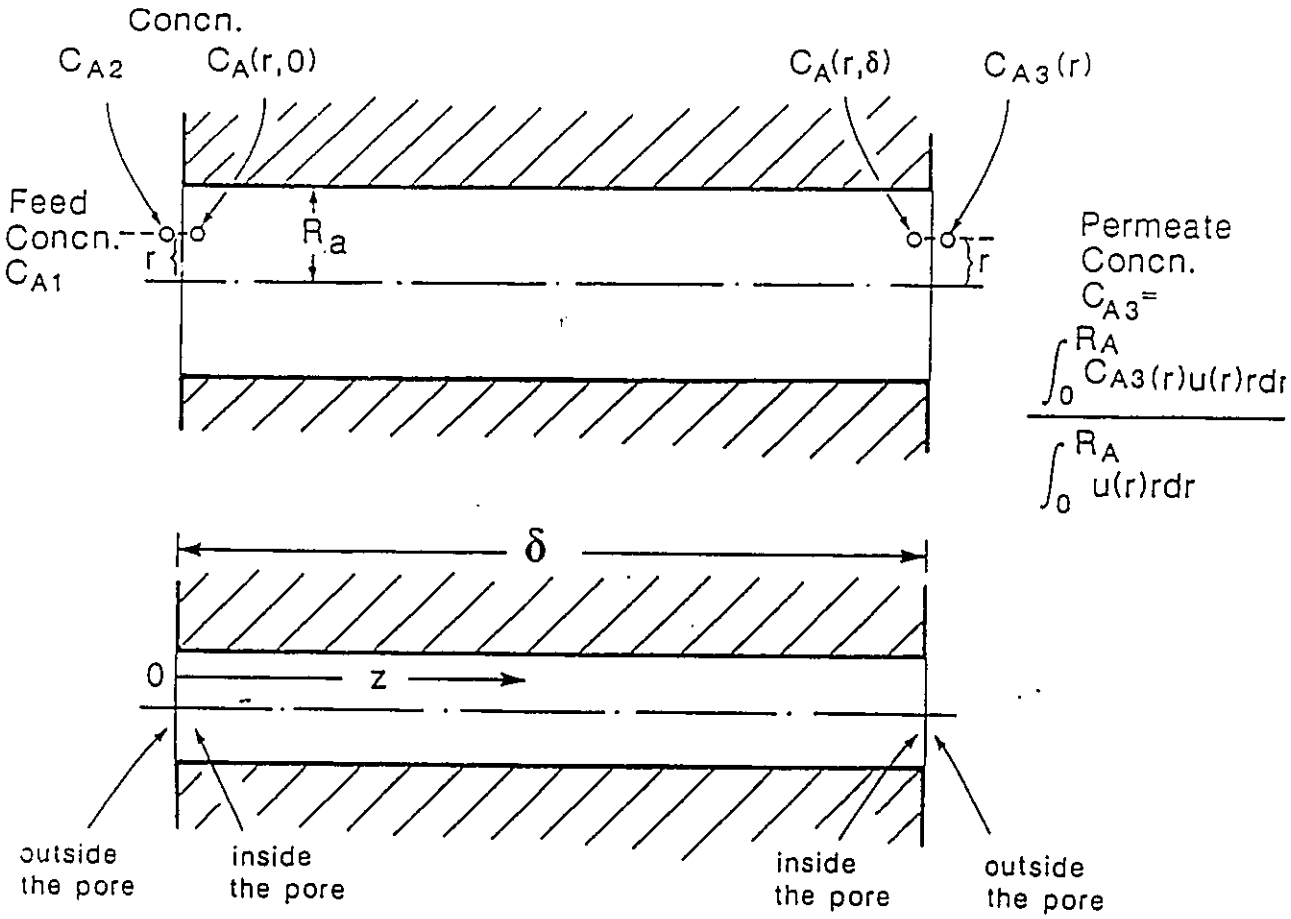


Figure 2: Cylindrical Coordinates(r,z) in Membrane Pores

two concentric cylinders of radii r and r + dr and between axial distances of z and z + dz ( as Figure 3).

The small ring-shaped space is acted on by three forces: diffusive forces, viscous forces and pressure forces. Under steady-state conditions, the total forces acting on the small ring-shaped space have to be balanced.

We first consider the diffusive forces. Letting $F_A$(r,z) and $F_B$(r,z) represent the diffusive forces acting on the component A and component B, respectively, they are given as

$$F_A(r,z) = -\frac{\partial \mu_A(r,z)}{\partial z}|_(r = r) \tag{3.1}$$

$$F_B(r,z) = -\frac{\partial \mu_B(r,z)}{\partial z}|_(r = r) \tag{3.2}$$

The chemical potentials at the position (r,z) can be expressed by

$$\mu_A(r,z) = \mu_A^0 + RTlna_A \tag{3.3}$$

$$\mu_B(r,z) = \mu_B^0 + RTlna_B \tag{3.4}$$

By using equations (3.3) and (3.4), equations (3.1) and (3.2) can be written as

$$F_A(r,z) = -RT\frac{\partial lna_A}{\partial z} \tag{3.5}$$

$$F_B(r,z) = -RT\frac{\partial lna_B}{\partial z} \tag{3.6}$$

Both $F_A(r,z)$ and $F_B(r,z)$ are given as forces acting on one mole of solution components. Since the number of moles of the component A and component B in the ring-shaped volume segment are $2\pi$rdrdz$C_A$(r,z) and $2\pi$rdrdz$C_B$(r,z), the total diffusive force acting on the segment is

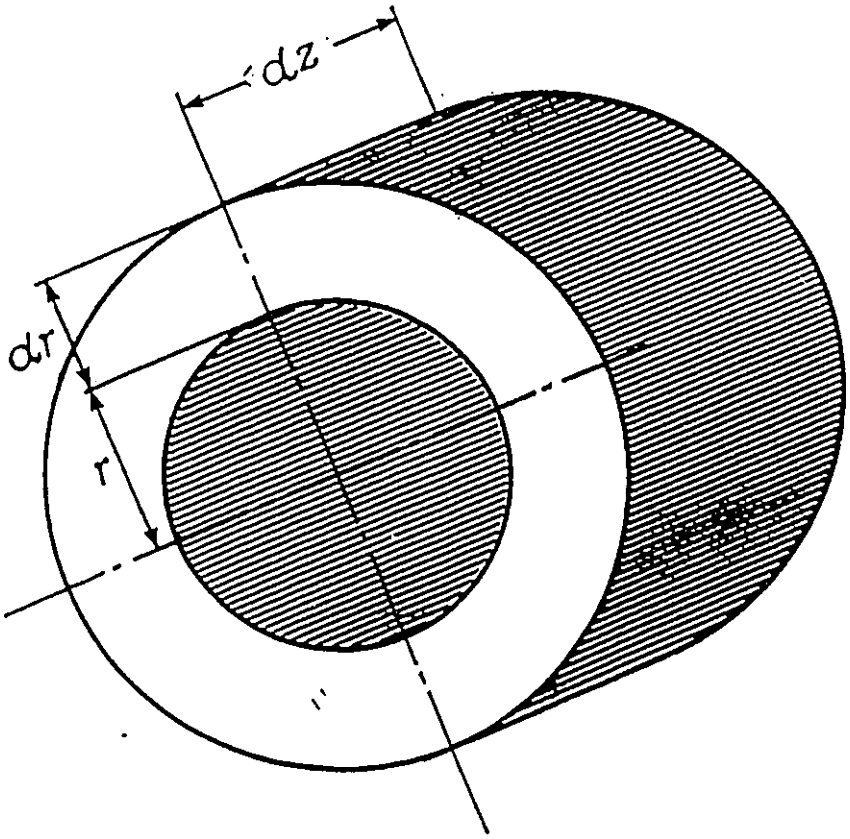


Figure 3: A Small Ring-Shaped Space Confined between two Concentric Cylinders of Radii r and r+dr and between Axial Distances of z and z+dz

$$2\pi r dr dz C_A(r,z)(-RT\frac{\partial ln a_A}{\partial z}) + 2\pi r dr dz C_B(r,z)(-RT\frac{\partial ln a_B}{\partial z}) \qquad (3.7)$$

By considering that the component A and component B in the spacial segment move together under the common diffusive force, it is shown that equation (3.7) is satisfied in most practical cases.

Osmotic pressure of the component A, $\pi_A$, and osmotic pressure of the component B, $\pi_B$, can be expressed by

$$\pi_A = -\frac{RT}{\bar{V}_B} ln a_B \qquad (3.8)$$

$$\pi_B = -\frac{RT}{\bar{V}_A} ln a_A \qquad (3.9)$$

Using the above relations, equation (3.7) becomes

$$2\pi r dr dz\{C_A(r,z)\bar{V}_A\frac{\partial \pi_B}{\partial z} + C_B(r,z)\bar{V}_B\frac{\partial \pi_A}{\partial z}\} \qquad (3.10)$$

Therefore the total diffusive forces can be given by equation (3.10). Now we begin our discussion of viscous forces by considering the momentum balance.

Momentum input through the cylindrical surface of radius r is

$$2\pi r dz\{-\eta\frac{du(r)}{dr}\} \qquad (3.11)$$

Momentum output through the cylindrical surface of radius r+dr is

$$2\pi(r+dr)dz\{-\eta\frac{du(r+dr)}{dr}\} \qquad (3.12)$$

$$\approx (2\pi r dz + 2\pi dr dz)\{-\eta\frac{du(r)}{dr} - \eta\frac{d^2u(r)}{dr^2}dr\} \qquad (3.13)$$

$$= 2\pi rdz\{-\eta\frac{du(r)}{dr}\}+2\pi rdz\{-\eta\frac{d^2u(r)}{dr^2}dr\}+2\pi drdz\{-\eta\frac{du(r)}{dr}\}+2\pi drdz\{-\eta\frac{d^2u(r)}{dr^2}dr\} \tag{3.14}$$

$$\approx 2\pi rdz\{-\eta\frac{du(r)}{dr}\} + 2\pi drdz\{-\eta\frac{du(r)}{dr}\} + 2\pi rdz\{-\eta\frac{d^2u(r)}{dr^2}dr\} \tag{3.15}$$

Therefore, increase in momentum in unit time is

$$2\pi rdz\{-\eta\frac{du(r)}{dr}\} - [2\pi rdz\{-\eta\frac{du(r)}{dr}\} + 2\pi drdz\{-\eta\frac{du(r)}{dr}\} + 2\pi rdz\{-\eta\frac{d^2u(r)}{dr^2}dr\}] \tag{3.16}$$

$$= 2\pi drdz\{\eta\frac{du(r)}{dr}\} + 2\pi rdrdz\{\eta\frac{d^2u(r)}{dr^2}\}] \tag{3.17}$$

$$= 2\pi rdrdz\{\eta\frac{d^2u(r)}{dr^2} + \eta\frac{1}{r}\frac{du(r)}{dr}\} \tag{3.18}$$

which is an expression for viscous force acting on the spacial segment.

For the pressure force acting on the volume segment, it can be given by

$$-\frac{\partial P}{\partial z}2\pi rdrdz \tag{3.19}$$

Under the steady-state conditions, the diffusive, viscous and pressure forces must be balanced. That is,

$$2\pi rdrdz\{\eta\tfrac{d^2u(r)}{dr^2} + \eta\tfrac{1}{r}\tfrac{du(r)}{dr}\} + 2\pi rdrdz\{C_A(r,z)\bar{V}_A\tfrac{\partial\pi_B}{\partial z}|(r=r)$$

$$+ C_B(r,z)\bar{V}_B\frac{\partial\pi_A}{\partial z}|(r=r)\} - \frac{\partial P}{\partial z}2\pi rdrdz = 0 \tag{3.20}$$

Dividing both sides of equation(3.20) by $2\pi rdrdz\eta$, one obtains

$$\frac{d^2u(r)}{dr^2} + \frac{1}{r}\frac{du(r)}{dr} + \frac{1}{\eta}\{C_A(r,z)\bar{V}_A\frac{\partial\pi_B}{\partial z}|(r=r) + C_B(r,z)\bar{V}_B\frac{\partial\pi_A}{\partial z}|(r=r) - \frac{\partial P}{\partial z}\} = 0 \tag{3.21}$$

Making the approximation that $C_A(r,z) \approx \bar{C}_A$ and $C_B(r,z) \approx \bar{C}_B$, and integrating the above equation from z=0 (pore inlet) to $z = \delta$ (pore outlet), we obtain,

$$\delta\frac{d^2u(r)}{dr^2}+\delta\frac{1}{r}\frac{du(r)}{dr}+\frac{1}{\eta}\{\bar{C}_A\bar{V}_A(\pi_{B,3}-\pi_{B,2})+\bar{C}_B\bar{V}_B(\pi_{A,3}-\pi_{A,2})-(P_3-P_2)\} = 0 \quad (3.22)$$

It should be noted that the integration should be extended to the position outside the pore. $\bar{C}_A$ and $\bar{C}_B$ are the average concentration of the component A and the component B in the pore, respectively. $P_2$, $\pi_{A,2}$ and $\pi_{B,2}$ are the hydraulic pressure, the osmotic pressure of the component A and the osmotic pressure of the component B at the pore inlet, respectively, all quantities corresponding to those outside the pore. Likewise, $P_3$, $\pi_{A,3}$ and $\pi_{B,3}$ are the hydraulic pressure, the osmotic pressure of the component A and that of the component B at the pore outlet, respectively, all quantities corresponding to those outside the pore.

Division by $\delta$ and rearrangement of equation (3.22) gives

$$\frac{d^2u(r)}{dr^2}+\frac{1}{r}\frac{du(r)}{dr}+\frac{1}{\eta\delta}\{(P_2-\bar{C}_A\bar{V}_A\pi_{B,2}-\bar{C}_B\bar{V}_B\pi_{A,2})-(P_3-\bar{C}_A\bar{V}_A\pi_{B,3}-\bar{C}_B\bar{V}_B\pi_{A,3})\} = 0 \quad (3.23)$$

By defining

$$\rho_2 = P_2 - \bar{C}_A\bar{V}_A\pi_{B,2} - \bar{C}_B\bar{V}_B\pi_{A,2} \quad (3.24)$$

$$\rho_3 = P_3 - \bar{C}_A\bar{V}_A\pi_{B,3} - \bar{C}_B\bar{V}_B\pi_{A,3} \quad (3.25)$$

By substituting equations (3.24) and (3.25) into equation (3.23), we can obtain

$$\frac{d^2u(r)}{dr^2} + \frac{1}{r}\frac{du(r)}{dr} + \frac{1}{\eta}\frac{\rho_2-\rho_3}{\delta} = 0 \quad (3.26)$$

To find a solution for the differential equation (3.26), we apply the boundary

conditions which are

$$\frac{du(r)}{dr} = 0 \; at \; r = 0 \tag{3.27}$$

$$and \; u(r) = 0 \; at \; r = R_a \tag{3.28}$$

where $R_a$ is the radius of the channel of the solution of the binary mixture and it can be given by $R_a = R_b$ - $D_A$. Note that $D_A < D_B$. By solving the differential equation together with the above boundary conditions, we can obtain a velocity profile in the radial direction in the cylindrical pore.

To find the concentration profile and the composition of the permeate solution, we derive a transport equation by applying the force balance with respect to the component A. The forces acting on the component A molecule in the volume segment of the cylindrical coordinate are the diffusive force and the friction force.

Let the diffusive force acting on the component A be denoted as $F_A(r, z)$ which is given by

$$F_A(r, z) = -RT\frac{\partial lna_A}{\partial z} \tag{3.29}$$

For the friction force between the component A and the component B we can write:

$$F_{AB}(r, z) = -\chi_{AB}\{u_A(r, z) - u_B(r, z)\} \tag{3.30}$$

where $\chi_{AB}$ is a proportionality constant to relate the friction force to the relative velocity of A to B.

Using the relations that

$$u_A(r,z) = \frac{J_A(r)}{C_A(r,z)} \tag{3.31}$$

$$and\ u_B(r,z) = \frac{J_B(r)}{C_B(r,z)} \tag{3.32}$$

Equation (3.30) can be expressed by

$$F_{AB}(r,z) = -\chi_{AB}\{\frac{J_A(r)}{C_A(r,z)} - \frac{J_B(r)}{C_B(r,z)}\} \tag{3.33}$$

Note that the flux of the component A and the component B, $J_A$ and $J_B$, are functions of the radial distance r alone and independent of the axial distance z.

The friction between the component A and the pore wall is given by

$$F_{AM}(r,z) = -\chi_{AM}\{\frac{J_A(r)}{C_A(r,z)}\} \tag{3.34}$$

where $\chi_{AM}$ is the proportionality constant between the friction force and the velocity of the component A molecule relative to the pore wall.

The above equation is valid since the velocity of the pore wall is equal to zero.

For steady-state conditions, all forces acting on the system have to be balanced, which yields:

$$-RT\frac{\partial lna_A}{\partial z} - \chi_{AB}\frac{J_A(r)}{C_A(r,z)} - \chi_{AM}\frac{J_A(r)}{C_A(r,z)} + \chi_{AB}\frac{J_B(r)}{C_B(r,z)} = 0 \tag{3.35}$$

Rearranging the above equations yields:

$$-RT\frac{\partial lna_A}{\partial z} - (\chi_{AB} + \chi_{AM})\frac{J_A(r)}{C_A(r,z)} + \chi_{AB}\frac{J_B(r)}{C_B(r,z)} = 0 \tag{3.36}$$

Using $J_A(r) = u(r)C_{A3}(r)$ and $J_B(r) = u(r)C_{B3}(r)$, equation (3.36) becomes

$$-RT\frac{\partial lna_A}{\partial z} - (\chi_{AB} + \chi_{AM})u(r)\frac{C_{A3}(r)}{C_A(r,z)} + \chi_{AB}u(r)\frac{C_{B3}(r)}{C_B(r,z)} = 0 \qquad (3.37)$$

By using appropriate boundary conditions, we can solve the above first order differential equation. Such boundary conditions can be obtained by applying the Maxwell-Boltzmann equation to both ends of the pore. They are given by

$$C_A(r,0) = C_{A2}e^{-\phi(C_{A2},r)/RT} \text{ at the pore inlet} \qquad (3.38)$$

$$C_A(r,\delta) = C_{A3}(r)e^{-\phi(C_{A3}(r),r)/RT} \text{ at the pore outlet} \qquad (3.39)$$

where $C_A$(r,o) and $C_{A2}$ are the concentration of component A at the pore inlet inside the pore and outside the pore, respectively. Likewise $C_A(r,\delta)$ and $C_{A3}(r)$ are the concentration of component A at the pore outlet inside the pore, and outside the pore, respectively. Note that the concentration of the boundary layer, $C_{A2}$, prevails at the pore inlet outside the pore and it does not depend on the radial coordinate r. On the other hand, the concentration at the pore outlet outside the pore $C_{A3}$(r) is considered to depend on the radial distance r. Since the interfacial interaction force constant depends on the composition of the binary mixture, as will be explained later, the potential function $\phi$ depends on both the distance from the pore wall (or the distance from the center of the pore, r) and the concentration of the component A outside the pore. It is assumed that the composition of the solution outside the pore is the bulk solution and the solution inside the pore is the interfacial solution.

The concentration of the component A in the permeate solution $C_{A3}$ is represented by

$$C_{A3} = \int_0^{R_a} C_{A3}(r) 2\pi r u(r) dr / \int_0^{R_a} 2\pi r u(r) dr \tag{3.40}$$

Furthermore, the following relation has to be satisfied in each phase in deriving above transport equations,

$$C_A \bar{V}_A + C_B \bar{V}_B = 1 \tag{3.41}$$

As well, the mole fraction of the component A at each phase can be given by

$$X_{A1} = \frac{C_{A1}}{C_{A1} + C_{B1}} \tag{3.42}$$

$$X_{A2} = \frac{C_{A2}}{C_{A2} + C_{B2}} \tag{3.43}$$

$$X_{A3} = \frac{C_{A3}}{C_{A3} + C_{B3}} \tag{3.44}$$

Considering the effect of concentration polarization, the following relation can be obtained:

$$X_{A2} - X_{A3} = (X_{A1} - X_{A3}) exp(\frac{v_s}{k_A}) \tag{3.45}$$

where $v_s$ is the membrane permeation velocity, $k_A$ is the mass transfer coefficient of the component A.

Using equations (3.26)–(3.28) and equations (3.37)–(3.45), one can calculate the mole fraction of the component A in the product permeate solution, $X_{A3}$, for a given mole fraction of the feed, $X_{A1}$, under given operating conditions including the operating pressure and the flow rate of the feed solution. The detailed calculation steps will be considered in section 3.4.

## 3.3 Numerical values

### 3.3.1 Determination of molecular radius

The molecular radius can be determined by the Stokes equation which is given by [29]

$$D_{AB} = \frac{kT}{6\pi\eta D_A} \tag{3.46}$$

Therefore

$$D_A = \frac{kT}{6\pi\eta D_{AB}} \tag{3.47}$$

where $D_{AB}$ is the diffusivity of component A in component B, $T$ is absolute temperature, $k$ is the Boltzmann constant, $\eta$ is solution viscosity, $D_A$ is the molecular radius of component A. Similarly, $D_B$ can be obtained from the diffusivity $D_{AB}$ by using above equation.

### 3.3.2 Activity Coefficients

Based on phase-equilibrium Data, activity coefficients can be calculated using the following equations [30]:

$$ln\gamma_A = ln\frac{y_A p}{x_A p_A} + \frac{(B_{AA} - V_A^L)(p - p_A) + p\delta_{AB}y_B^2}{RT} \tag{3.48}$$

$$ln\gamma_B = ln\frac{y_B p}{x_B p_B} + \frac{(B_{BB} - V_B^L)(p - p_B) + p\delta_{AB}y_A^2}{RT} \tag{3.49}$$

where $\delta_{AB} = 2B_{AB} - B_{AA} - B_{BB}$, $\gamma_A$ and $\gamma_B$ are the activity coefficient in liquid phase of component A and component B, respectively; $p$, $p_A$ and $p_B$ are the total vapor

pressure, the vapor pressure of component A and the vapor pressure of component B, respectively; $B_{AA}$ and $B_{BB}$ are the second virial coefficient for component A and for component B, respectively; $B_{AB}$ is the second cross virial coefficient, $x_A$ and $x_B$ are the mole fraction of component A and component B in liquid phase, respectively; $y_A$ and $y_B$ are the mole fraction of component A and component B in vapor phase, respectively; $T$ is absolute temperature, $R$ is universal gas constant.

### 3.3.3 Interaction Force Constant

The solute - solvent - membrane material interaction force constant, B, for the organic liquid systems can be determined by liquid chromatography experiments [31,32]. The detailed method can be given as follows :

According to the Maxwell-Boltzmann equation

$$C_{A,i}(\underline{d}) = C_{A,b}exp(-\Phi(\underline{d})) \tag{3.50}$$

The surface excess can be given by [7]

$$\Gamma_A/C_{A,b} = \int_{DA}^{\infty}\{exp(-\phi(\underline{d})/RT) - 1\}d(\underline{d}) \tag{3.51}$$

$$= \int_{DA}^{\infty}\{exp(-\Phi(\underline{d})) - 1\}d(\underline{d}) \tag{3.52}$$

where $C_{A,i}$ is molar concentration of the component A in the interfacial solution, $C_{A,b}$ is molar concentration of the component A in the bulk solution, $\phi(\underline{d})$ is a potential as a function of distance $\underline{d}$ from the interface and $\Phi(\underline{d})$ is its dimensionless form. Special considerations have to be given to the potential function when the radius of the component A molecule, designated as $D_A$, is smaller than that of the component B molecule, designated as $D_B$. It should be noted that a molecule is

considered to be spherical in this model and its position is represented by that of the molecular center. Then, in the vicinity of the polymer–solution interface there is a space which is unoccupied by the center of the component B molecule but can be occupied by that of the component A molecule as shown in Figure 4 by a shadowed region near the interface. Considering the existence of such a region the concentration profile of the component A molecule at the polymer–solution interface becomes such as illustrated in Figure 5. The potential function which represents the above concentration profile should then be such as given in Figure 6, which can be expressed by [33]

$$\phi = \begin{cases} \infty & \text{when } \underline{d} \leq D_A \\ -ln\frac{C_{A,pure}}{C_{A,b}}RT & \text{when } D_A < \underline{d} \leq D_B \\ -\frac{B_A RT}{(\underline{d})^3} & \text{when } \underline{d} > D_B \end{cases} \tag{3.53}$$

Substituting the relation $C_{A,pure}\bar{V}_A = 1$ into above equation, one gets

$$\phi = \begin{cases} \infty & \text{when } \underline{d} \leq D_A \\ -ln\frac{1}{C_{A,b}\bar{V}_A}RT & \text{when } D_A < \underline{d} \leq D_B \\ -\frac{B_A RT}{(\underline{d})^3} & \text{when } \underline{d} > D_B \end{cases} \tag{3.54}$$

A theory for liquid chromatography was established to relate the surface excess of the component A and the component B, $\Gamma_A/C_{A,b}$ and $\Gamma_B/C_{B,b}$, to the retention volume data [34].

According to the theory,

$$\Gamma_A/C_{A,b} = \frac{X_{B,b}\bar{V}_B([V_R']_A^{mixt} - [V_R']_B^{mixt})}{X_{A,b}\bar{V}_A + X_{B,b}\bar{V}_B}/A_p \tag{3.55}$$

$$\Gamma_B/C_{B,b} = \frac{X_{A,b}\bar{V}_A([V_R']_B^{mixt} - [V_R']_A^{mixt})}{X_{A,b}\bar{V}_A + X_{B,b}\bar{V}_B}/A_p \tag{3.56}$$

Therefore, the surface excess of the component A and the component B, $\Gamma_A/C_{A,b}$ and $\Gamma_B/C_{B,b}$, can be obtained from liquid chromatography experiment and using the above relations.

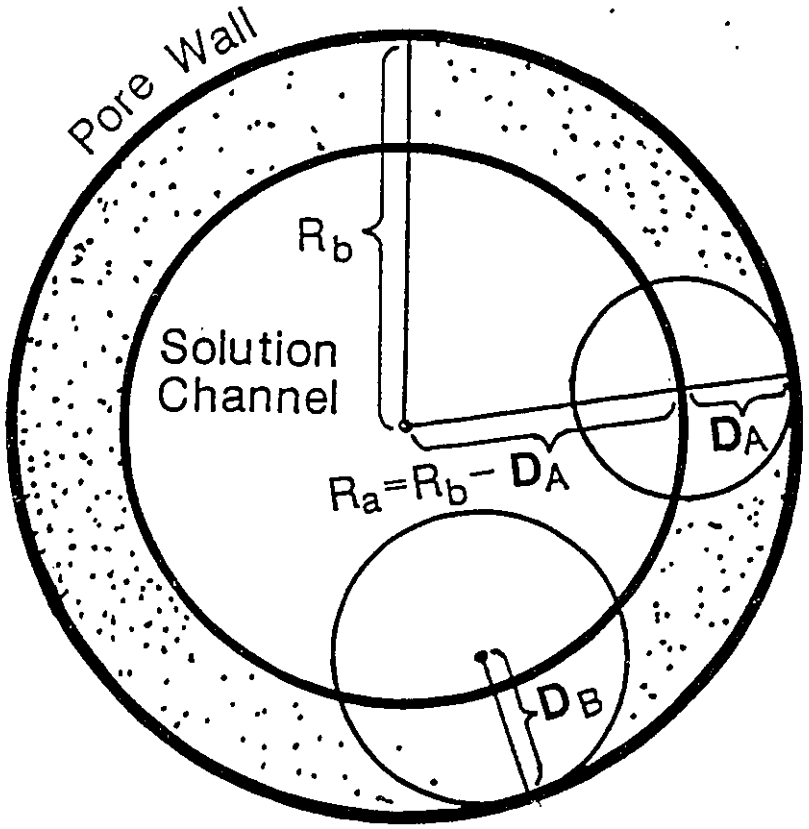


Figure 4: A Shadowed Region which is unoccupied by the Center of the Component B Molecule but can be occupied by that of the Component A Molecule

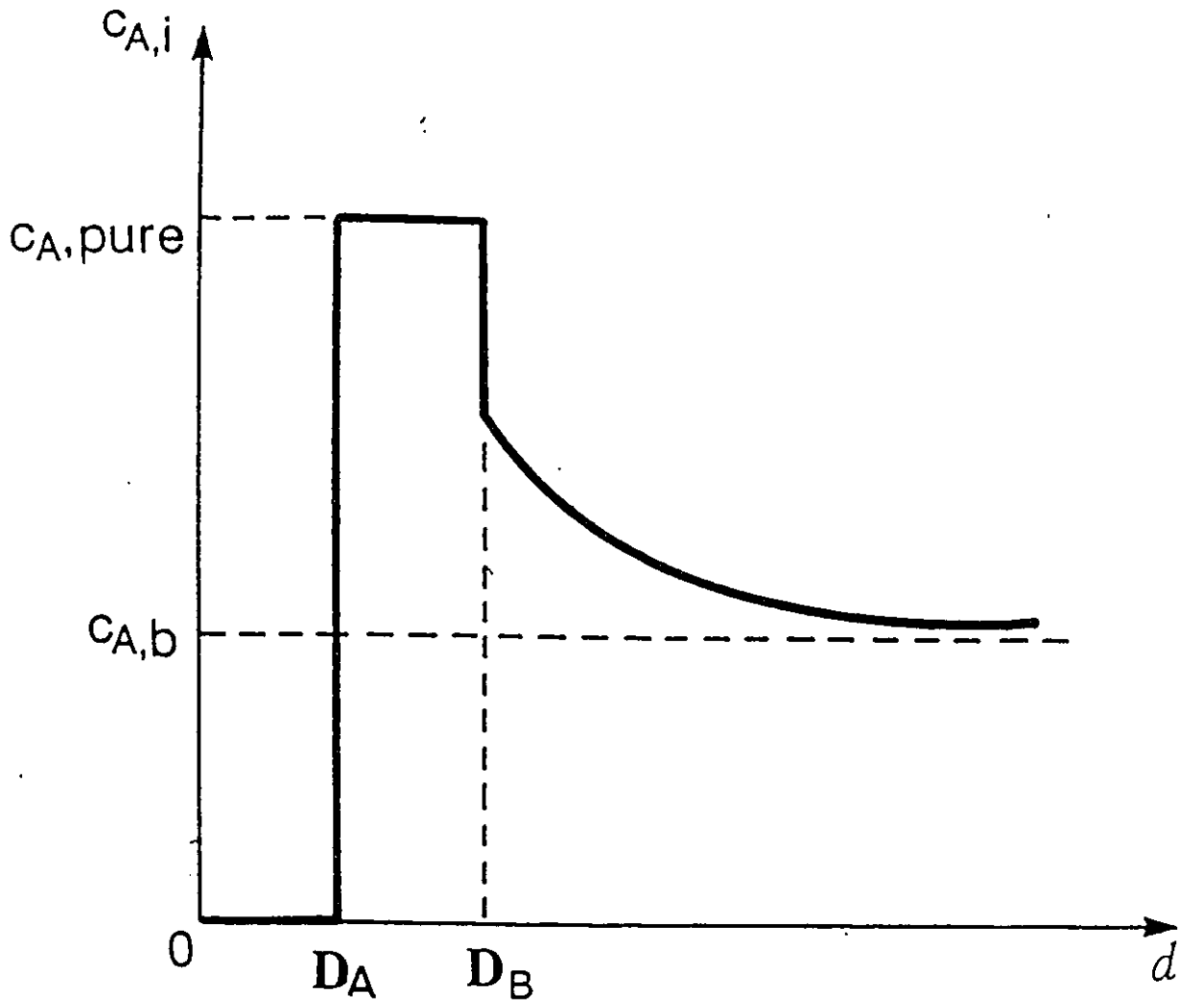


Figure 5: The Concentration Profile of the Component A at the Polymer–Solution Interfaces in the Case of Preferential Sorption of Component A

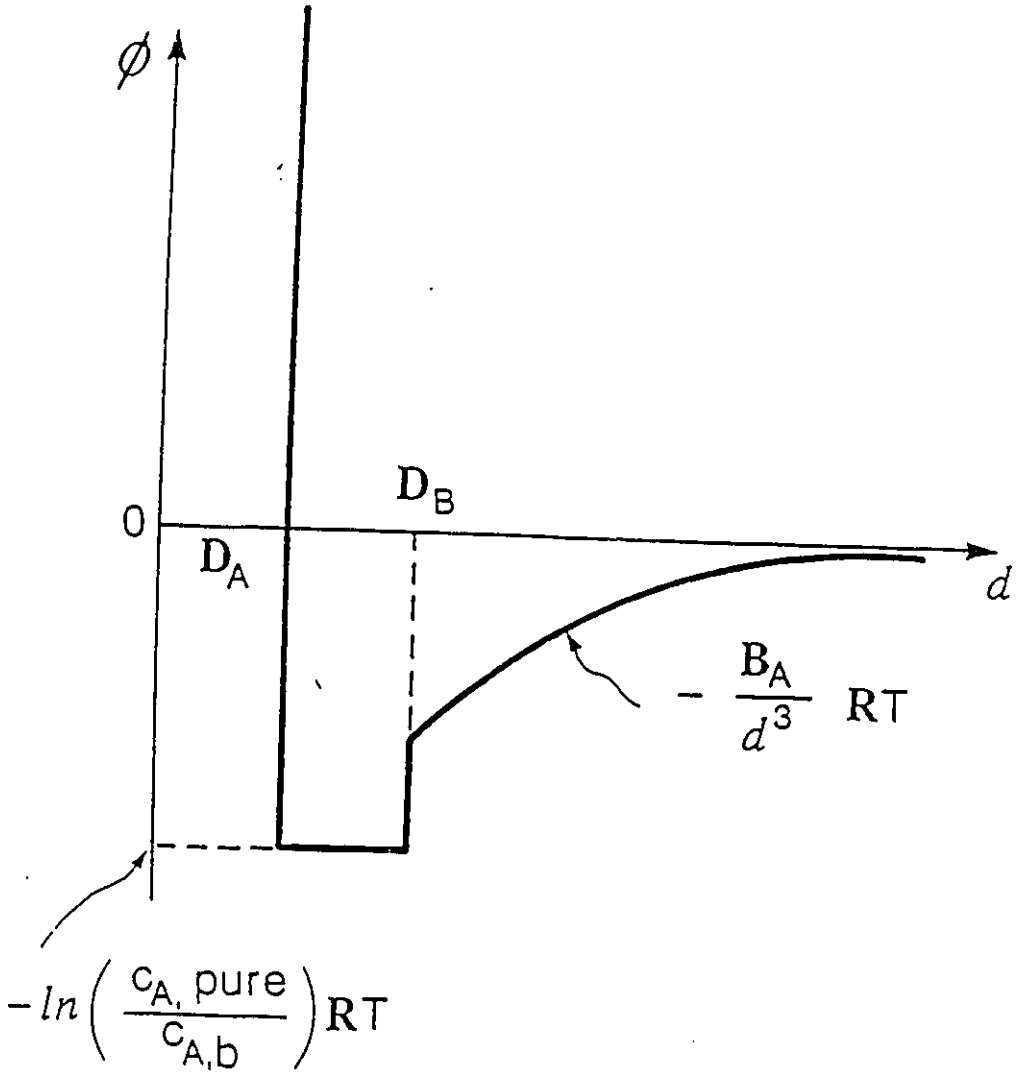


Figure 6: The Potential Profile of the Component A at the Polymer–Solution Interfaces in the Case of Preferential Sorption of Component A

In eq.(3.55), $A_p$ is the surface area of the polymer powder which is measured independently from the liquid chromatography experiment by gas chromatography method [35,36,37]; $X_{A,b}$, $X_{B,b}$, $\bar{V}_A$ and $\bar{V}_B$ indicate the mole fraction of the component A and component A in the solvent mixture which is used as the mobile phase in the chromatography, the average molar volume of the component A and that of component B, respectively; the quantities $C_{A,b}$ and $C_{B,b}$ are molar concentrations of the component A and that of the component B, respectively; and, $[V_R']_A^{mixt}$ and $[V_R']_B^{mixt}$ are the retention volume data of the component A and the component B which can be obtained from the chromatography experiment. The superscript $mixt$ indicates that a binary mixture is used for the solvent in the chromatographic experiment. $\Gamma_A/C_{A,b}$ and $\Gamma_B/C_{B,b}$ values obtained for the system ethanol - heptane - cellulose polymer are given in Table 1 as a function of $X_{A,b}$.

The interaction force constant $B_A$, can be obtained for a given value of $\Gamma_A/C_{A,b}$ by solving equations (3.52) and (3.54). The $B_A$ values obtained for the system ethanol - heptane - cellulose polymer are also given in Table 1 as a function of $X_{A,b}$.

Table 1. Surface Excess and Interfacial Interaction Force constant for the System Ethyl Alcohol (A) – Heptane (B)– Cellulose

| $X_{A,b}$ | $\Gamma_A/C_{A,b} \times 10^{10} m^a$ | $\Gamma_B/C_{B,b} \times 10^{10} m^a$ | $B_A \times 10^{30} m^3$ |
|---|---|---|---|
| 0 | 48.82 | 0 | 10.9 |
| 0.073 | 54.09 | -17.00 | 11.2 |
| 0.200 | 5.07 | -0.502 | 5.34 |
| 0.277 | 3.63 | -0.558 | 4.41 |
| 0.387 | 0 | 0 | 0 |
| 0.543 | 0 | 0 | 0 |
| 0.656 | -1.59 | 1.2 | -15.6 |
| 0.714 | -1.39 | 1.39 | -13.0 |
| 0.779 | 0 | 0 | 0 |
| 0.827 | 4.32 | -8.23 | 4.90 |
| 0.891 | 5.24 | -17.07 | 5.43 |
| 0.934 | 6.95 | -39.08 | 6.19 |
| 1.000 | 0 | -30.69 | 0 |

[a] data based on $A_p = 71.69\ m^2$

## 3.4 Calculation steps

Several steps are required to calculate the membrane performance data by using the above transport equations. The full sequence of calculations is as follows.

Step 1. Assume $X_{A3}$ and calculate $X_{A2}$ by equation (3.45), in which $v_s$ is the permeation velocity of the pure liquid. The mass transfer coefficient $k_A$ is ob-

tained from the Sherwood-Schmidt equation based on the mass transfer coefficient of sodium chloride $k_{NaCl}$ in an aqueous solution determined for a given experimental setup. It is given by [38]

$$k_A = \{\frac{(D_A)\ in\ B}{(D_{NaCl})\ in\ Water}\}^{2/3}(k_{NaCl})\ in\ water \tag{3.57}$$

Step 2. $C_{A2}$ and $C_{B2}$ can be calculated by equation (3.41) and (3.43) using $X_{A2}$ value above obtained. Similarly, $C_{A3}$ and $C_{B3}$ can be calculated by equations (3.41) and (3.44).

Step 3. Equation (3.23) is solved by using the boundary conditions given by equation (3.27) and (3.28). As $\bar{C}_A$ and $\bar{C}_B$ used in equation (3.22) $C_{A3}$ and $C_{B3}$ are chosen assuming the solution composition prevailing in the membrane pore is close to that of the permeate solution. This assumption may not always be correct. As the viscosity required in equation (3.26), that of the permeate solution is chosen. Activity data are necessary for this calculation and they are listed in Table 2.

Step 4. Assume $C_{A3}(r)$ and calculate $C_{B3}$(r) by equation (3.41).

Step 5. $C_A(r,0)$ is calculated for a given r value by equation (3.38) using $C_{A2}$ obtained in Step 2. $X_{A2}$ can be obtained by equation (3.43), in which $C_{A2}$ and $C_{B2}$ are from Step 2. $C_{A2}$ prevails at the pore inlet outside the pore and is considered to be the bulk concentration, that is, $C_{A,b} = C_{A2}$ at the pore inlet. Similarly $C_{B,b} = C_{B2}$. Furthermore, $X_{A,b} = X_{A2}$. $D_A$ and $D_B$ value are obtained by equation (3.47). $B_A$ can be determined from $X_{A,b}$ and Table 1. By using $\underline{d} = R_b$ - r, we can get

$$\phi = \begin{cases} \infty & \text{when } R_b - r \leq D_A \\ -ln\frac{1}{C_{A,b}V_A}RT & \text{when } D_A < R_b - r \leq D_B \\ -\frac{B_A RT}{(R_b - r)^3} & \text{when } R_b - r > D_B \end{cases} \tag{3.58}$$

Note that $B_A$ is the function of $X_{A,b}$, that is, the function of $C_{A2}$. Consequently, $\phi$ is the function of both $C_{A2}$ and r for given $R_b$, $D_A$ and $D_B$ values. Hence, $\phi$ is written as $\phi(C_{A2}, r)$ in equation (3.38). Then, $C_A$ (r,0) can be obtained from equation (3.38) by using values of $\phi(C_{A2}, r)$ and $C_{A2}$, $C_B(r, 0)$ is obtained from equation (3.41). $a_A$ (r,0) can be obtained from the $C_A$(r,0) above determined by using the relation between $C_A$ and $a_A$ such as given in Table 2. Starting from the latter $a_A$ (r,0) value the integration is performed from z=0 to z=$\delta$ by equation (3.37) using u(r) values obtained in step 3. In order to perform this integration, equation (3.37) is approximated by

$$\Delta lna_A(r,z) = \{\frac{-(\chi_{AB}+\chi_{AM})}{RT}u(r)\frac{C_{A3}(r)}{C_A(r,z)} + \frac{\chi_{AB}}{RT}u(r)\frac{C_{B3}(r)}{C_B(r,z)}\}\Delta z \qquad (3.59)$$

starting from $a_A(r, 0)$ the numerical value of $a_A(r, \Delta z)$ is given by

$$lna_A(r,\Delta z) = lna_A(r,0) + \{\frac{-(\chi_{AB}+\chi_{AM})}{RT}u(r)\frac{C_{A3}(r)}{C_A(r,0)} + \frac{\chi_{AB}}{RT}u(r)\frac{C_{B3}(r)}{C_B(r,0)}\}\Delta z \qquad (3.60)$$

where $\chi_{AB}$ is equal to $RT/D_{AB}$. $\chi_{AM}$ can be obtained from an equation by using value of $b_A$

$$b_A = \frac{\chi_{AB}+\chi_{AM}}{\chi_{AB}} \qquad (3.61)$$

where the friction constant $b_A$ is given by [39,40,41,42]

$$b_A = \begin{cases} [1 - 2.104\lambda_f + 2.09\lambda_f^3 - 0.95\lambda_f^5]^{-1} & \text{when } \lambda_f \le 0.22 \\ 44.57 - 416.2\lambda_f + 934.9\lambda_f^2 + 302.4\lambda_f^3 & \text{when } 0.22 < \lambda_f < 1 \end{cases} \qquad (3.62)$$

where $\lambda_f = D_A$ / $R_b$, u(r) is from Step 3. The values for $C_{A3}$(r) and $C_{B3}$(r) are from Step 4. $C_(r, 0)$ and $C_B(r, 0)$ are also from the foregoing calculation. The numerical value for $a_A(r, \Delta z)$ is then used to obtain $C_A(r, \Delta z)$ from Table 2. and $C_B(r, \Delta z)$ from equation (3.41). Using these numerical values we can further cal-

culate $a_A(r, 2\Delta z)$ by

$$ln a_A(r, 2\Delta z) = ln a_A(r, \Delta z) + \{\frac{-(\chi_{AB} + \chi_{AM})}{RT} u(r) \frac{C_{A3}(r)}{C_A(r, \Delta z)} + \frac{\chi_{AB}}{RT} u(r) \frac{C_{B3}(r)}{C_B(r, \Delta z)}\} \Delta z \tag{3.63}$$

These calculations are proceeded until $a_A(r, \delta)$ are obtained.

Step 6. Using Table 2, we will find $C_A(r, \delta)$ corresponding to $a_A(r, \delta)$ obtained above. Then, we shall examine if the above $C_A(r, \delta)$ and $C_{A3}(r)$ assumed in Step 4 satisfy equation (3.39). If equation (3.39) is satisfied the assumed $C_{A3}$(r) is right, otherwise we shall go back to the Step 4. In some cases $a_A(r, \delta)$ becomes more than unity. Corresponding to $a_A(r, \delta) > 1$, $C_A(r, \delta) = C_{A,pure}$ is used, where $C_{A,pure}$ denotes the molar concentration of the component A in the pure component A liquid. In such a case there are many $C_{A3}(r)$ values which can satisfy equation (3.39) and $C_{A3}$(r) is undetermined. As an approximation $C_{A3}(r) = C_{A,pure}$ is also used.

Step 7. We repeat steps 4 to 6 for r=0, $r = \Delta r$, $r = 2\Delta r$,..., $r = R_a$ where $\Delta r$ is a small increment in r value and for each r value $C_{A3}$(r) and $C_{B3}$(r) which satisfy the relation given by equation (3.39) are determined.

Step 8. The above $C_{A3}(r)$ values are used together with u(r) in equation (3.40) to calculate $C_{A3}$. This $C_{A3}$ value should agree with $C_{A3}$ obtained in Step 2. If they agree the value $X_{A3}$ assumed in Step 1 is right and we can go to the next Step. Otherwise, we have to go back to Step 1 and reassume $X_{A3}$.

Step 9. Using numerical values for u(r), $C_{A3}$ and $C_{B3}$ obtained above we can further calculate $[PR]/[PSP]_B$ ratio by

$$[PR]/[PSP]_B = \frac{(\int_0^{R_a} u(r)2\pi r dr) \times \rho_{mixture}/\rho_B}{\pi R_a^4 (P_2 - P_3)/8\eta_B \delta} \tag{3.64}$$

$$= \frac{(\int_0^{R_a} u(r)2\pi r dr) \times \frac{(C_{A3}M_A + C_{B3}M_B)V_B}{M_B}}{\pi R_a^4 (P_2 - P_3)/8\eta_B \delta} \tag{3.65}$$

where $\eta_B$ is the viscosity of the pure B component liquid.

Table 2. Mole Fraction, Molar Concentration and Activity Data for the Ethyl Alcohol (A) – Heptane (B)– Cellulose System

| $X_A$ | $C_A \times 10^{-3}$ mol/$m^3$ | $C_B \times 10^{-3}$ $mol/m^3$ | $C_{total} \times 10^{-3}$ $mol/m^3$ | $a_A$ | $a_B$ |
|---|---|---|---|---|---|
| 0 | 0 | 6.823 | 6.823 | 0 | 1.000 |
| 0.01 | 0.069 | 6.792 | 6.861 | 0.226 | 0.992 |
| 0.025 | 0.173 | 6.748 | 6.921 | 0.562 | 0.986 |
| 0.05 | 0.351 | 6.675 | 7.026 | 0.659 | 0.979 |
| 0.075 | 0.535 | 6.599 | 7.134 | 0.708 | 0.974 |
| 0.1 | 0.725 | 6.521 | 7.246 | 0.740 | 0.971 |
| 0.150 | 1.122 | 6.360 | 7.482 | — | — |
| 0.200 | 1.547 | 6.187 | 7.734 | 0.812 | 0.956 |
| 0.300 | 2.490 | 5.807 | 8.297 | 0.836 | 0.947 |
| 0.400 | 3.58 | 5.369 | 8.949 | 0.848 | 0.940 |
| 0.500 | 4.857 | 4.857 | 9.714 | 0.859 | 0.930 |
| 0.600 | 6.378 | 4.252 | 10.63 | 0.86 | 0.929 |
| 0.700 | 8.211 | 3.519 | 11.73 | 0.879 | 0.892 |
| 0.800 | 10.48 | 2.62 | 13.10 | 0.902 | 0.824 |
| 0.900 | 13.35 | 1.48 | 14.83 | 0.934 | 0.661 |
| 1.000 | 17.13 | 0.000 | 17.13 | 1.000 | 0 |

data from Van Ness et al., 1967

# Chapter 4

# Results and Discussion

Based on the surface force-pore flow model, a computer program to calculate the membrane performance for the separation of organic liquid mixture under different conditions has been developed. The calculation procedure of the computer program has been described in detail in Section 3.4. Using the computer program, a series of the membrane performance data, such as the mole fraction of both components in the product solution, the ratio of the permeation rate of the product solution to the permeation rate of pure solvent can be obtained. The results show that the interaction force, pore radius on the membrane surface and the relative radius of component molecules are three important factors to govern the membrane separation.

The calculated data are tested by the experimental data on reverse osmosis separation of ethanol-heptane mixtures by cellulose membrane [17]. The agreement between the experimental data and calculated data shows that the transport equations for organic liquid mixture systems which were derived from surface force-pore flow model have truly predictive capabilities.

## 4.1 Effect of Molecular Radius on the Membrane Performance

Figures 7 – 10 show the effect of molecular radii of the component A and component B of the liquid mixtures on the membrane performance. It has to be noted that the membrane pore radius of membrane, $R_b = 5.2 \times 10^{-10}$ m, and the operating gauge pressure of 1700 $kPa$ were used throughout the calculation. Values listed in Table 1 for the interaction force parameter $B_A$ and the activity coefficient data listed in Table 2 have been used in this calculation. It should be recalled that both tables corresponding to the system ethanol(A) –n–heptane(B)–cellulose. As for the radii of the component A and B molecules, which are denoted as $D_A$ and $D_B$, $D_A = 1.2 \times 10^{-10}$ m corresponding to that of ethanol molecule $D_B = 2.56 \times 10^{-10}$ m corresponding to that of n–heptane molecule. Therefore, the combinations of the above $D_A$ and $D_B$ values reflect truly the situation occurring in the separation of ethanol–n–heptane mixtures by cellulose membranes. Other combinations of $D_A$ and $D_B$ values lead to the calculation for some imaginary systems.

In Figure 7, $D_A$ was fixed at $1.2\times10^{-10}$ m while $D_B$ was changed from $2.56\times10^{-10}$ m to $4.5\times10^{-10}$ m.

Figure 7 shows that a larger $D_B$ results in greater $X_{A3}$. The difference between the values of $X_{A3}$ at $D_B = 4.5 \times 10^{-10}m$ and $D_B = 2.56 \times 10^{-10}$ m is significant in the range of $X_{A1}$ below 0.6 and the difference shows a maximum at about $X_{A1} =$ 0.2.

Figure 8 shows the effect of molecular radius of component B on $[PR]/[PSP]_B$ ratio under the same conditions as Figure 7. The results in Figure 8 show that $[PR]/[PSP]_B$ ratio decreases drastically in the initial increase of $X_{A1}$ and changes

only little when $X_{A1} > 0.3$.

Figure 9 shows the effect of molecular radius of component A on the mole fraction of component A in the permeate. In Figure 9, $D_B$ was fixed at $2.56 \times 10^{-10}$ m, $D_A$ was changed from $1.0 \times 10^{-10}$ m to $1.5 \times 10^{-10} m$. $X_{A3}$ decreases drastically with an increase in $D_A$. When $D_A = 1.5 \times 10^{-10}$ m, $X_{A3}$ is nearly equal to $X_{A1}$ in the range $X_{A1} > 0.6$.

Both Figures 7 and 9 show that the preferential permeation of component A molecule increases when the relative radius of component A and component B molecule increases.

Figure 10 shows the effect of molecular radius of component A on $[PR]/[PSP]_B$ ratio under the same conditions as Figure 9. The results in Figure 10 indicates that curves for different molecular radii of component A have a similar pattern. With an increase of $X_{A1}$, $[PR]/[PSP]_B$ ratio drops to a lower level at the beginning but the ratio changes only little in a higher $X_{A1}$ range. The change from $D_A = 1.0 \times 10^{-10} m$ to $1.2 \times 10^{-10} m$ has more significant effect on the above ratio than the change in $D_A$ from $1.2 \times 10^{-10} m$ to $1.5 \times 10^{-10} m$.

It is interesting to note that the minimum value in the $[PR]/[PSP]_B$ ratio appearing at $X_{A1} \approx 0.15$ tends to be lower as preferential permeation of the component A increases by decreasing $D_A$ value.

Figure 11 shows the results of the calculation in which the conditions are almost the same as Figure 9. The interaction force parameters, $B_A$, listed in Table 3 were used instead of those listed in Table 2. Note that all $B_A$ values in Table 3 are negative, indicating that the interaction force between the component A and the membrane polymer material is rejective in the entire range of the feed mole fraction.

In other words the component B is preferentially attracted to the membrane. The effect is clearly seen by comparing Figure 9 and Figure 11, i.e. the mole fraction of the component A in the permeate is less in Figure 11 than in Figure 9 in the almost entire range of feed mole fraction. It is natural since the component B molecule is more strongly attracted to the membrane in the calculation of Figure 11. The effect is seen more strongly in the higher range of feed mole fraction. Figures 7, 9 and 11 show that the permeate composition is governed by the relative size of the component A and B as well as the interaction force working between the component molecules and the membrane material.

Figure 12 shows that $[PR]/[PSP]_B$ ratio changes with the feed mole fraction. The above ratio exhibits a more complicated pattern than those observed in Figure 8 and 10. It is interesting to note that ratio decreases twice, in the lower ($X_{A1} \approx 0.15$) and the higher lower ($X_{A1} \approx 0.65$) feed mole fraction value. Looking into Figure 11, it is found that $X_{A3}$ values are farther away from the diagonal line at the above $X_{A1}$ values, which means that the $[PR]/[PSP]_B$ ratio decreases significantly when the separation of component A and B is effective regardless of which component permeates the membrane preferentially.

Table 3. Surface Excess and Interfacial Interaction Force Constant for the Preferential Sorption of Component B System

| $X_{A,b}$ | $\Gamma_A/C_{A,b} \times 10^{10} m^a$ | $B_A \times 10^{30} m^3$ |
|---|---|---|
| 0 | – | – |
| 0.01 | -0.5 | -4.8 |
| 0.025 | -1.0 | -9.64 |
| 0.050 | -1.5 | -14.4 |
| 0.075 | -2.0 | -28.8 |
| 0.1 | -2.4 | -37.4 |
| 0.15 | -3.1 | -47.8 |
| 0.20 | -3.6 | -63.5 |
| 0.3 | -4.3 | -142 |
| 0.4 | -4.8 | -171 |
| 0.5 | -5.0 | -183 |
| 0.6 | -4.8 | -171 |
| 0.7 | -4.3 | -142 |
| 0.8 | -3.6 | -63.5 |
| 0.9 | -2.4 | -37.4 |
| 1.000 | 0 | – |

[b] data based on $A_p = 71.69\ m^2$

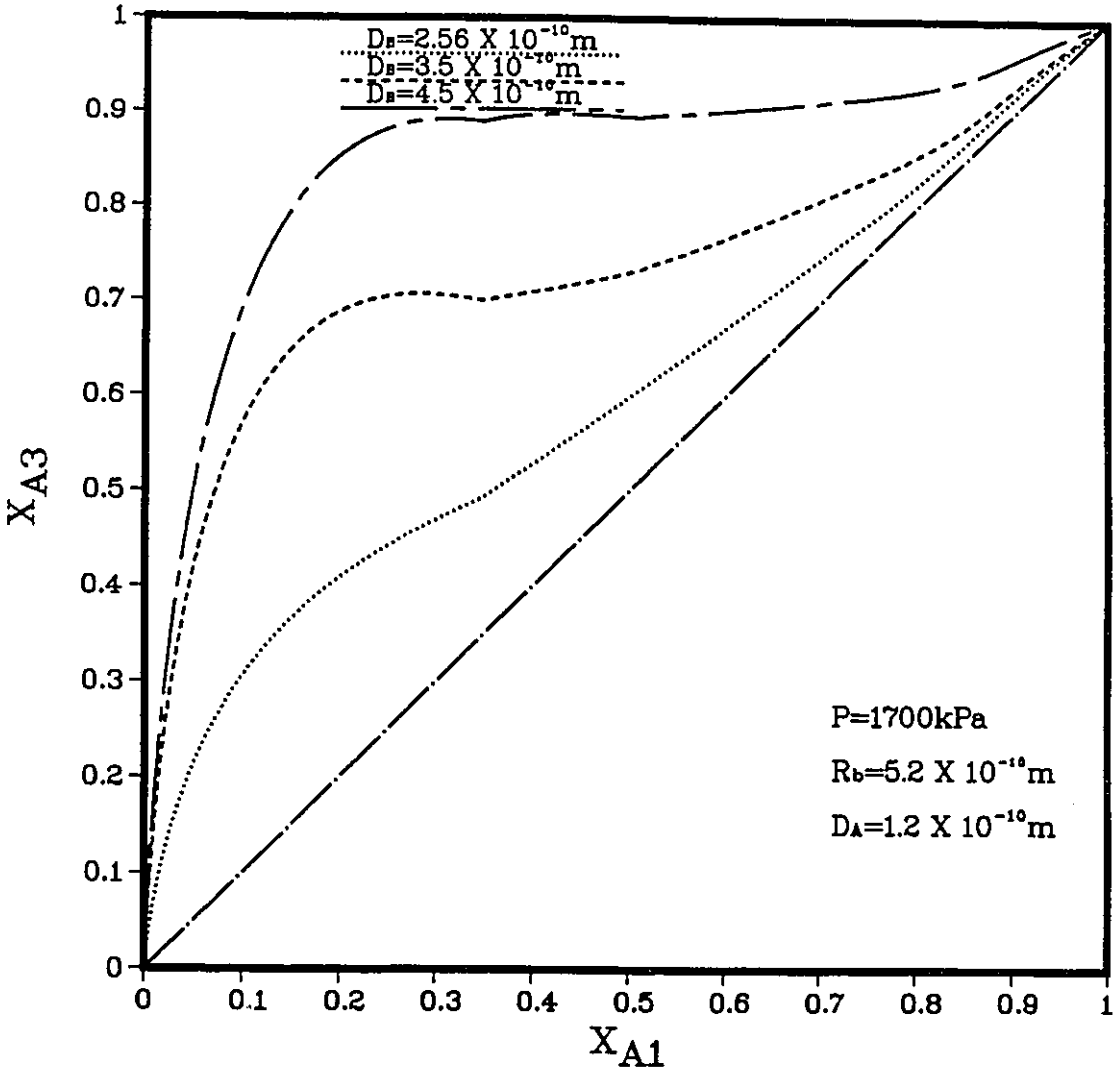


Figure 7 : Effect of Molecular Radius of Component B on Mole Fraction of Component A in the Permeate

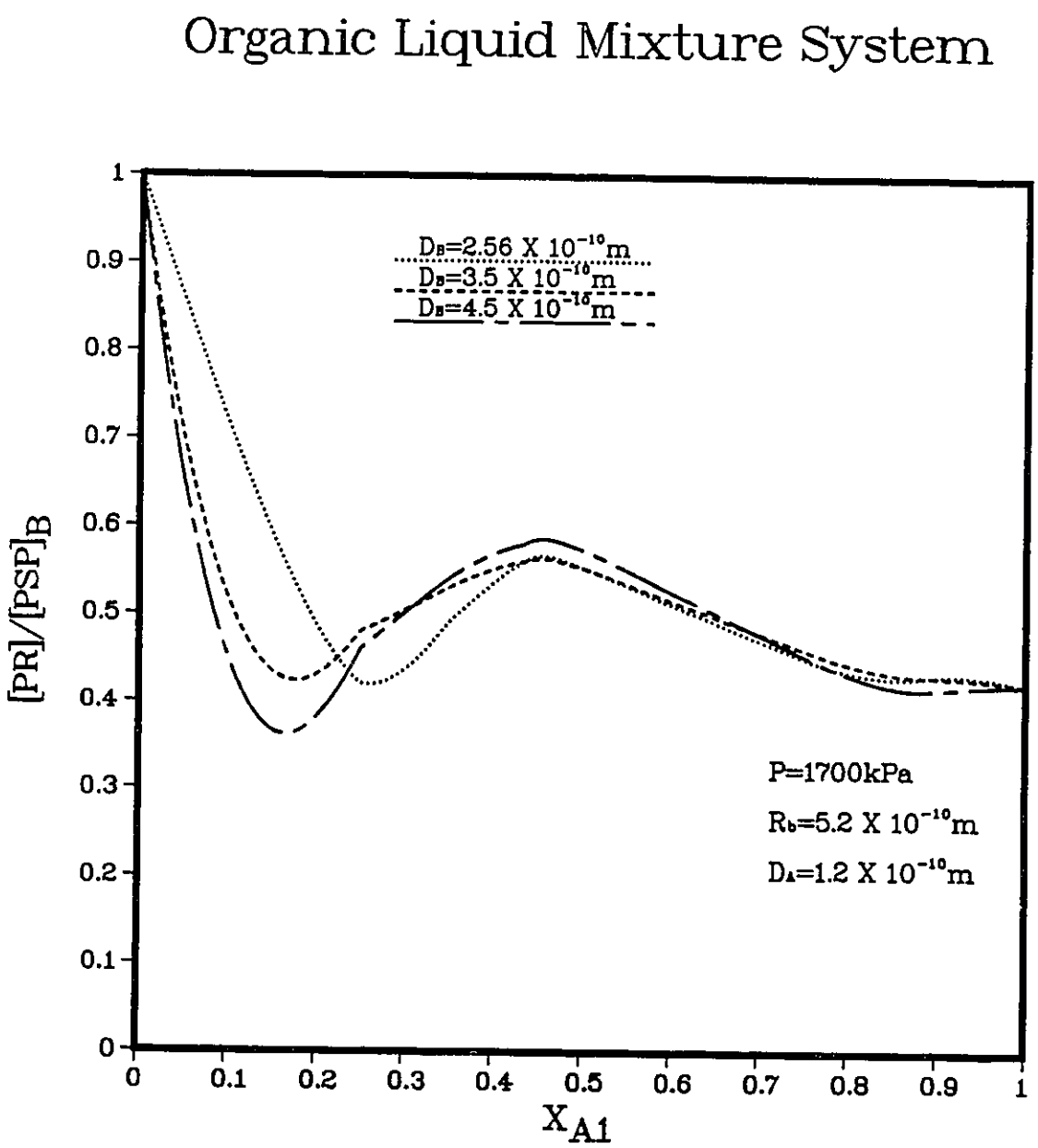


Figure 8 : Effect of Molecular Radius of Component B on $[PR]/[PSP]_B$ Ratio

# Organic Liquid Mixture System

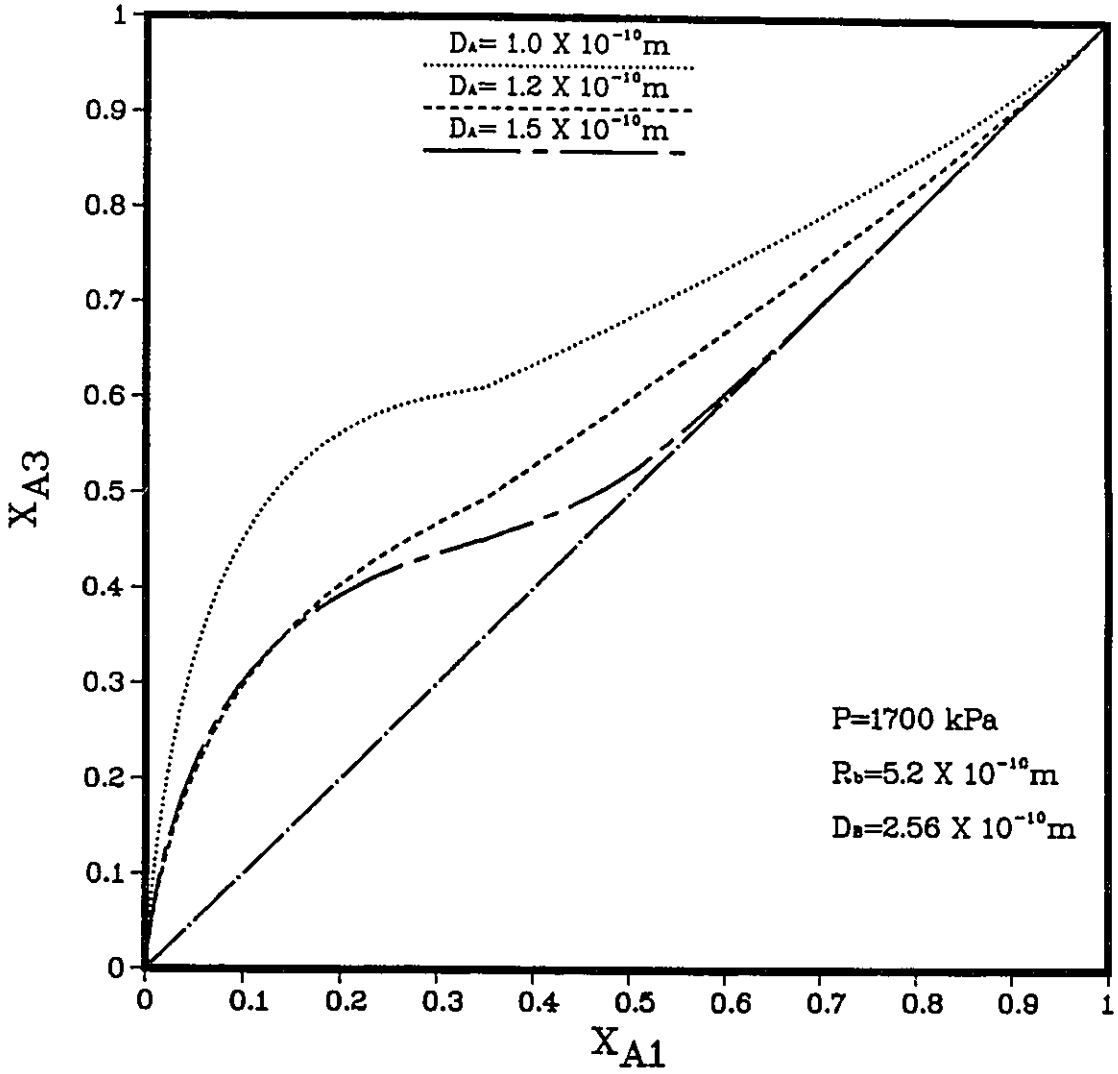


Figure 9 : Effect of Molecular Radius of Component A on Mole Fraction of Component A in the Permeate

# Organic Liquid Mixture System

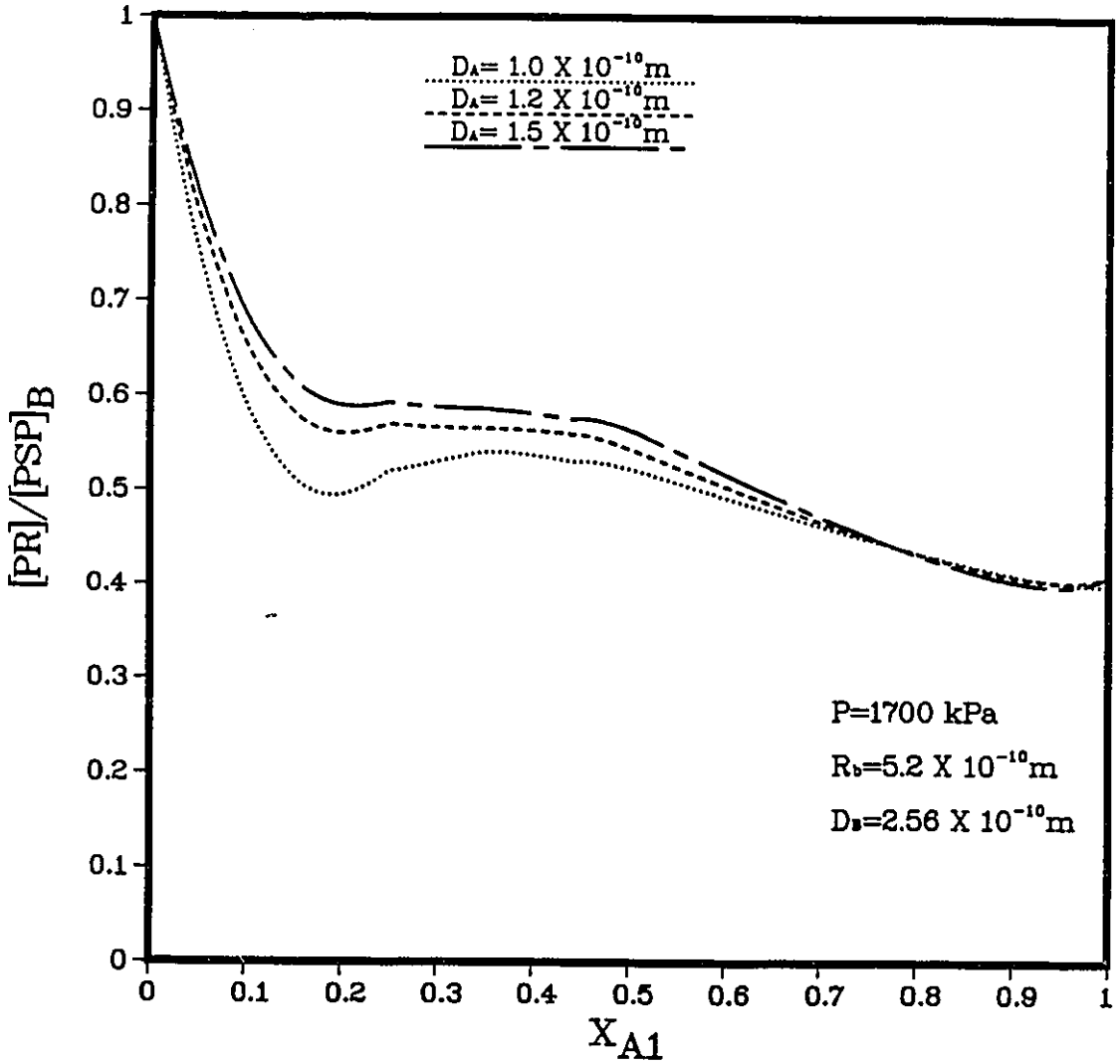


Figure 10: Effect of Molecular Radius of Component A on [PR]/[PSP]$_B$ Ratio

# Organic Liquid Mixture System

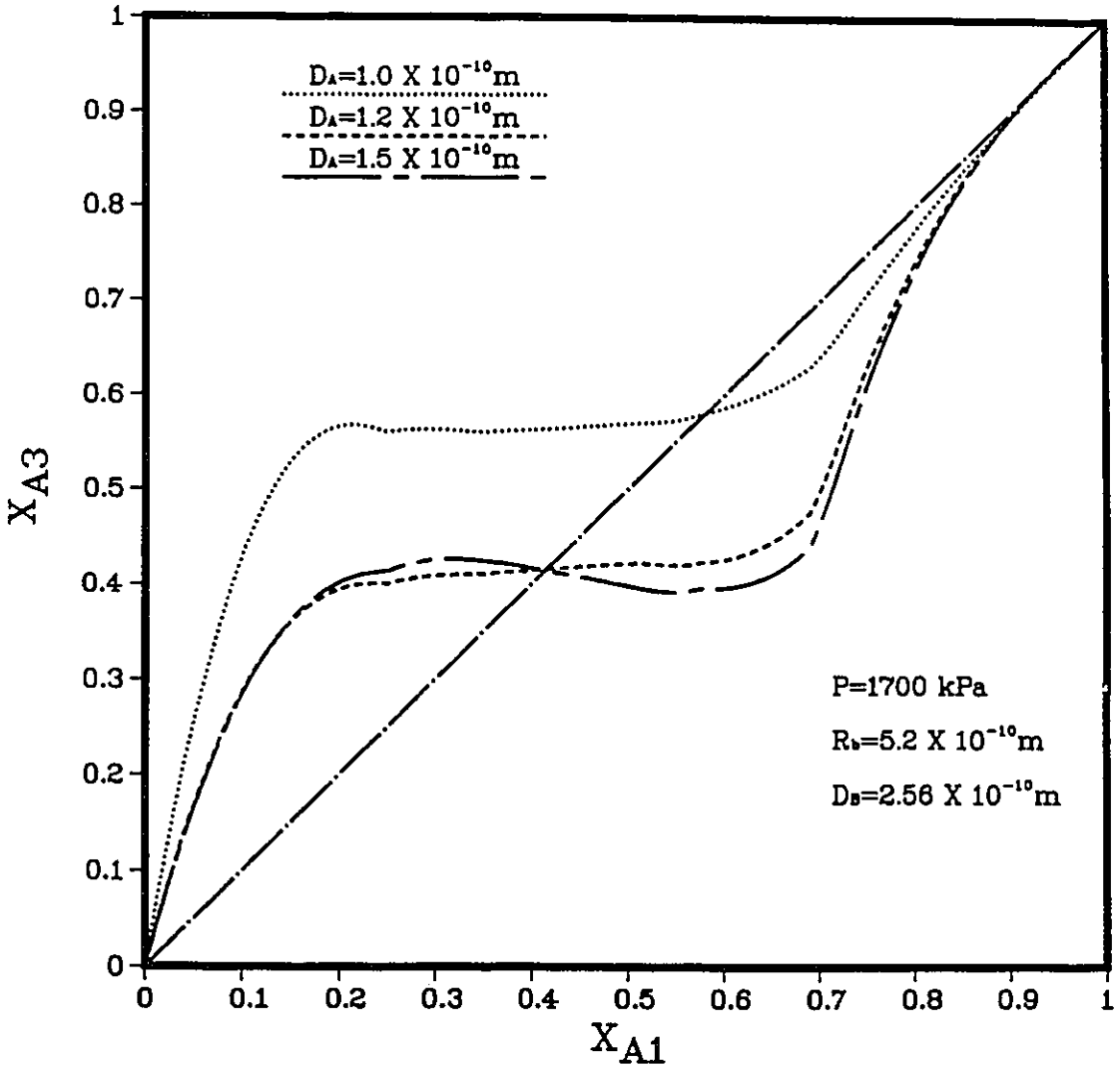


Figure 11 : Effect of Molecular Radius of Component A on Mole Fraction of Component A in the Permeate

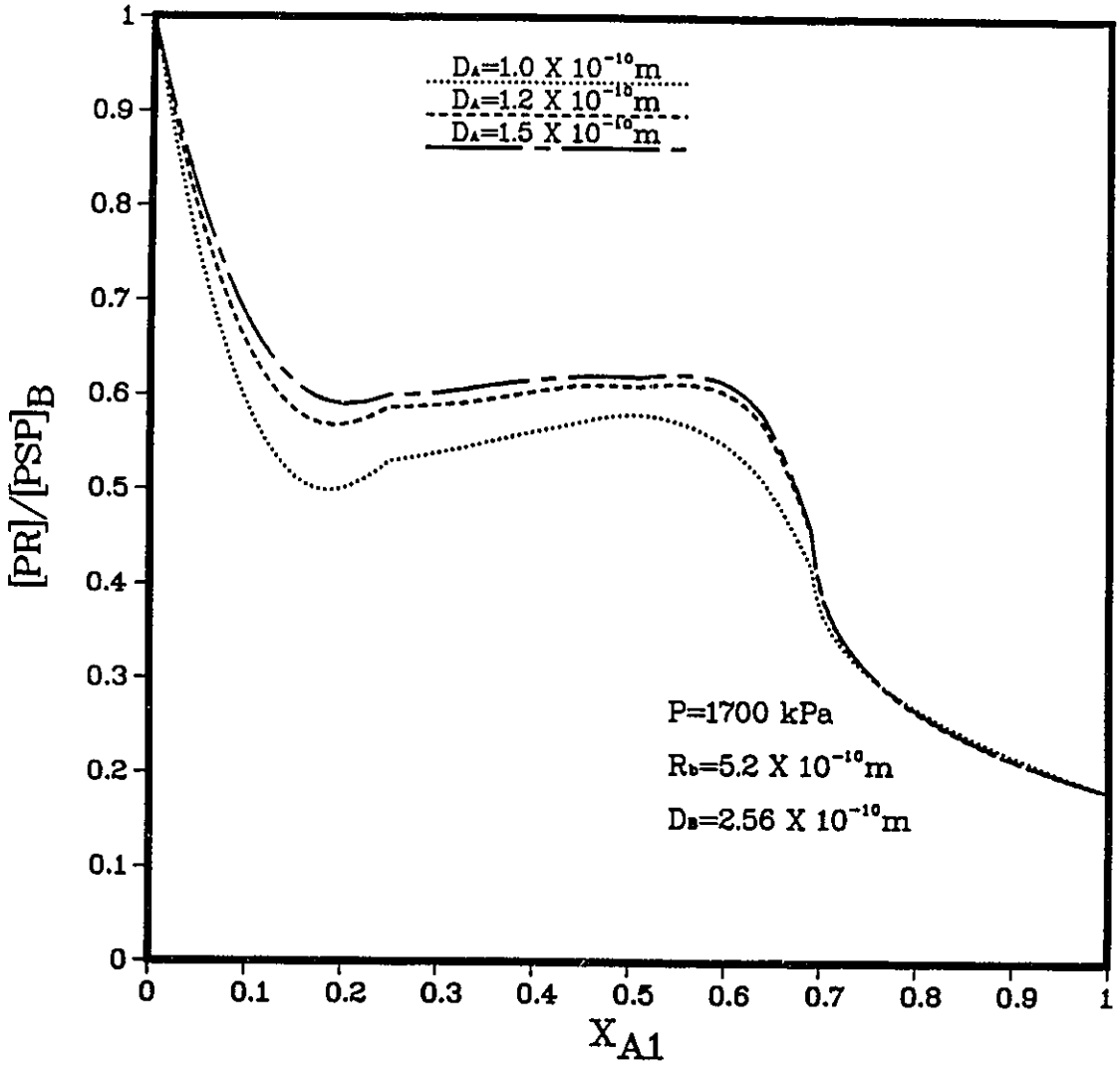


Figure 12: Effect of Molecular Radius of Component A on $[PR]/[PSP]_B$ Ratio

## 4.2 Effect of Pore Radius on the Membrane Performance

Figure 13 shows the effect of pore radius $R_b$ on the mole fraction of component A in the permeate.

The calculation was made under the conditions P = 1700 $kPa$, $D_A = 1.2 \times 10^{-10}$ m and $D_B = 2.56 \times 10^{-10}$ m. As for the interaction force parameter $B_A$ the values in Table 1 are used. Therefore, this calculation is truly applied to the separation of ethanol–n–heptane mixture by cellulose membranes. It is obvious that the preferential permeation of the component A becomes less as the pore radius increases. When $R_b = 16.2 \times 10^{-10}$ m, $X_{A3} = X_{A1}$, indicating such a large pore does not contribute to the separation of ethanol–n–heptane any longer.

The effect of pore radius on $[PR]/[PSP]_B$ is shown in Figure 14. The minimum value in the ratio appearing at $X_{A1} \approx 0.2$ tends to become lower as the preferential permeation of the component A is intensified by decreasing the pore radius on membrane surface.

# Organic Liquid Mixture System

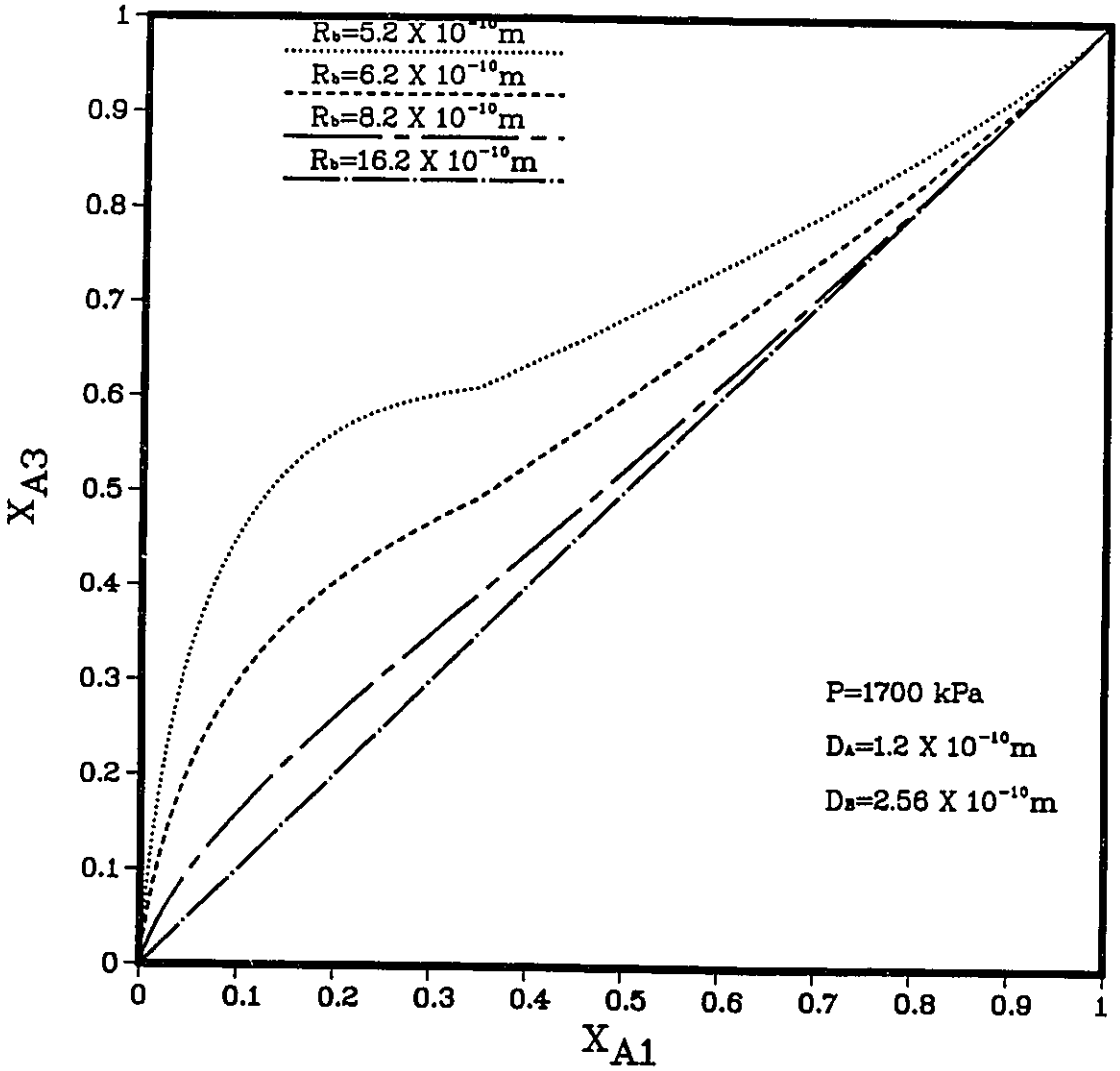


Figure 13 : Effect of Pore Radius on Mole Fraction of Component A in the Permeate

# Organic Liquid Mixture System

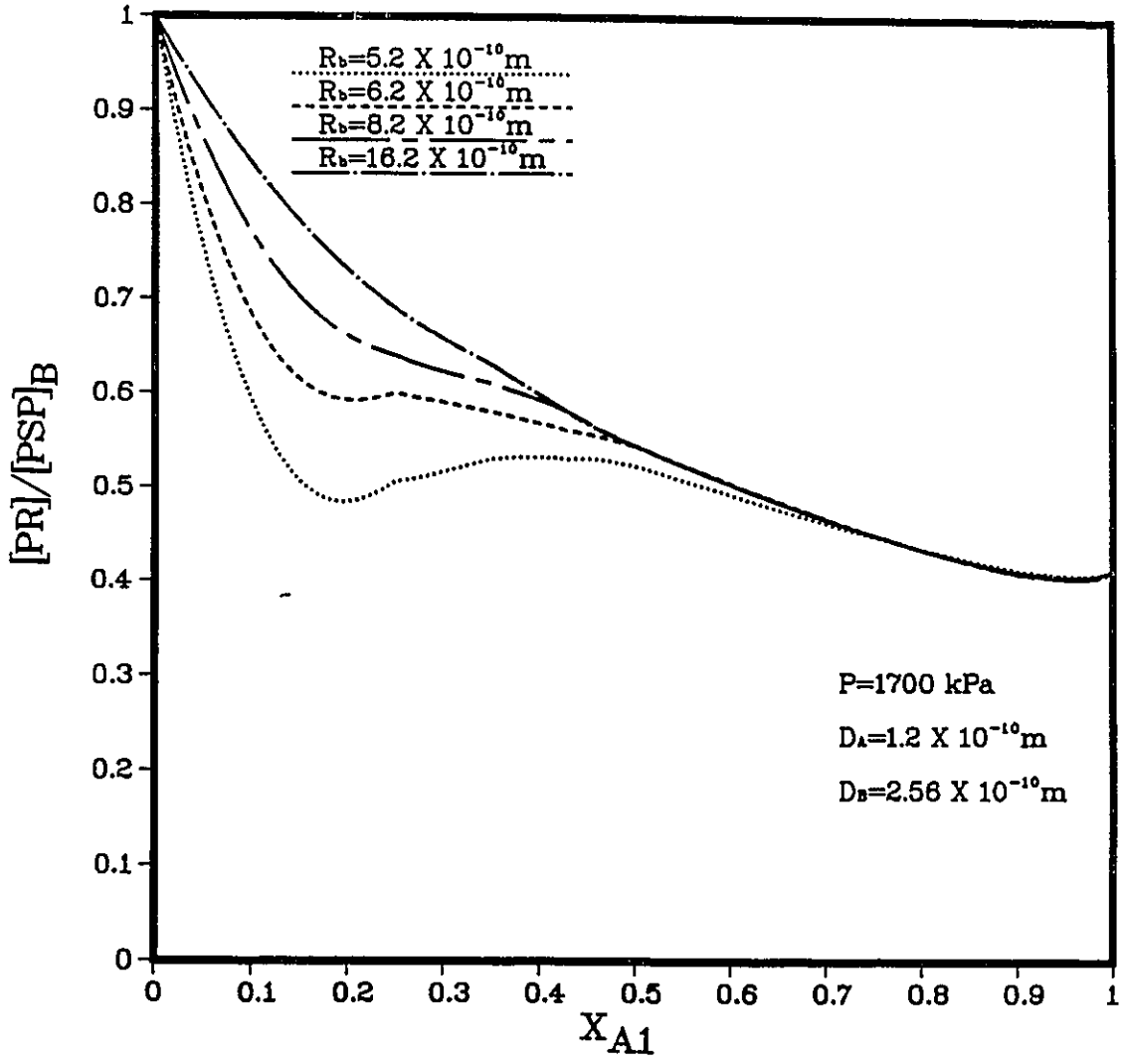


Figure 14: Effect of Pore Radius on $[PR]/[PSP]_B$ Ratio

## 4.3 Effect of Operating Pressure on the Membrane Performance

Figures 15 and 16 show the effect of operating pressure on mole fraction of component A in the permeate and on $[PR/PSP]_B$ ratio, respectively. The conditions for the calculation were: $D_A$=1.2 $\times$ $10^{-10}$ m, $D_B$=2.56 $\times$ $10^{-10}$ m, $R_b$=5.2 $\times$ $10^{-10}$ m and $B_A$ values in Table 1 are used. Therefore, this calculation applies again to ethanol–n–heptane cellulose system. Both figures show that there is practically no effect of operating pressure on $X_{A3}$ and $[PR]/[PSP]_B$ ratio.

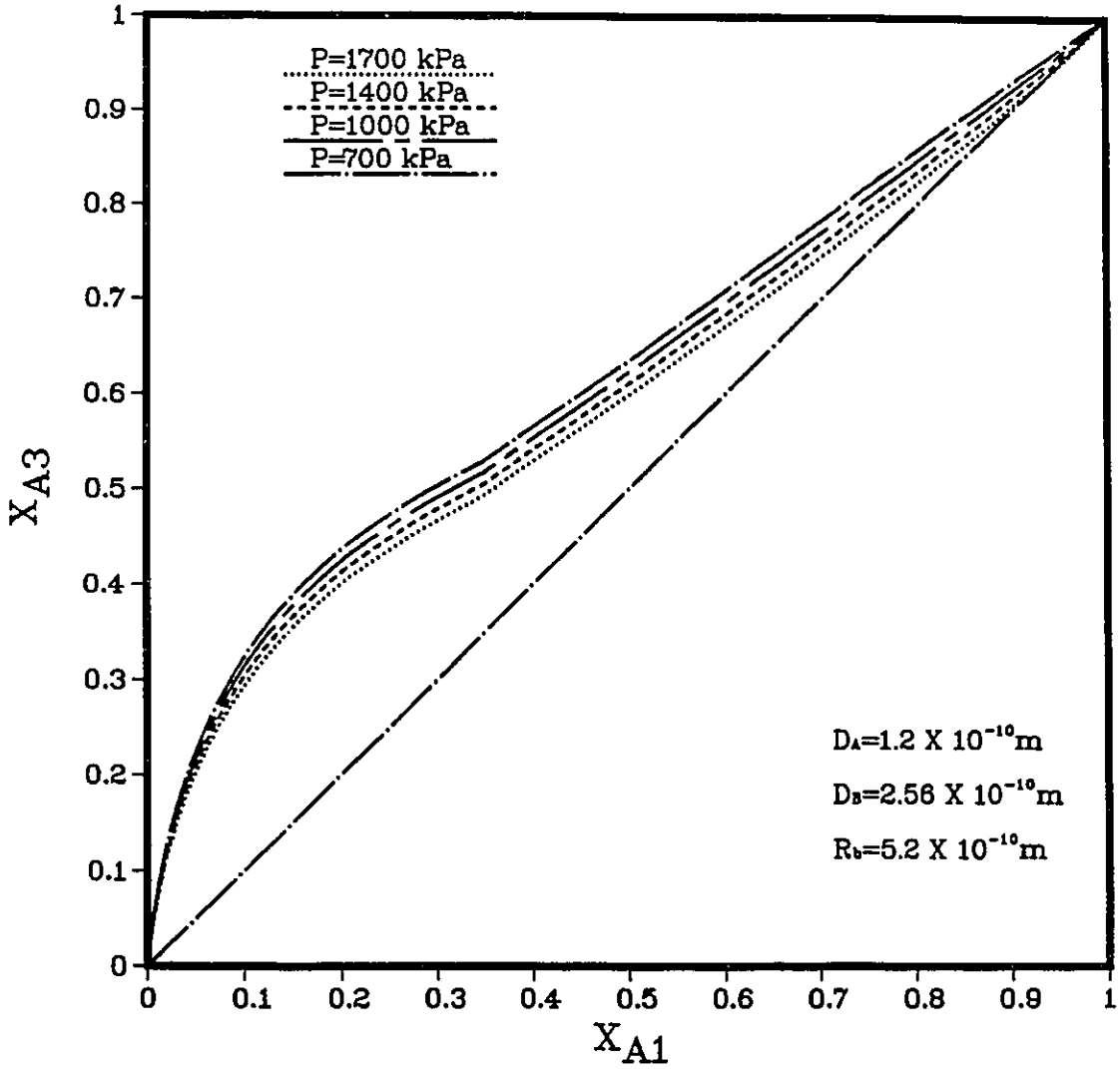


Figure 15: Effect of Operating Pressure on Mole Fraction Component A in the Permeate

# Organic Liquid Mixture System

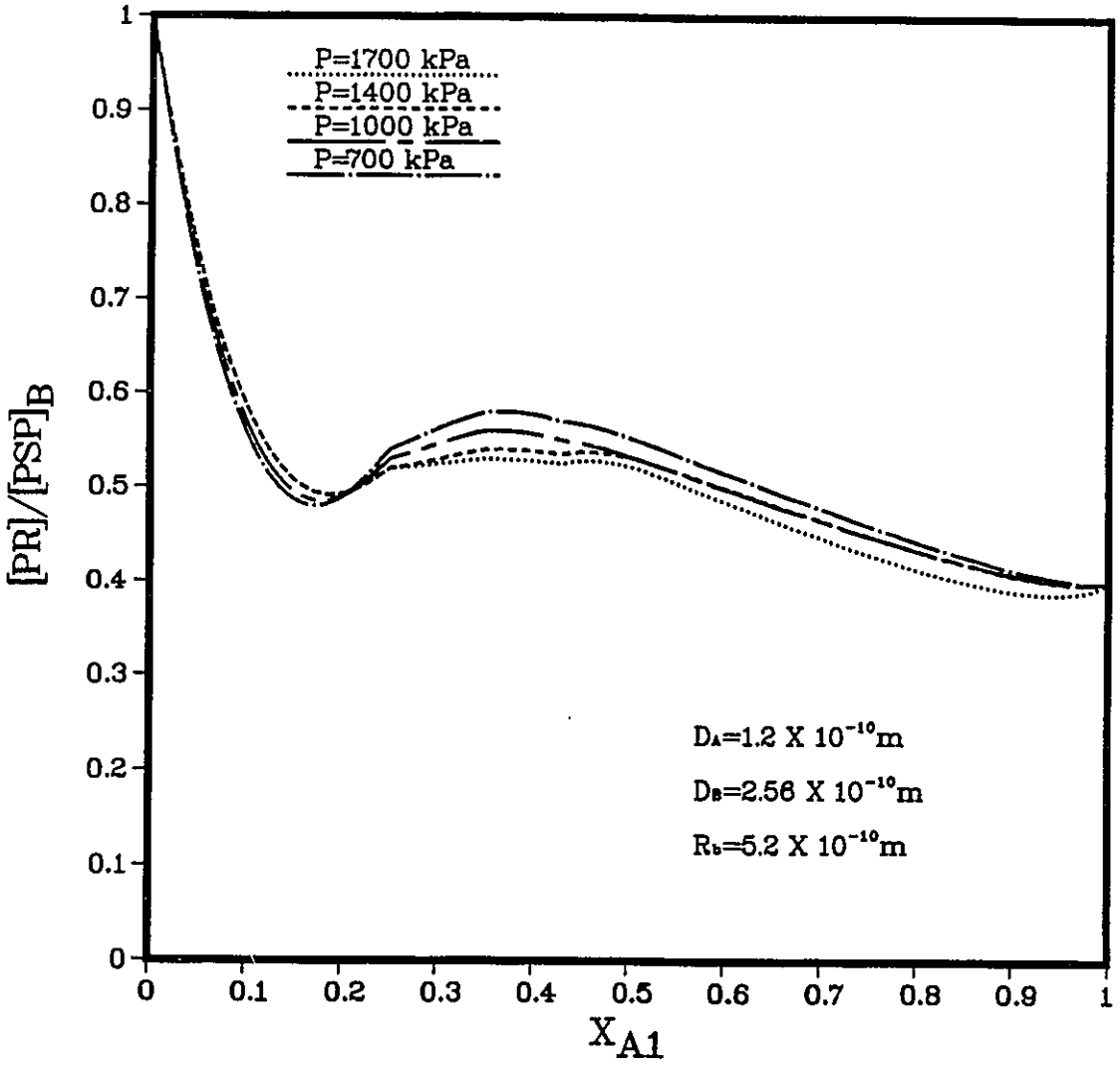


Figure 16: Effect of Operating Pressure on $[PR]/[PSP]_B$ RATIO

## 4.4 Effect of Interaction Force Constant on the Membrane performance

Figures 17–22 show the effect of interaction force constants on the membrane performance.

In Figure 17, the calculation is made under the conditions $D_A = 1.2 \times 10^{-10}$ m, $D_B = 2.56 \times 10^{-10}$ m, $R_b = 5.2 \times 10^{-10}$ m, $P = 1700kPa$ and three imaginary $B_A$ values are used for this calculations. Therefore, the calculation is truly applies to some imaginary systems. In Figure 17, $B_A = -3200 \times 10^{-30}m^3$, $200 \times 10^{-30}m^3$ and $400 \times 10^{-30}m^3$, are used. Note that $B_A$ value changes from $-3200 \times 10^{-30}m^3$ to $400 \times 10^{-30}m^3$, indicating that the interaction force between the component A and the membrane polymer material changes from strong repulsive interfacial force to strong attractive interfacial force. Figure 17 shows that the shapes of the mole fraction curves for different $B_A$ have a great change. When $B_A = 400 \times 10^{-30}m^3$, $X_{A3}$ increases drastically up to 0.99 in the initial increase of $X_{A1}$ and changes only little when $X_{A1} > 0.25$. From Figure 17, it can be seen that $X_{A3}$ values are farther away from the diagonal line when $B_A$ value becomes larger, which means the separation of the organic liquid mixture is very effective when the interaction force between the component A and the membrane polymer material becomes stronger.

Figure 18 shows the effect of interaction force constant on $[PR]/[PSP]_B$ at same conditions as in Figure 17. $[PR]/[PSP]_B$ curves for different $B_A$ values have different shapes. It should be noted that the ratio decreases twice, in the lower ($X_{A1} \approx 0.15$) and the higher ($X_{A1} \approx 0.60$) feed mole fraction value. The change from $B_A = -3200 \times 10^{-30}m^3$ to $B_A = 200 \times 10^{-30}m^3$ has more significant effect on the above ratio than the change in $B_A$ from $200 \times 10^{-30}m^3$ to $400 \times 10^{-30}m^3$.

Figure 19 shows the results of the calculation in which the conditions are almost the same as Figure 17. Three imaginary $B_A$ values are used for this calculation, which are $B_A = -3200 \times 10^{-30} m^3$, $-200 \times 10^{-30} m^3$ and $-400 \times 10^{-30} m^3$. Note that all $B_A$ values in Figure 19 are negative, indicating that the interaction force between the component A and the membrane polymer material is rejective in the entire range of feed mole fraction. The curves for different $B_A$ values have a very similar pattern, which cross the diagonal. As shown in Figure 19, $X_{A3} > X_{A1}$ in the range of lower $X_{A1}$; then $X_{A3} = X_{A1}$; $X_{A3} < X_{A1}$ in the range of higher $X_{A1}$. The effect of interaction force constants on $[PR]/[PSP]_B$ is shown in Figure 20. The results in Figure 20 show that the above ratio curves for different $B_A$ values have a general tendency. The minimum in the $[PR]/[PSP]_B$ ratio for different $B_A$ is almost same. It should also be noted that the ratio decreases twice.

In Figure 21 , a further computer simulation is made for the case $D_A = D_B = 1.2 \times 10^{-10}$ m, indicating that the molecular radius of both component A and component B are identical. Three different values of interfacial interaction force constants, i.e. $B_A = 50 \times 10^{-30}$ $m^3$, 0, - $50 \times 10^{-30}$ $m^3$, are chosen. The above $B_A$ values corresponding to a strong attraction, no interaction, and a strong repulsion between the membrane material. As illustrated in Figure 21, for the case of a strong attraction, $X_{A3}$ is always greater than $X_{A1}$ , the separation is very effective. For the case of no interaction, $X_{A3}$ is always equal to $X_{A1}$, that is, no separation happens in this situation; For the case of a strong repulsion, $X_{A3}$ is always less than $X_{A1}$, that also means that the separation is very effective.

A significant effect of interaction force constant on $[PR]/[PSP]_B$ ratio is observed in Figure 22. The ratio curve for $B_A = 0$ and that for $B_A = -50 \times 10^{-30}$ $m^3$ have a very similar pattern, which is that $[PR]/[PSP]_B$ ratio decreases with an increase of $X_{A1}$ for both $B_A$ values. However, when $B_A = 50 \times 10^{-30}$ $m^3$, $[PR]/[PSP]_B$

ratio exhibits a complicated pattern, which is that the ratio decreases twice with an increases in $X_{A1}$.

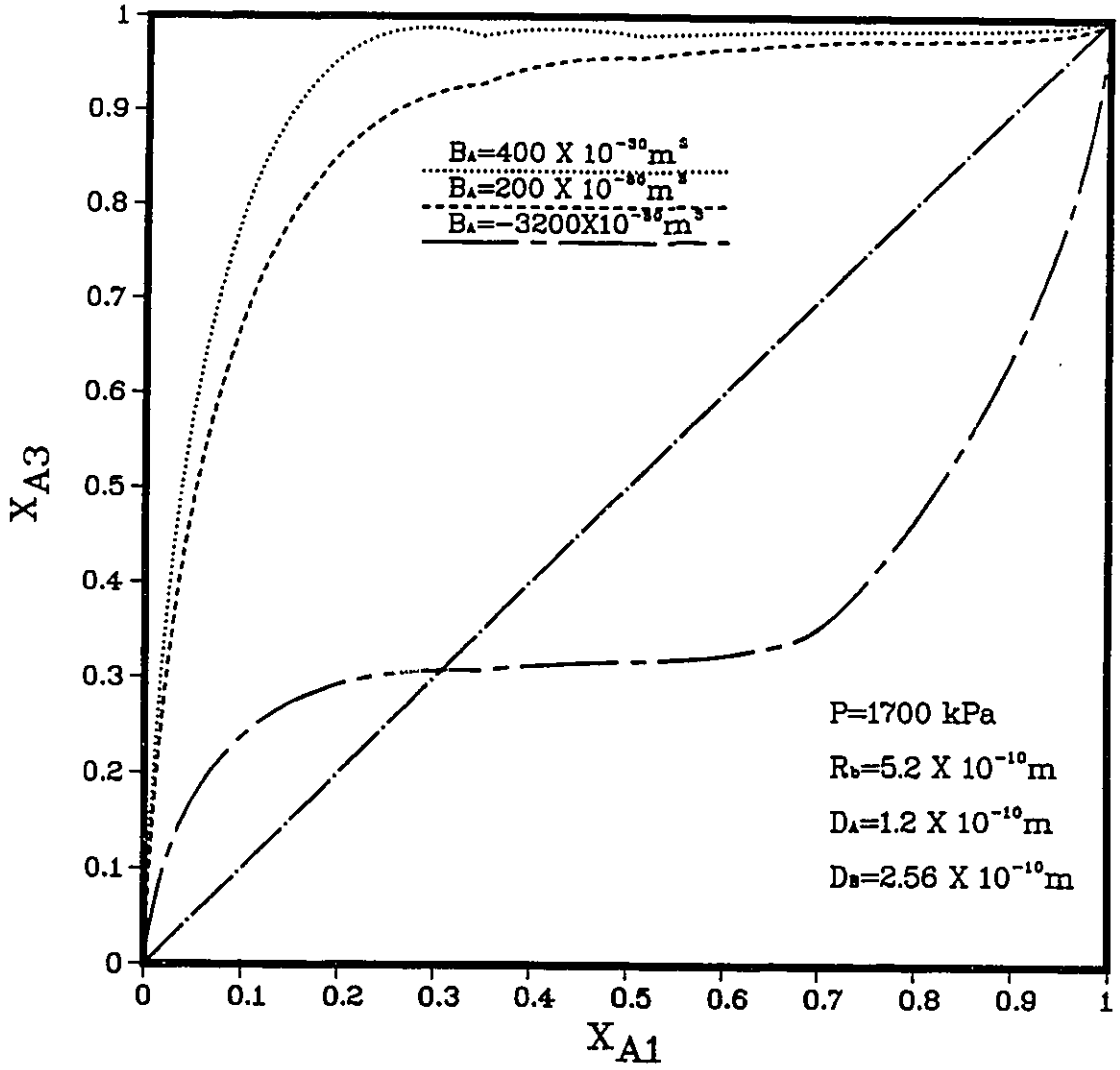


Figure 17: Effect of Interaction Force Constant on Mole Fraction of Component A in the permeate

# Organic Liquid Mixture System

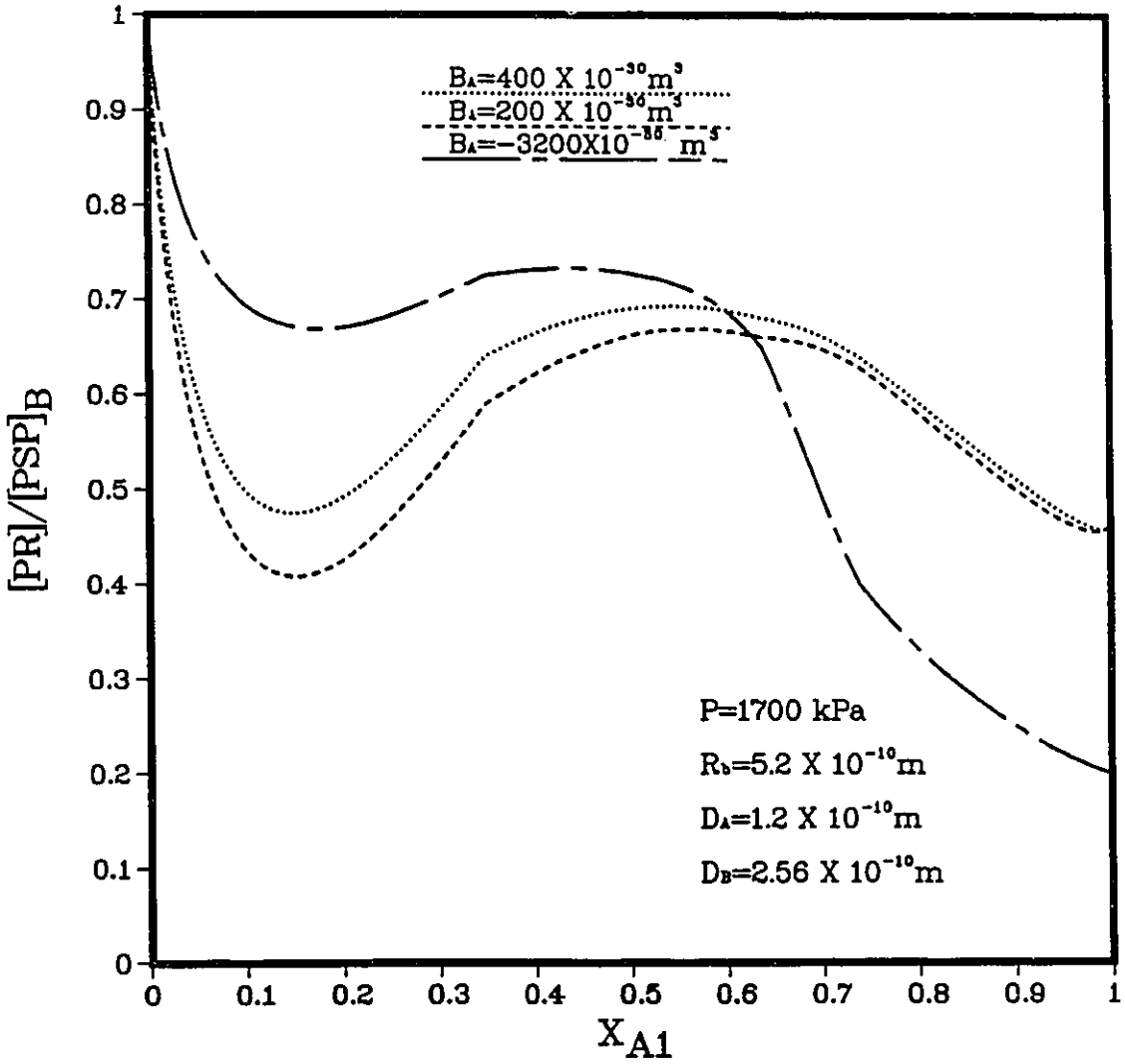


Figure 18 : Effect of Interaction Force Constant on $[PR]/[PSP]_B$

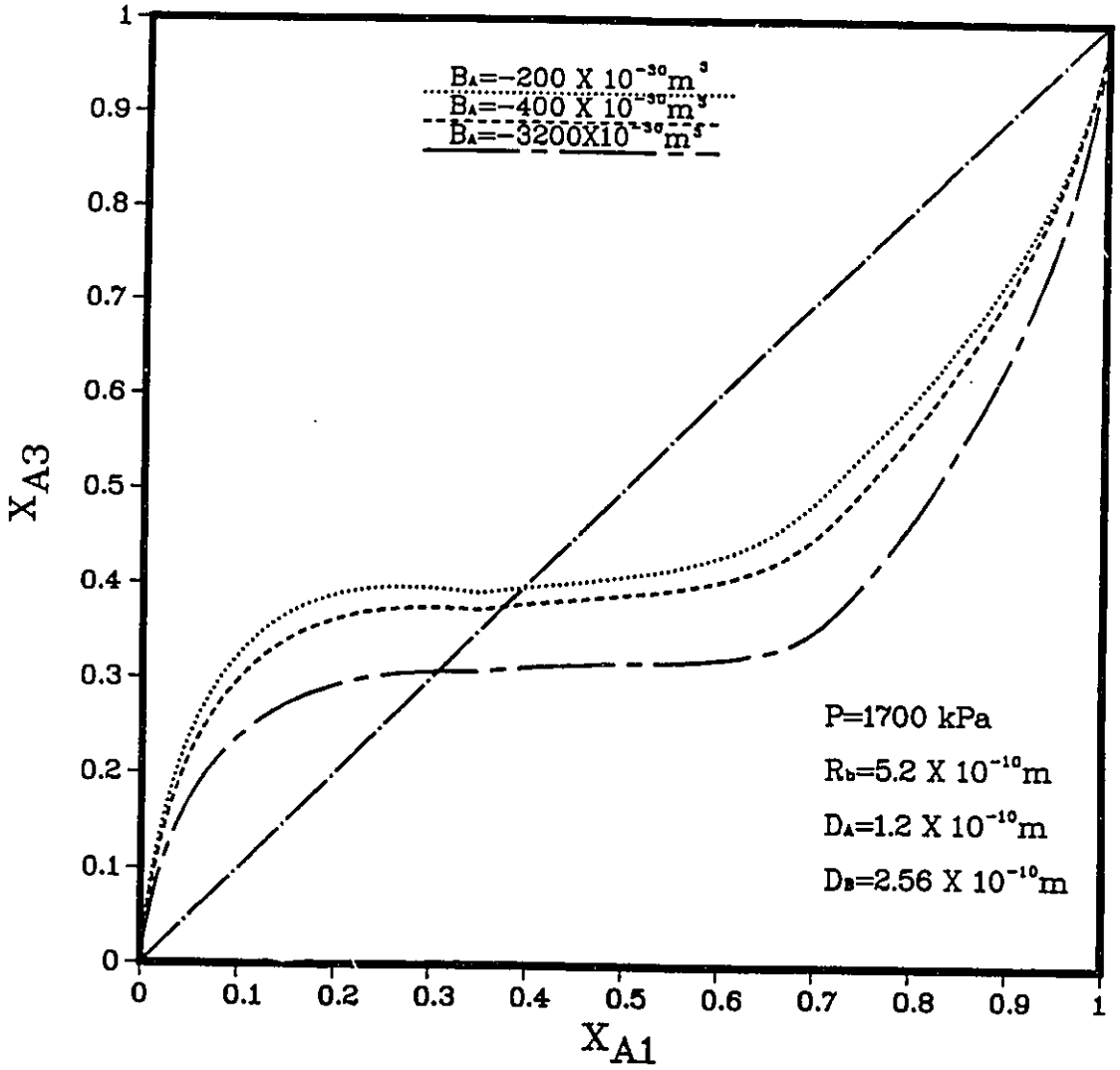


Figure 19 : Effect of Interaction Force Constant on Mole Fraction of Component A in the Permeate

# Organic Liquid Mixture System

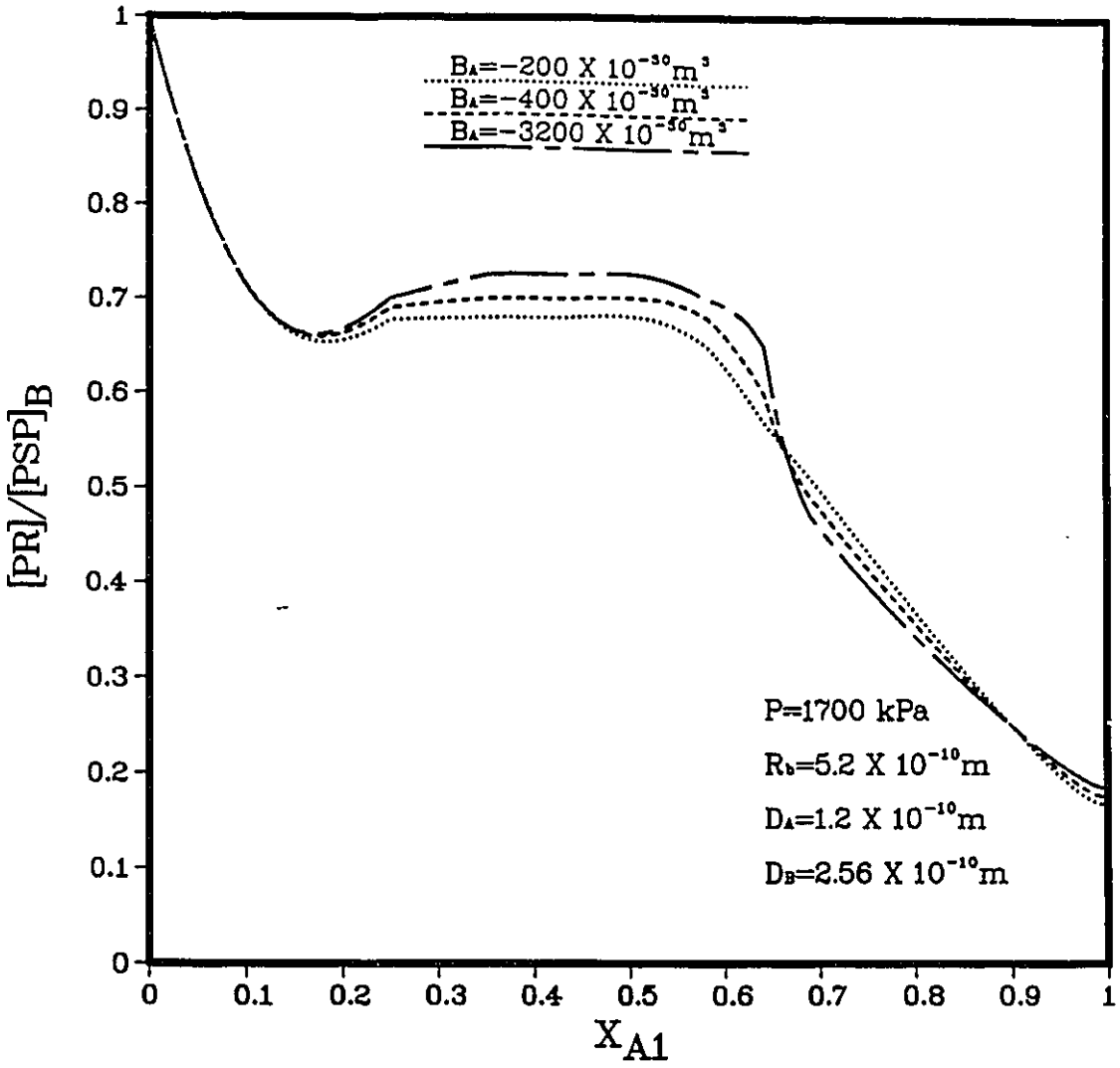


FIGURE 20 : Effect of Interaction Force Constant on $[PR]/[PSP]_B$ Ratio

# Organic Liquid Mixture System

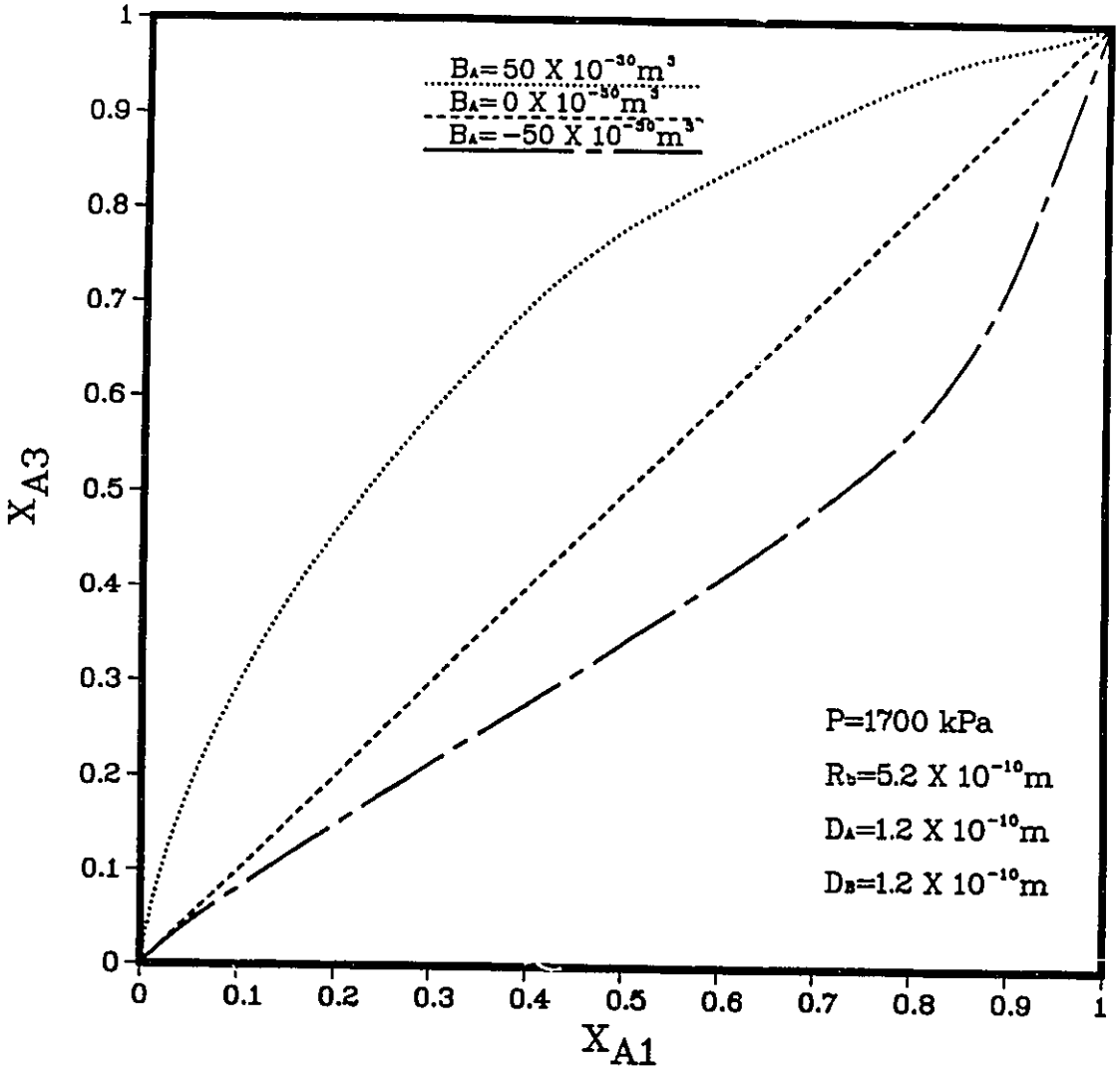


Figure 21 : Effect of Interaction Force Constant on Mole Fraction of Component A in the Permeate

# Organic Liquid Mixture System

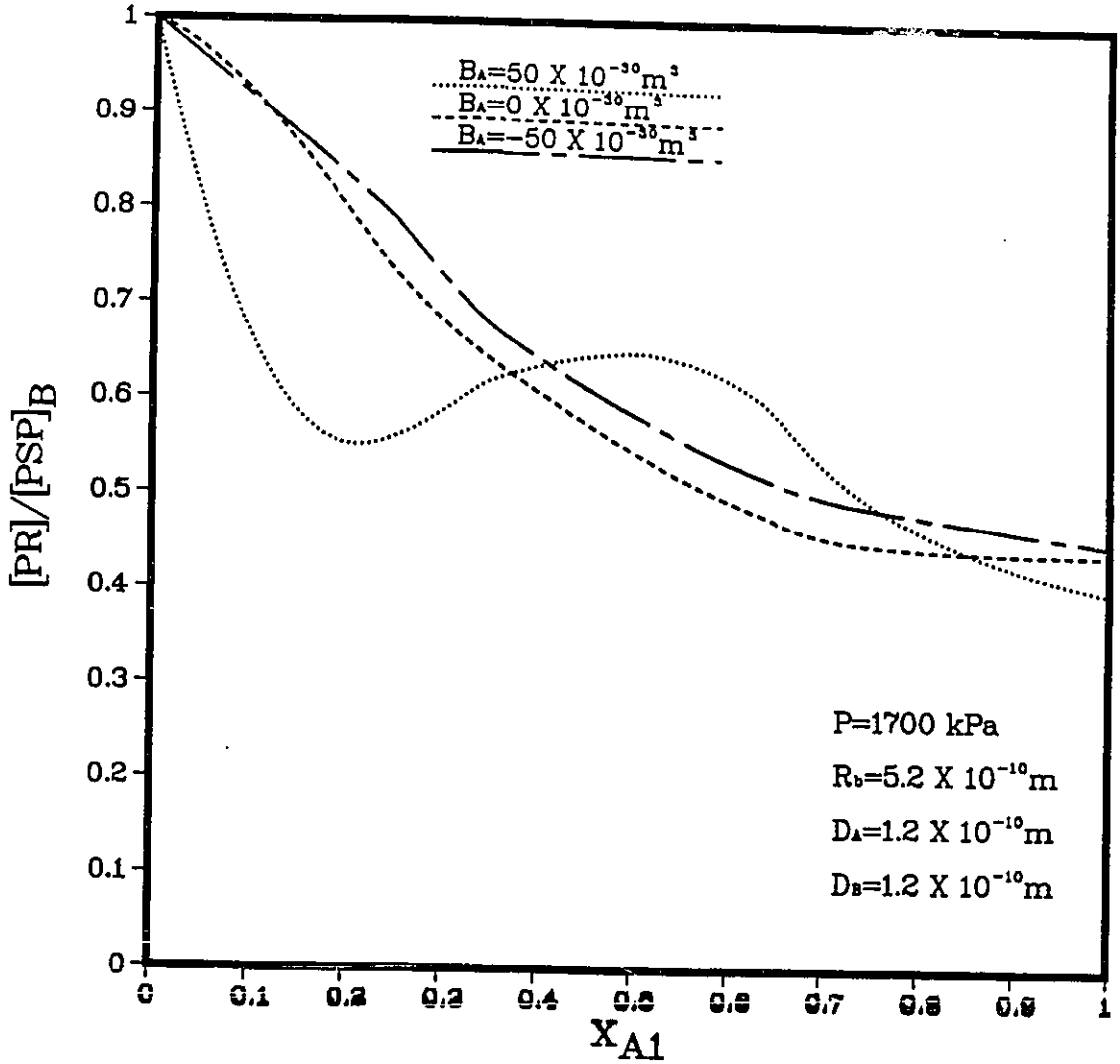


Figure 22 : Effect of Interaction Force Constant on $[PR]/[PSP]_B$

## 4.5 Analysis of Data on Membrane Fractionation of Organic Liquid Mixtures

As stated above, the membrane performance is governed by pore radius on the membrane surface. The satisfactory membrane performance can be obtained by using the membrane with appropriate pore radius on the membrane surface. In order to determine the pore radius on the membrane surface, analysis of a series of experimental data has been carried out by using computer model developed above.

In this analysis, a series of reverse osmosis experimental data for the ethanol–heptane system with cellulose RO membrane [17] at the conditions, where P = 6900 kPag, t =25$^0$C, $D_A$= 1.2×10$^{-10}$ m and $D_B$= 2.56×10$^{-10}$ m, are used to compare with calculation data at the same conditions as the experimental conditions. The results of comparison are shown in Figures 23–28. In the Figures, four curves are different types of theoretical curves with four different uniform pore radius and the points in the figures represent experimental results. It can be seen that the experimental results vary between the theoretical curve with a pore radius of $5.2 \times 10^{-10}$ m and the theoretical curve with a pore radius of $6.2 \times 10^{-10}$ m. Therefore, cellulose membranes have similar pore radius distributions ranging from $5.2 \times 10^{-10}$ m to $6.2 \times 10^{-10}$ m.

The agreement between calculated data and experimental data is shown in Figures 29–34 which demonstrates the validity of the transport equations for the organic liquid mixtures. From Figures 29–34, it can be seen that the experimemtal data is a little lower than calculated data in most cases, which indicates the sub-structure of cellulose membrane affects [PR]/[PSP]$_B$ ratio in membrane separation processes.

The analysis of RO data on the basis of the transport equations arising from the surface force-pore flow model yields quantitative information on the average pore radius and pore radius distribution on the surface of the available RO membranes. The above method of obtaining such information opens new direction and offers new possibilities in RO membrane research and development, particularly through the establishment of precise cause–effect relationships governing the ultimate pore radius and pore radius distribution on the surface of resulting membranes in the membrane making process, and also through the establishment of appropriate quality control techniques for the production of membranes with the desired surface pore structure.

# Organic Liquid Mixture System

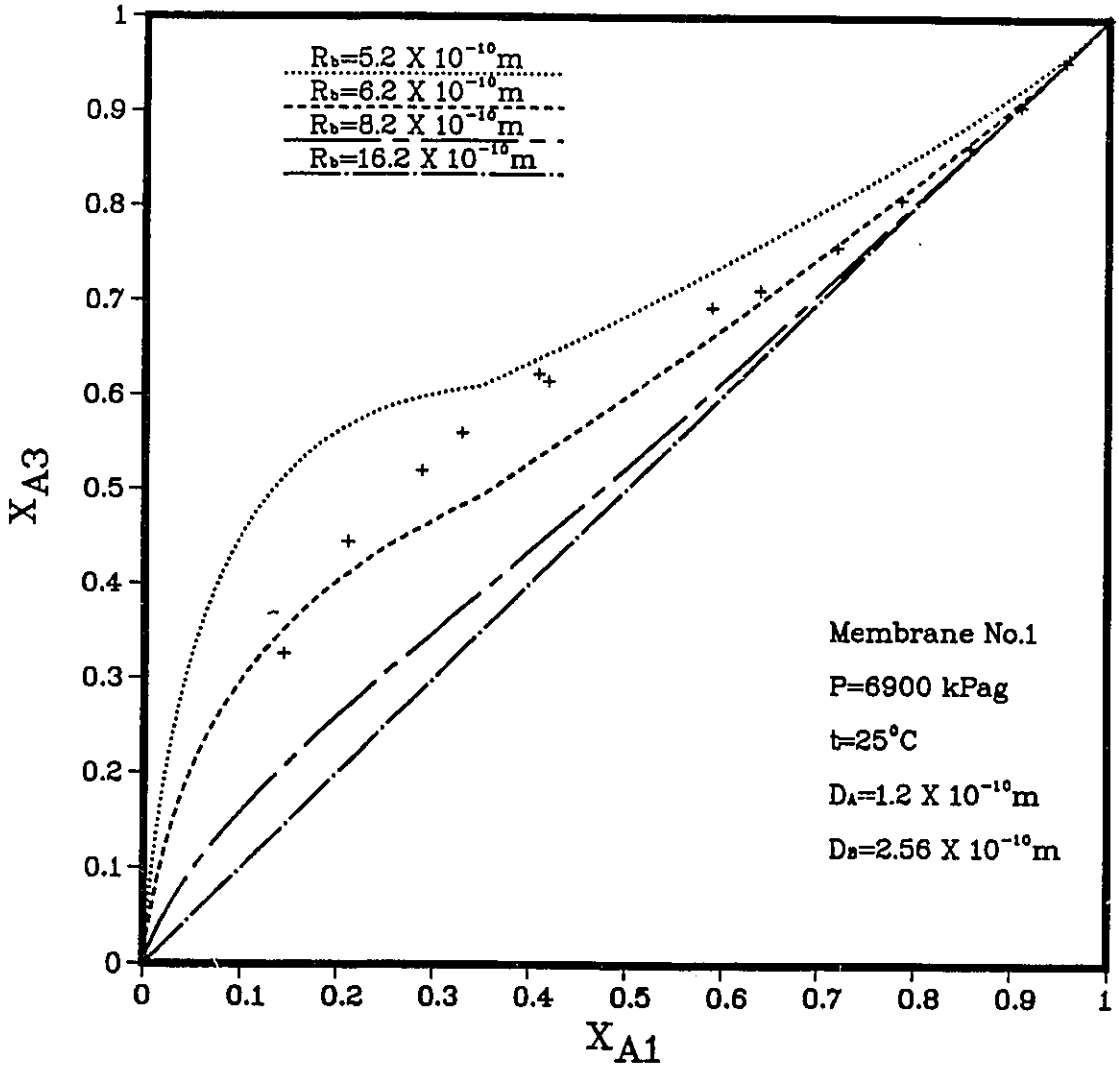


Figure 23: Comparison of Experimental Data with Calculated Data for the Ethanol–Heptane System

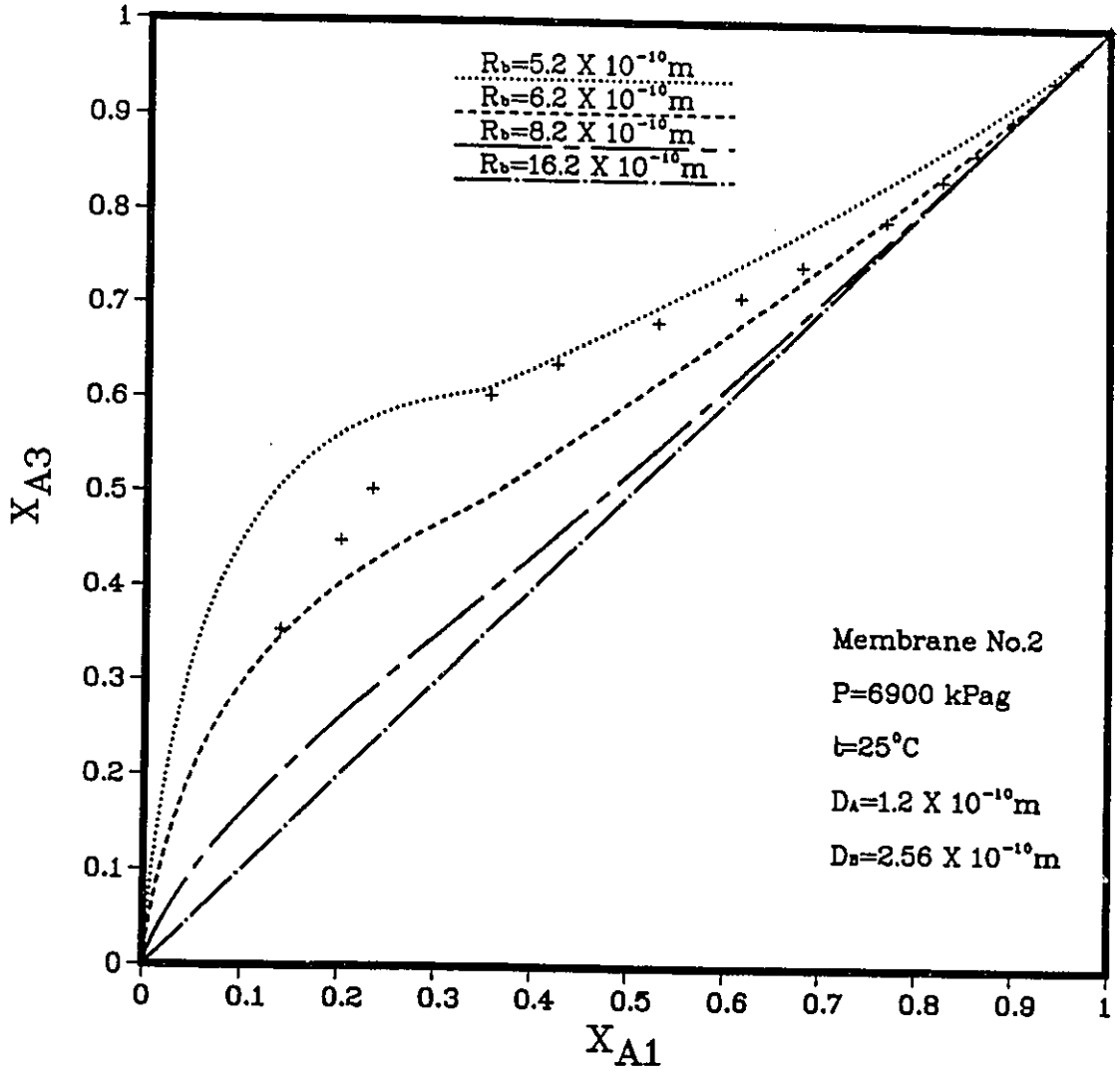


Figure 24: Comparison of Experimental Data with Calculated Data for the Ethanol–Heptane System

# Organic Liquid Mixture System

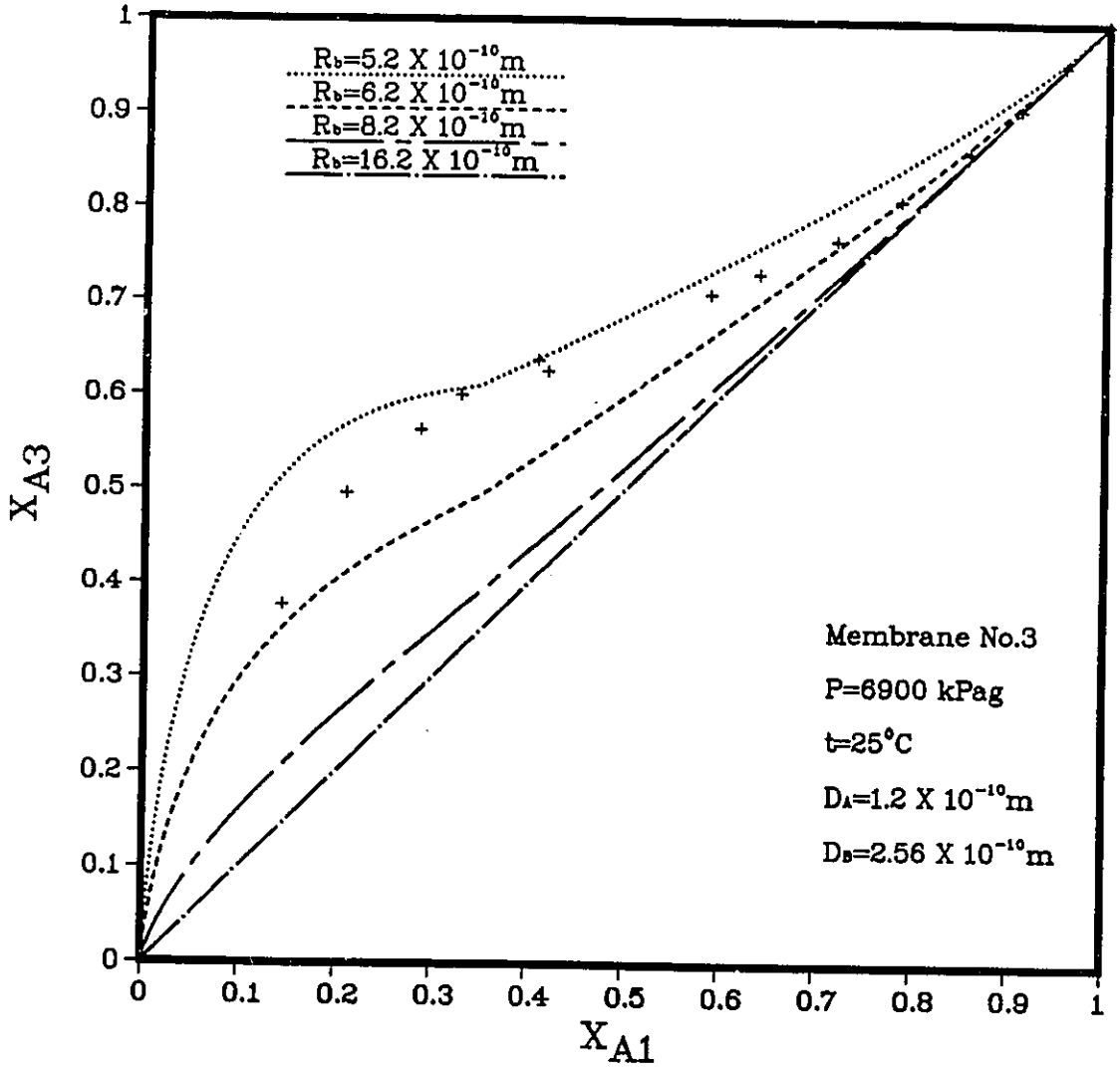


Figure 25: Comparison of Experimental Data with Calculated Data for the Ethanol–Heptane System

# Organic Liquid Mixture System

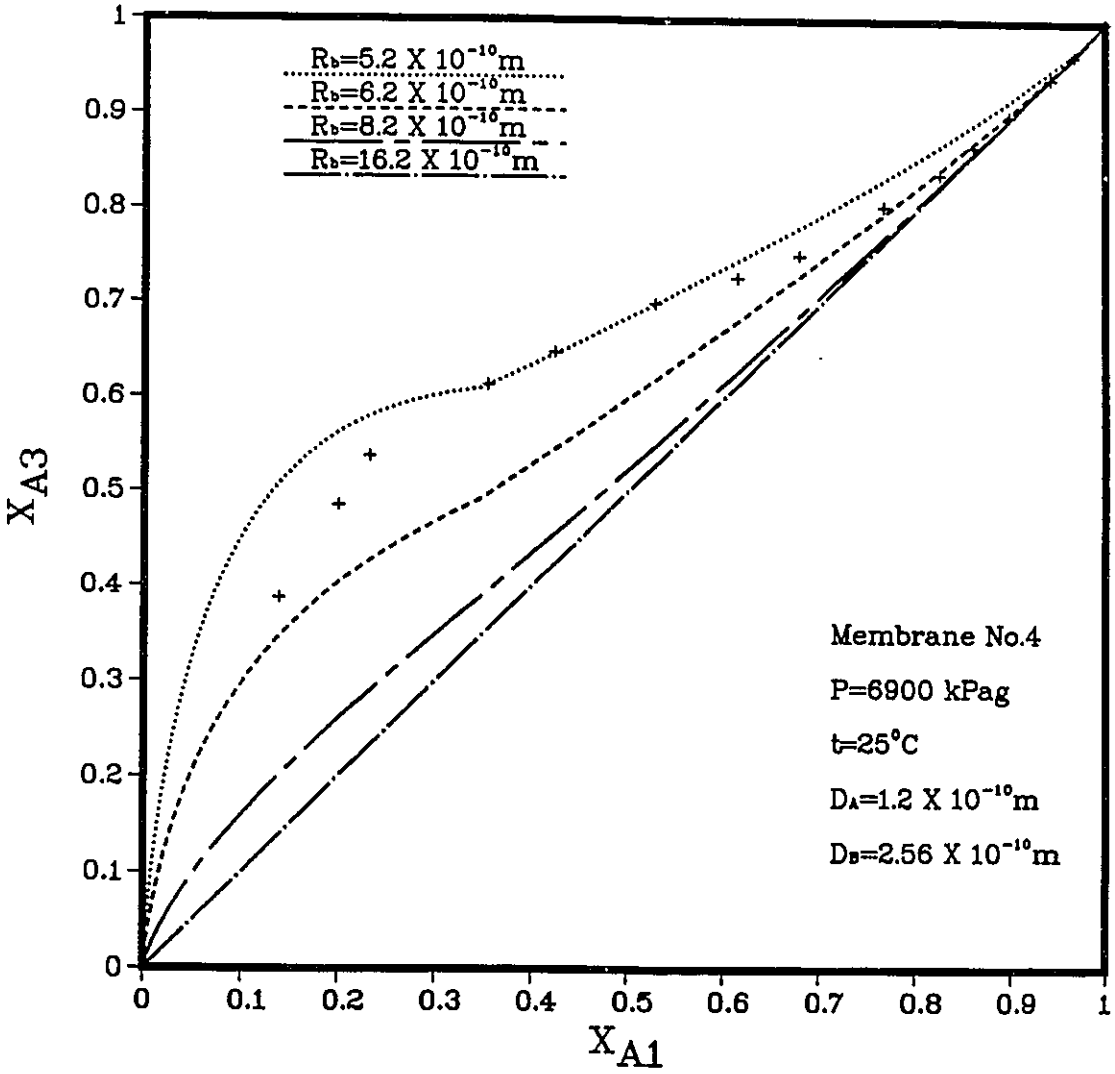


Figure 26: Comparison of Experimental Data with Calculated Data for the Ethanol–Heptane System

# Organic Liquid Mixture System

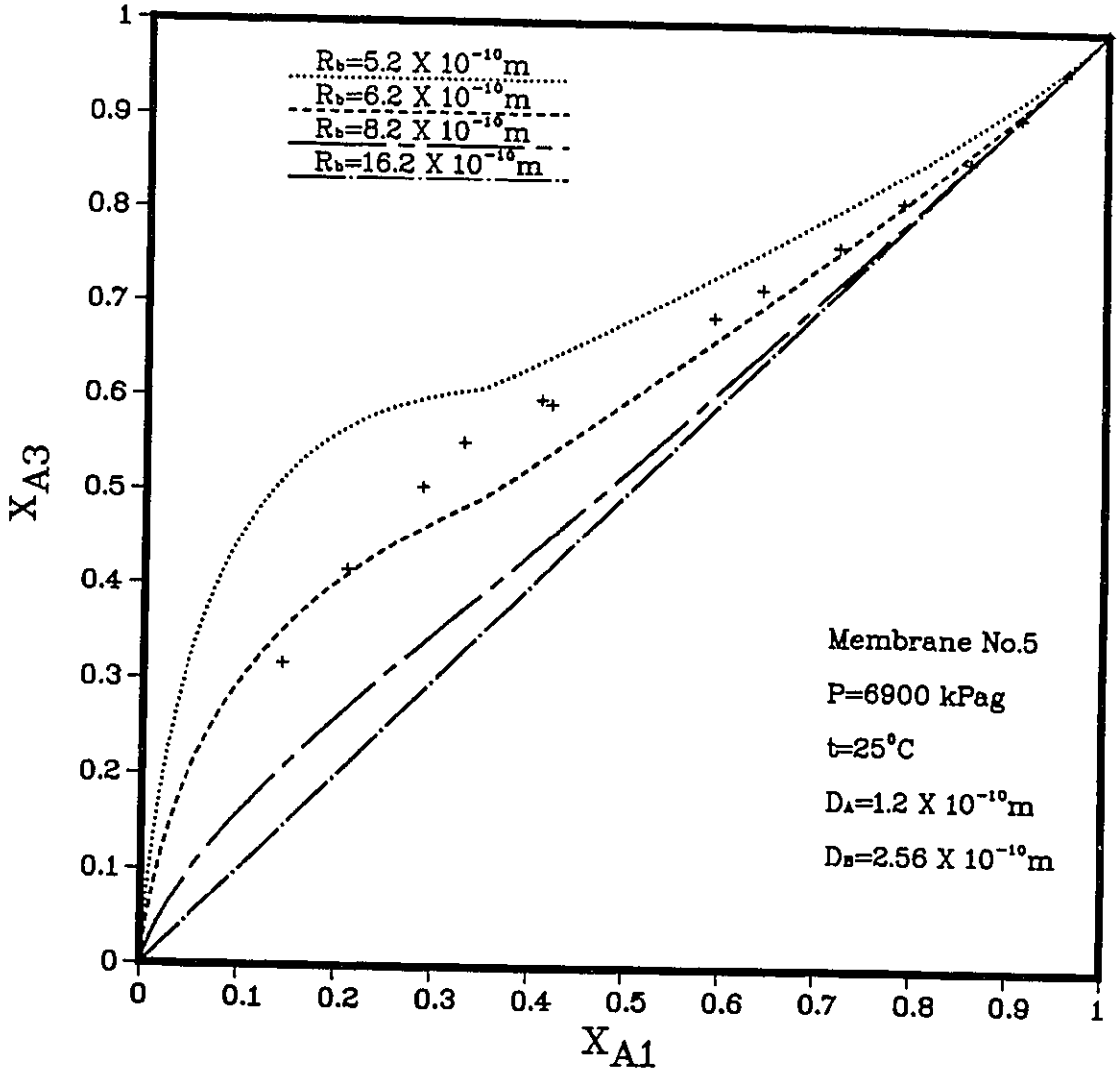


Figure 27: Comparison of Experimemtal Data with Calculated Data for the Ethanol–Heptane System

# Organic Liquid Mixture System

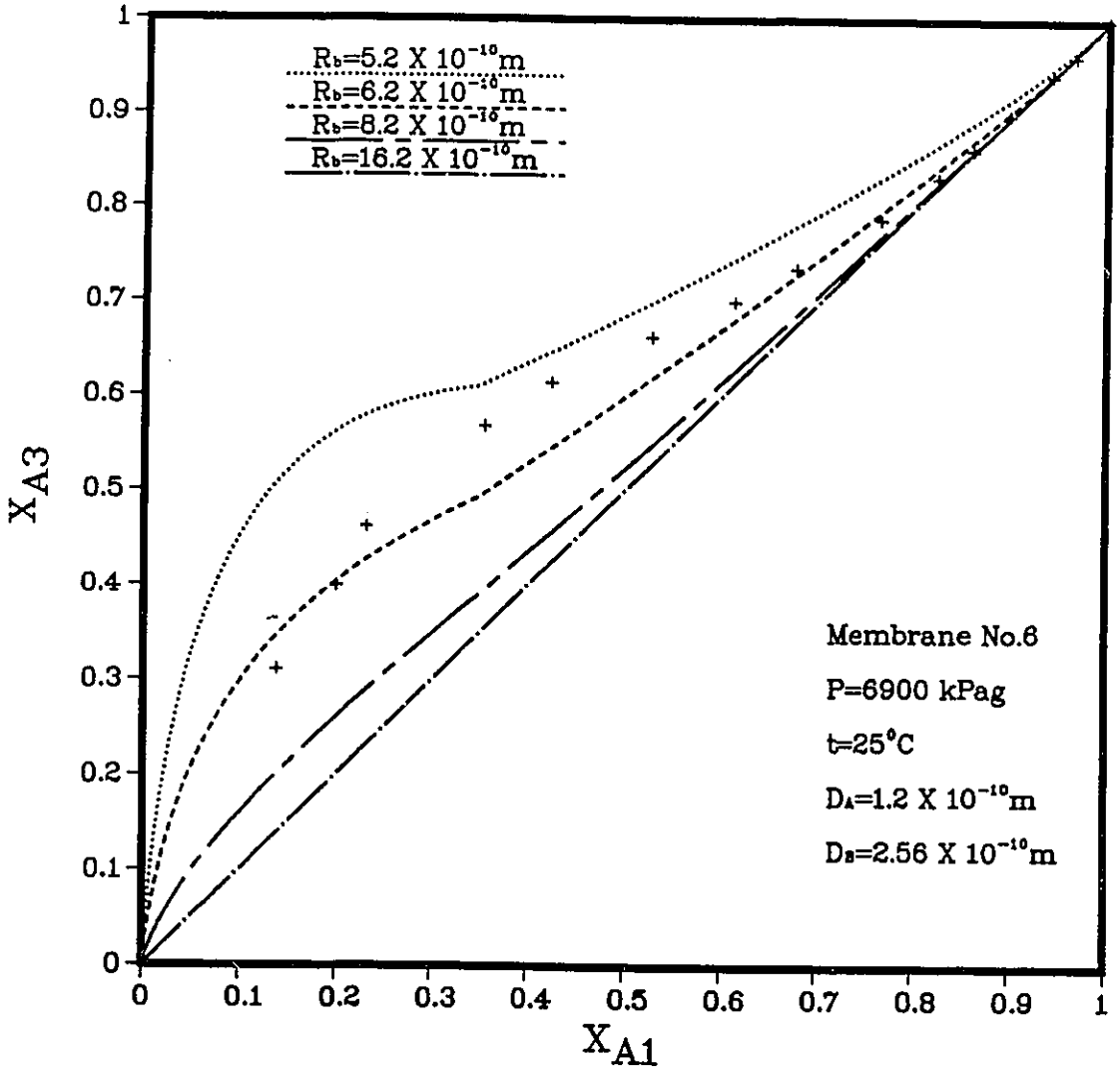


Figure 28 : Comparison of Experimental Data with Calculated Data for the Ethanol–Heptane System

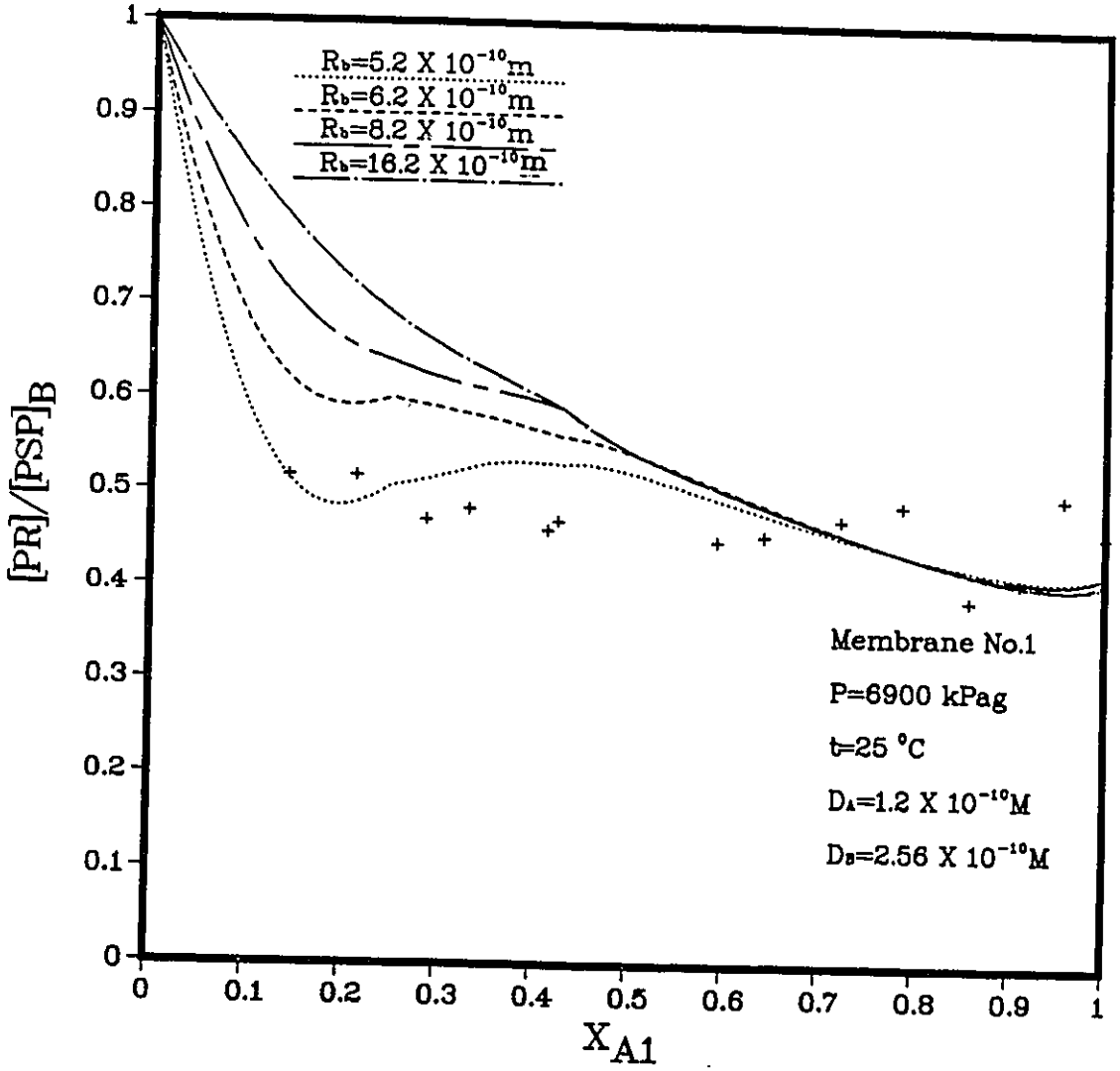


Figure 29: Comparison of Experimental Data with Calculated Data for the Ethanol–Heptane System

# Organic Liquid Mixture System

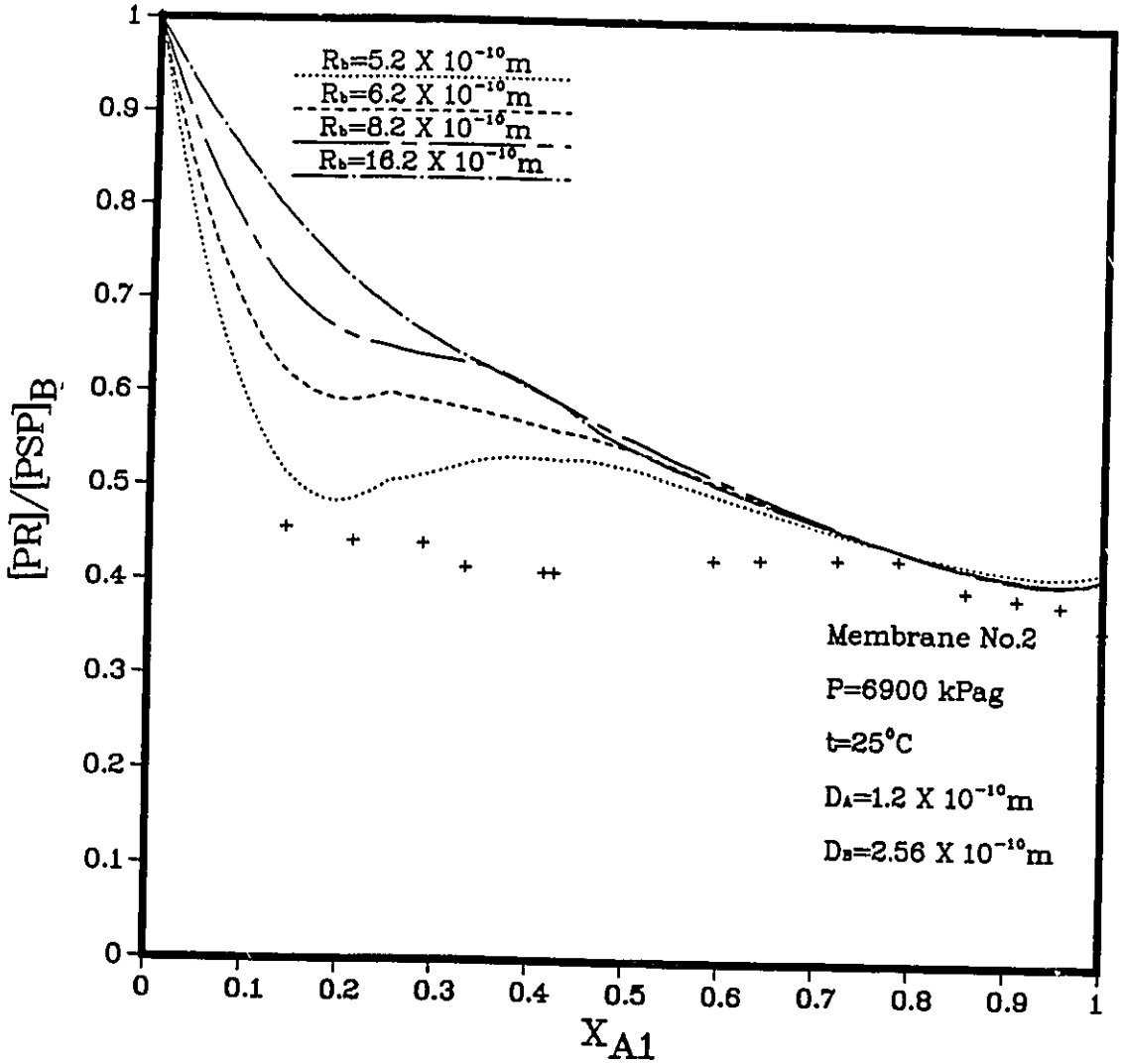


Figure 30 : Comparison of Experimental Data with Calculated Data for the Ethanol–Heptane System

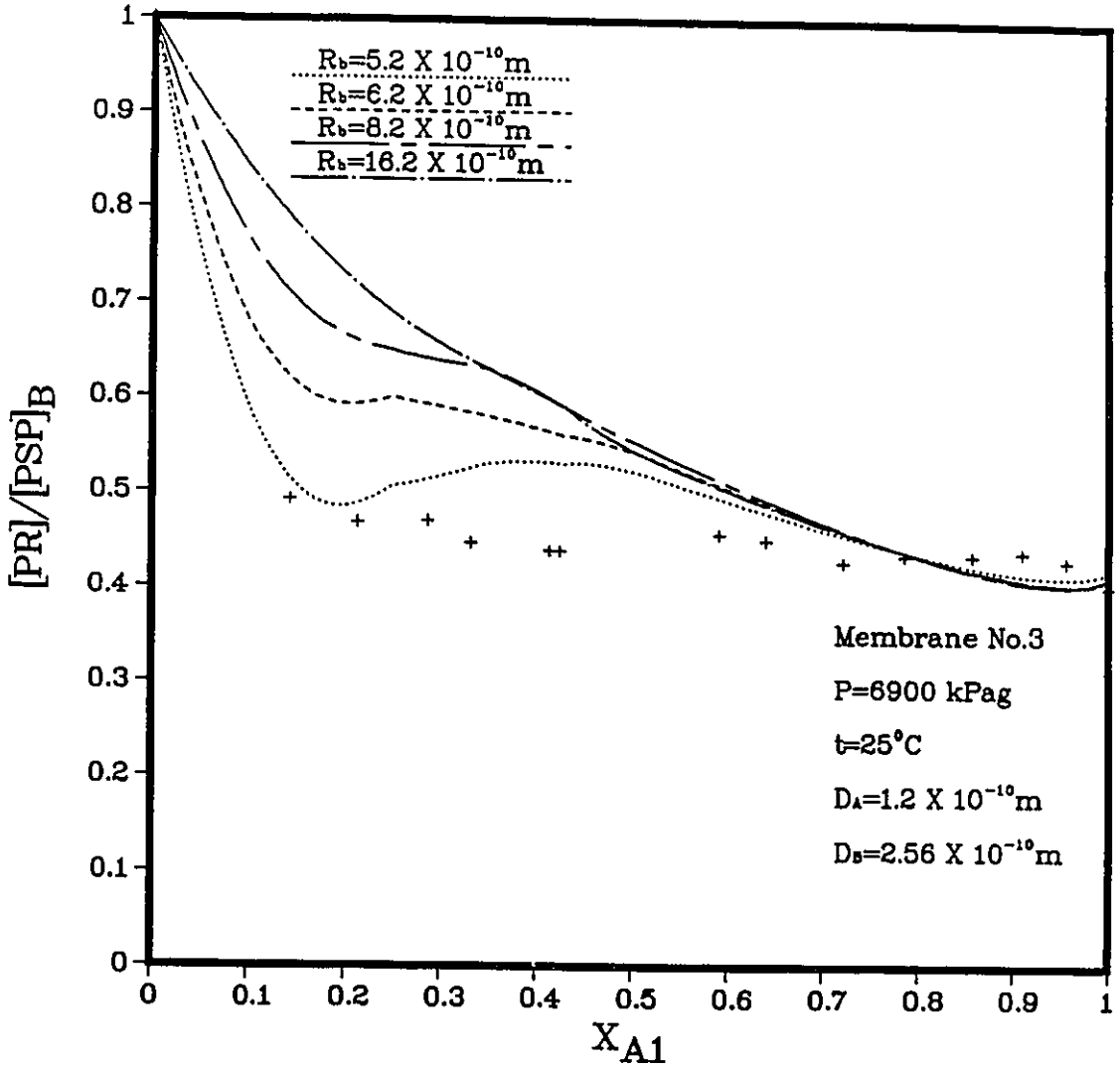


Figure 31: Comparison of Experimental Data with Calculated Data for the Ethanol–Heptane System

# Organic Liquid Mixture System

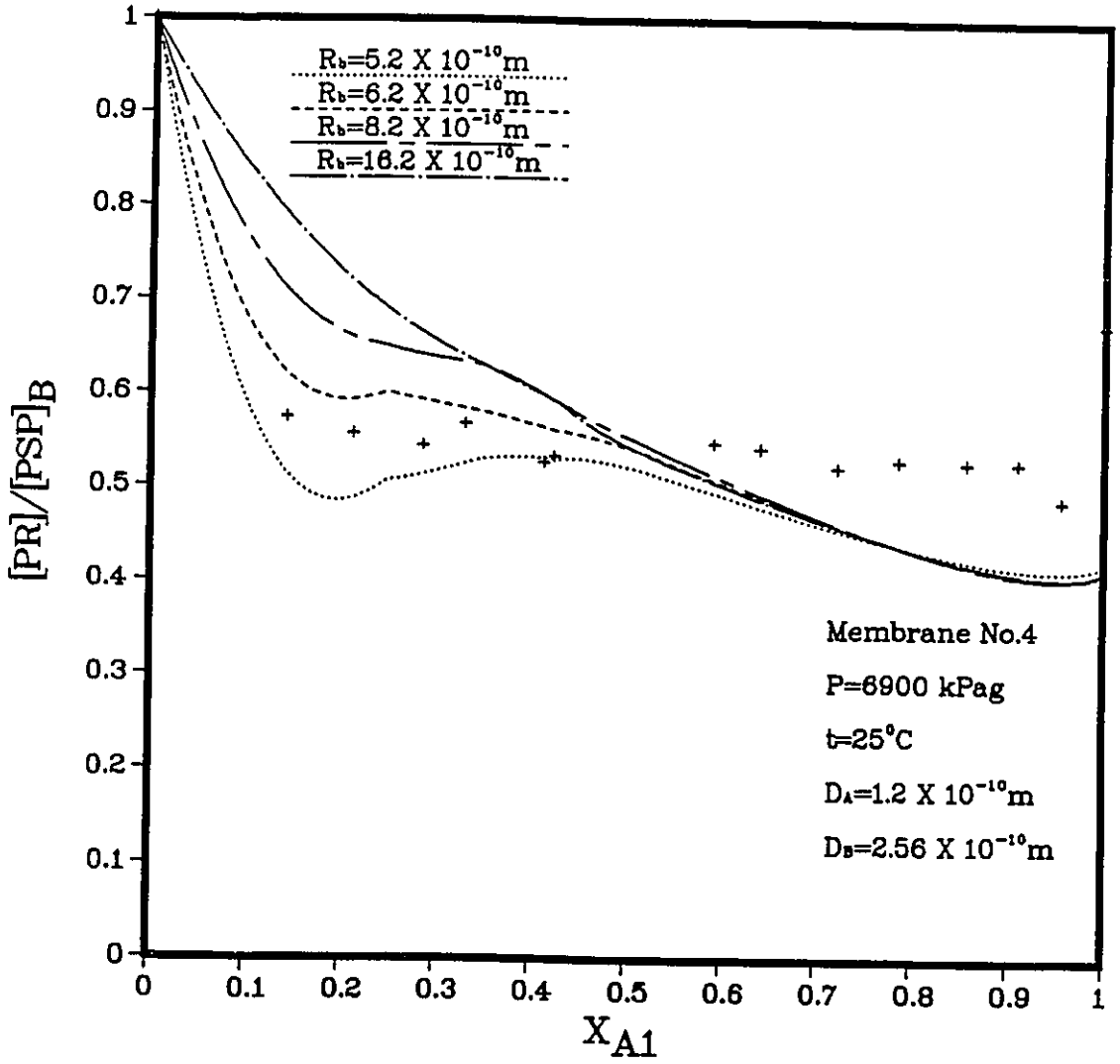


Figure 32 : Comparison of Experimental Data with Calculated Data for the Ethanol–Heptane System

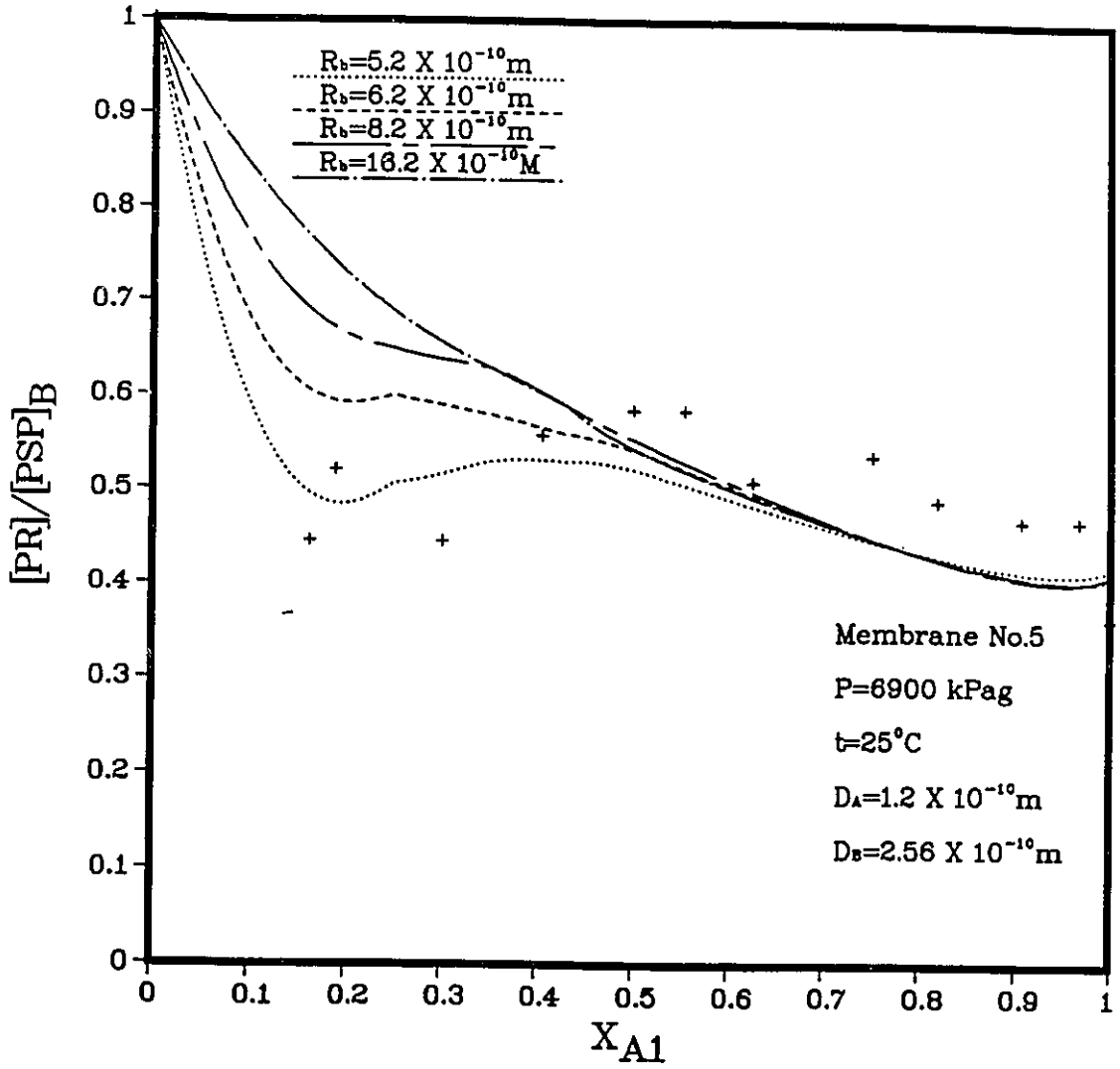


FIGURE 33 : Comparison of Experimental Data with Calculated Data for the Ethanol–Heptane System

# Organic Liquid Mixture System

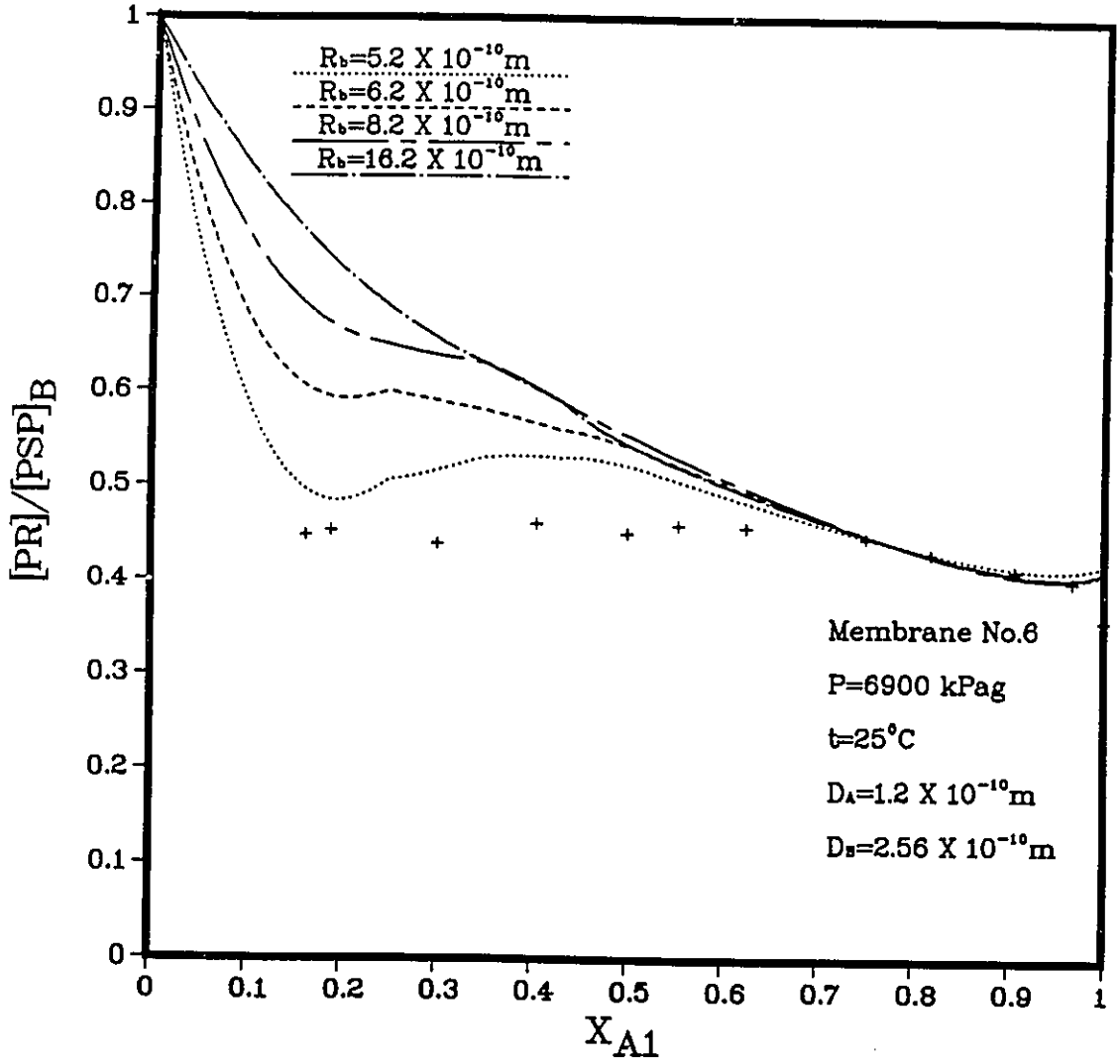


Figure 34: Comparison of Experimental Data with Calculated Data for the Ethanol–Heptane System

# Chapter 5

# Conclusions

A set of transport equations based on the surface force–pore flow model have been derived for the RO membrane separation of organic liquid mixtures. By using the transport equations, a study with computer calculation on reverse osmosis separation of organic liquids has been presented. It has been shown that the parameters such as the radius of component molecule, the interaction force and the pore radius on the membrane surface have a significant effect on the membrane performance. However, the operating pressure has a little effect on the membrane performance. For organic liquid mixture systems, the membrane with a smaller pore radius can result in superior separation. A large difference in molecular radius of component A and component B also can result in superior separation. Furthermore, it was found that the separation becomes more effective when one liquid component is more strongly attracted to the membrane material than the other.

Most importantly, the effects of the pore radius, effects of the component molecule radius and the interaction force are incorporated in the transport equations, which enable us to predict quantitatively the membrane performance data

under given operating conditions. The results obtained from this work provide new information that is very useful for understanding the nature of RO separation of organic liquid systems. It has been proved that the interaction forces acting on the solution–membrane system, an appropriate pore radius on the membrane surface and relative molecular radius are the three factors governing the RO separation. Therefore, for a given separation process, it is much possible to obtain satisfactory separation by choosing an appropriate membrane with the required pore radius and interaction force.

Because the transport equations on the basis of the surface force–pore flow model incorporate the interfacial interaction force and the pore radius, they permit an accurate description and prediction of membrane separation performance. By using the transport equations, we can analyze the experimental data of binary organic liquids separation to determine pore radius on the membrane surface. Such analysis provides a new direction in membrane design for organic liquid separation.

# Chapter 6

# Recommendations

Although the developed transport equations are found generally suitable for reverse osmosis membrane separation of organic liquid systems, it also appears that further improvements of these equations are possible. Based on the results of this work, some recommendations are made for possible future research endeavours in three directions.

- The transport equations could be extended to incorporate the effect of pore size distributions and the effect of activity coefficients of organic liquids on membrane performance.
- A method could be developed to determine the pore length of the membrane to calculate membrane permeated product rate.
- The computer program could be modified in order to calculate the effect of a wider range of parameters.

# Bibliography


[1] M. Soltanieh and W.N. Gill. Review of reverse osmosis membranes and transport models. *Chem. Eng. Commun.*, 12:279-363, 1981.

[2] J.G.A. Bitter. *Transport Mechanisms in Membrane Separation Processes*, Koninklijke / Sell-laboratorium, Amsterdam, 1988.

[3] W. Banks and A. Sharples. Studies on desalination by reverse osmosis; III. Mechanism of solute rejection. *J. Appl. Chem.*, 16:153-158, 1966.

[4] A. Katchalsky and P.F. Curran. *Non-equilibrium Thermodynamics in Biophysics*. Harvard University Press, 4th printing, 1975.

[5] S. Loeb and S. Sourirajan. Sea water demineralization by means of an osmotic membrane. *Saline Water Conversion-II*, Advances in Chemistry Series 38, pages 117-132, 1963.

[6] S. Sourirajan. Reverse osmosis: A new field of applied chemistry and chemical engineering. *Synthetic Membrane Vol. I*, edited by A.F. Turbak, ACS Symposium series 153, pages 11-62, 1981.

[7] S. Sourirajan and T. Matsuura. *Reverse Osmosis /Ultrafiltration Process Principles*. National Research Council of Canada, 1985.

[8] T. Matsuura and S. Sourirajan. Reverse osmosis transport through capillary pores under the influence of surface forces. *Ind. Eng. Chem. Process Des. Dev.*, 20:273-282, 1981.

[9] T. Matsuura, S. Sourirajan, B. Farnand and F.D.F. Talbot. Studies on the reverse osmosis separation of binary mixtures of organic liquids. *The 1987 International Congress on Membranes and Membrane Processes*, Tokyo, Japan, pages 293-294, 1987.

[10] K. Kammermeyer and D.H. Hagerbaumer. Membrane separations in the liquid phase. *A.I.Ch.E.J.*, 1:215, 1955.

[11] S. Sourirajan. Separation of hydrocarbon liquids by flow under pressure through porous membranes. *Nature*, 203:1348, 1964.

[12] J. Kopecek and S. Sourirajan. Performance of porous cellulose acetate membranes for the reverse osmosis separation of mixtures of organic liquids. *Ind. Eng. Chem. Process Des. Dev.*, 9:5, 1970.

[13] H. Strathmann. Asymmetric polyimide membranes for filtration of nonaqueous solutions. *Desalination*, 26:85, 1978.

[14] H. Nomura, S. Yoshida, M. Seno, H. Takahashi and T. Yamabe. Permselectivities of some aromatic compounds in organic medium through cellulose acetate membranes by reverse osmosis. *J. Appl. Polym. Sci.*, 22:2609, 1978.

[15] A. Iwama and Y. Kazuse. New polyimide ultrafiltration membranes for organic use. *J. Memb. Sci.*, 11:297, 1982.

[16] W.J. Adam, B. Luke and P. Meares. The separation of mixtures of organic liquids by hyperfiltration. *J. Memb. Sci.*, 13:127, 1983.

[17] B. Farnand. *A Study of Reverse Osmosis Separations involving Nonaqueous Solution.* PhD thesis, University of Ottawa, 1983.

[18] B. Farnand and H. Sawatsky. Reverse osmosis and the selective permeation and rejection of methanol from hydrocarbon mixtures. *Proceedings of the International Membrane Conference on the 25th Anniversary of Membrane Research in Canada*, edited by M. Malaiyandi, O. Kutowy and F. Talbot, pages 229-240. National Research Council of Canada, 1986.

[19] J. Hazlett, O. Kutowy, T.A. Tweddle, M.D. Guiver and T.W. McCracken. Polysulfone membranes in non-aqueous applications. *Proceedings of the International Membrane Conference on the 25th Anniversary of Membrane Research in Canada*, edited by M. Malaiyandi, O. Kutowy and F. Talbot, pages 241-256. National Research Council of Canada, 1986.

[20] T. Matsuura and S. Sourirajan. preferential sorption-capillary flow mechanism and surface force-pore flow model applicability to different membrane separation processes. *Advances in Reverse Osmosis and Ultrafiltration*, edited by T. Matsuura and S. Sourirajan, pages 139-176. National Research Council of Canada, 1989.

[21] B. Farnand. Reverse osmosis fractionation of organic solutes in nonaqueous solutions. *Advances in Reverse Osmosis and Ultrafiltration*, edited by T. Matsuura and S. Sourirajan, pages 177-184. National Research Council of Canada, 1989.

[22] O. Kedem and A. Katchalsky. Thermodynamic analysis of the permeability of biological membranes to non-electrolytes. *Biochimica et Biophysica Acta*, 27:229, 1958.

[23] H.K. Lonsdale, U. Merten and R.L. Riley. Transport properties of cellulose acetate osmotic membranes. *J. Appl. Polym. Sci.*, 9:1341-1362, 1965.

[24] T.K. Sherwood, P.L.T. Brian and R.E. Fisher. Desalination by reverse osmosis. *I & EC Fund.*, 6:2, 1967.

[25] J.M. Dickson, T. Matsuura, P. Blais and S. Sourirajan. Reverse osmosis separation of some organic and inorganic solutes in aqueous solutions using aromatic polyamide membranes. *J. Appl. Polym. Sci.*, 19:801-819, 1975.

[26] J.M. Dickson, T. Matsuura, P. Blais and S. Sourirajan. Some transport characteristics of aromatic polyamide membranes in reverse osmosis. *J. Appl. Polym. Sci.*, 20:1491-1499, 1976.

[27] S. Sourirajan. *Reverse Osmosis.* Academic Press, 1970.

[28] S. Sourirajan. *Lectures on Reverse Osmosis*, pages 275-353. National Research Council of Canada, 1983.

[29] S. Sourirajan and T. Matsuura. *Reverse Osmosis and Ultrafiltration*, edited by N.P. Cheremisinoff, pages 50-51, 1984.

[30] H. C. Van Ness, C. A. Soczek and N. K. Kochar. Thermodynamic excess properties for ethanol–n–heptane. *J. Chem. Eng. Data*, 12:346-351, 1967.

[31] T. Matsuura and S. Sourirajan. Properties of polymer-solution interfacial fluid from liquid chromatography data. *J. Coll. Int. Sci.*, 66:589-592, 1978.

[32] T. Matsuura and S. Sourirajan. *Desalination*, 38:319, 1981.

[33] I. Prigogine. *The Molecular Theory of Solutions.* North-Holland, Amsterdam, 1957.

[34] B. Farnand, F.D.F. Talbot, T. Matsuura and S. Sourirajan. *Fifth Canadian Bioenergy R&D Seminar*, edited by S. Hasnein, pages 195-200. Elsevier, New York, 1984.

[35] T. Matsuura, Y. Taketani and S. Sourirajan. Interfacial parameters governing reverse osmosis for different polymer material-solution systems through gas and liquid chromatography data. *J. Coll. Int. Sci.*, 95(1):10-22, 1983.

[36] J.F.K. Huber and R.G. Gertise. Evaluation of dynamic gas chromatography methods for the determination of adsorption and solution isotherm. *J. Chromatogr.*, 95(1):137-158, 1971.

[37] U-B. Mohlin and D.G. Gray. Gas chromatography on polymer surfaces adsorption on cellulose. *J. Coll. Int. Sci.*, 47(3):747-754, 1974.

[38] T. Matsuura and S. Sourirajan. *Fundamentals of Reverse Osmosis*. National Research Council of Canada, 1985.

[39] H. Faxen. About T. Bohlin's paper: On the drag on rigid spheres, moving in a viscous liquid inside cylindrical tubes. *Kolloid Z*, 167:146, 1959.

[40] C.N. Satterfield, C.K. Colton and W.H. Pitcher Jr.. Restricted diffusion in liquids within fine pores.*A.I.Ch.E. J.*, 19:628-635.

[41] J.A. Lane and J.W. Riggle. Dialysis. *Chem. Eng. Progr. Symp. Ser.*, 55 (24), pages 127-143, 1959.

[42] T. Matsuura, Y. Taketani and S. Sourirajan. Estimation of interfacial forces governing reverse osmosis system nonionized polar organic solute-water-cellulose Acetate membrane. *Synthetic Membranes*. Vol. II, edited by A.F. Turbak, ACS Symposium Series 154, pages 315-338, 1981.

# Appendix A

# Program Listing

```
FILE: DDD      FORTRAN  *   UNIV D'/OF OTTAWA CMS

      THIS PROGRAM IS FOR THE CALCULATION OF SEPARATION                 DDD00010
      OF ORGANIC LIQUID MIXTURES                                        DDD00020
     ------------------------------------------------------------       DDD00030
      REAL ALPH01,RATIO,SEP,CONC1,CA1,CA2,CA3,SEP1,                     DDD00040
     1SEP2,APSP,PSP,TRANSN,TRANS,V,DIFF,DIFFF,CA3GUE                    DDD00050
     2,ROH00,VOLMOL,CA1TOT,MOLFR1,CA3TOT,MOLFR3,MOLFR2                  DDD00060
      INTEGER MMM,NNN,NN                                                DDD00070
      COMMON /BAKE/X1,X2,EH,K,L,M,KK,N,N0,CONC,CONST2,                  DDD00080
     1CONST,RADIUS,PRESS,D00,D01,Q,CTOTAI(16),                          DDD00090
     2CABAR,CBBAR,VISSOT,VISSOL,CONCET(16),CB(16),                      DDD00100
     3AM,ROH0,ROH1,CONACT,GASCOT,ACTIT(16),IMAX,I0,CONST3               DDD00110
     4,CONCE2(16),ACTIT2(16)                                            DDD00120
      OPEN(5,FILE='DATA')                                               DDD00130
      READ(5,21) ALPH01,EH,PRESS,D01,ROH00                              DDD00140
         WRITE(6, 98)                                                   DDD00150
  98 FORMAT(3X,'ALPH01',6X,'EH',6X,'PRESS',6X,'D01',6X,'ROH00')         DDD00160
     WRITE(6, 21) ALPH01,EH,PRESS,D01,ROH00                             DDD00170
  21 FORMAT(6E10.3)                                                     DDD00180
     READ(5,33) K,L,M,KK,MMM,NNN,NN                                     DDD00190
         WRITE(6, 99)                                                   DDD00200
  99 FORMAT(2X,'K',2X,'L',2X,'M',1X,'KK',1X,'MMM',1X,'NNN',1X,'NN')     DDD00210
     WRITE(6,33) K,L,M,KK,MMM,NNN,NN                                    DDD00220
  33 FORMAT(7I3)                                                        DDD00230
     DO 41 J=1,MMM                                                      DDD00240
        READ(5,34) D00,Q,CONC1                                          DDD00250
        WRITE(6, 100)                                                   DDD00260
 100 FORMAT(3X,'D00',9X,'Q',9X,'CONC1')                                 DDD00270
        WRITE(6,38)D00,Q,CONC1                                          DDD00280
        READ(5,34) CONST,CONST2,CONST3,VISSOT,VISSOL                    DDD00290
        WRITE(6, 101)                                                   DDD00300
 101 FORMAT(3X,'CONST',4X,'CONST2',4X,'CONST3',4X,'VISSOT',4X,'VISSOL')DDD00310
        WRITE(6,38) CONST,CONST2,CONST3,VISSOT,VISSOL                   DDD00320
        READ(5,34) VOLMOL,GASCOT,CA3GUE                                DDD00330
        WRITE(6, 102)                                                   DDD00340
 102 FORMAT(3X,'VOLMOL',4X,'GASCOT',4X,'CA3GUE')                        DDD00350
        WRITE(6,38) VOLMOL,GASCOT,CA3GUE                                DDD00360
  34    FORMAT(7E10.3)                                                  DDD00370
        READ(5,39) IMAX                                                 DDD00380
        WRITE(6,*)'IMAX = ',IMAX                                        DDD00390
  39    FORMAT(I3)                                                      DDD00400
        READ(5,38) (CONCET(I),I=1,IMAX)                                 DDD00410
        WRITE(6, 103)                                                   DDD00420
 103 FORMAT(9X,'CONCET(I),I=1,IMAX')                                    DDD00430
        WRITE(6,38)(CONCET(I),I=1,IMAX)                                 DDD00440
        READ(5,38) (CB(I),I=1,IMAX)                                     DDD00450
        WRITE(6, 104)                                                   DDD00460
 104 FORMAT(9X,'CB(I),I=1,IMAX')                                        DDD00470
        WRITE(6,38)(CB(I),I=1,IMAX)                                     DDD00480
        READ(5,38)(CTOTAI(I),I=1,16)                                    DDD00490
        WRITE(6, 105)                                                   DDD00500
 105 FORMAT(9X,'CTOTAI(I),I=1,IMAX')                                    DDD00510
        WRITE(6,38)(CTOTAI(I),I=1,IMAX)                                 DDD00520
        READ(5,38) (ACTIT(I),I=1,IMAX)                                  DDD00530
        WRITE(6, 106)                                                   DDD00540
 106 FORMAT(9X,'ACTIT(I),I=1,IMAX')                                     DDD00550
```

```
FILE: DDD      FORTRAN  *   UNIV D'/OF OTTAWA CMS

      WRITE(6,38)(ACTIT(I),I=1,IMAX)                                          DDD00560
      READ(5,38) (CONCE2(I),I=1,16)                                           DDD00570
      WRITE(6, 107)                                                           DDD00580
107 FORMAT(9X,'CONCE2(I),I=1,IMAX')                                           DDD00590
      WRITE(6,38)(CONCE2(I),I=1,IMAX)                                         DDD00600
      READ(5,38) (ACTIT2(I),I=1,IMAX)                                         DDD00610
      WRITE(6, 108)                                                           DDD00620
108 FORMAT(9X,'ACTIT2(I),I=1,IMAX')                                           DDD00630
      WRITE(6,38)(ACTIT2(I),I=1,IMAX)                                         DDD00640
 38   FORMAT(7E10.3)                                                          DDD00650
      DO 42 IJ=1,NNN                                                          DDD00660
         READ(5,35) RADIUS, PSP                                               DDD00670
      WRITE(6, 109)                                                           DDD00680
109 FORMAT(3X,'RADIUS',6X,'PSP')                                              DDD00690
         WRITE(6, 35) RADIUS,PSP                                              DDD00700
 35      FORMAT(2E10.3)                                                       DDD00710
         AM=FLOAT(M)                                                          DDD00720
         APSP=PSP/0.00141/3600.0/100.0/(PRESS*0.00001*101.325)*0.001          DDD00730
         IF(NN-1) 12,12,13                                                    DDD00740
 13      TRANSN=1.0E+6                                                        DDD00750
         GO TO 16                                                             DDD00760
 12      IF(APSP-6.32E-7) 14,14,15                                            DDD00770
 14      TRANSN=83.60E+0+APSP+40.05E-6                                        DDD00780
         GO TO 16                                                             DDD00790
 15      TRANSN=23.81E+0+APSP+40.05E-6                                        DDD00800
 16      TRANS=TRANSN*(Q/1.61E+0)**0.6667E+00                                 DDD00810
         V=APSP*(PRESS*1.0E-5*1.01325E+02)/17.13E0                            DDD00820
         V=V/TRANS                                                            DDD00830
         CA1=CONC1                                                            DDD00840
         CA2=CONC1                                                            DDD00850
         CONC=CONC1                                                           DDD00860
         WRITE(6,*)'CONC',CONC                                                DDD00870
         CALL ACTIV(CONC,CONACT)                                              DDD00880
         WRITE(6,*) 'CONACT',CONACT,'VOLMOL',VOLMOL                           DDD00890
 51      FORMAT(5E12.3)                                                       DDD00900
         CALL TOTCON(CONC1,CA1TOT)                                            DDD00910
         WRITE(6,*)'B1',B1,'B2',B2,'B3',B3                                    DDD00920
         WRITE(6,*) 'CONC1',CONC1,'CA1TOT',CA1TOT                             DDD00930
         MOLFR1=CONC1/CA1TOT                                                  DDD00940
         WRITE(6,*)'MOLFR1',MOLFR1                                            DDD00950
         CALL GUESC3(CA3GUE,SEP,RATIO,ALPH01,VOLMOL)                          DDD00960
 52      FORMAT(5D12.3)                                                       DDD00970
 18      SEP1=SEP                                                             DDD00980
         CALL TOTCON(SEP,CA3TOT)                                              DDD00990
         MOLFR3=SEP/CA3TOT                                                    DDD01000
         MOLFR2=MOLFR3+(MOLFR1-MOLFR3)*EXP(V)                                 DDD01010
         CALL MOLFRS(MOLFR2,CA2)                                              DDD01020
         CONC=CA2                                                             DDD01030
         WRITE(6,*)'CONC',CONC,'CA2',CA2                                      DDD01040
         CALL ACTIV(CONC,CONACT)                                              DDD01050
         CA3GUE=7.2E+00                                                       DDD01060
         SEP=SEP                                                              DDD01070
         CALL GUESC3(CA3GUE,SEP,RATIO,ALPH01,VOLMOL)                          DDD01080
         SEP2=SEP                                                             DDD01090
         DIFF=ABS(SEP2-SEP1)                                                  DDD01100
```

```
FILE: DDD      FORTRAN  *   UNIV D'/OF OTTAWA CMS

      CALL FRIC1(ROH,FUNCB)                                                    DDD01660
      CAR1=CA3RGE                                                              DDD01670
      IF(CAR-1713.E01) 31,31,32                                                DDD01680
   31 CALL TOTCON(CAR1,CTOTA1)                                                 DDD01690
      CALL TOTCON(CAR,CTOTA2)                                                  DDD01700
      AA=(CTOTA1-CAR1)/(CTOTA2-CAR)                                            DDD01710
      IF(AA-10.0E+0) 33,33,32                                                  DDD01720
   33 BB=CAR1/CAR                                                              DDD01730
      IF(BB-10.0E+0) 34,34,35                                                  DDD01740
   34 DO 11 I=1,10                                                             DDD01750
      CALL TOTCON(CAR1,CTOTA1)                                                 DDD01760
      CALL TOTCON(CAR,CTOTA2)                                                  DDD01770
      GASCOT=2400.0E+0                                                         DDD01780
14    ACTLN=ACTLN+(-FUNCB*ALPH*CAR1                                            DDD01790
     1/CAR+1.0E+0*ALPH*(CTOTA1-CAR1)/(CTOTA2-CAR))*0.10E+00                    DDD01800
113   IF(ACTLN.LE.-10.00E+1)  GO TO 36                                         DDD01810
   12 ACTITY=EXP(ACTLN)                                                        DDD01820
   15 CALL ACTINV(ACTITY,CAR)                                                  DDD01830
   11 CONTINUE                                                                 DDD01840
      CAR=CAR                                                                  DDD01850
      GO TO 36                                                                 DDD01860
   32 CAR=1713.0E+01                                                           DDD01870
      GO TO 36                                                                 DDD01880
   35 CAR=0.0E+00                                                              DDD01890
   36 RETURN                                                                   DDD01900
      END                                                                      DDD01910
      SUBROUTINE ACTIV(CONCEN,ACTITY)                                          DDD01920
      REAL CONCEN,ACTITY,B1,B2,B3                                              DDD01930
      COMMON /BAKE/X1,X2,EH,K,L,M,KK,N,NO,CONC,CONST2,                         DDD01940
     1CONST,RADIUS,PRESS,D00,D01,Q,CTOTAI(16),                                 DDD01950
     2CABAR,CBBAR,VISSOT,VISSOL,CONCET(16),CB(16),                             DDD01960
     3AM,ROHO,ROH1,CONACT,GASCOT,ACTIT(16),IMAX,IO,CONST3                      DDD01970
     4,CONCE2(16),ACTIT2(16)                                                   DDD01980
      DO 10 I=2,16                                                             DDD01990
      IF(CONCEN-CONCET(I)) 20,50,10                                            DDD02000
   10 CONTINUE                                                                 DDD02010
   20 IF(I-16) 30,25,600                                                       DDD02020
   25 IF(CONCEN-CONCET(I)) 30,50,600                                           DDD02030
   30 B1=(ACTIT(I)-ACTIT(I-1))/(CONCET(I)-CONCET(I-1))                         DDD02040
      B2=CONCEN-CONCET(I-1)                                                    DDD02050
      B3=ACTIT(I-1)                                                            DDD02060
      ACTITY=B1*B2+B3                                                          DDD02070
      GO TO 600                                                                DDD02080
   50 ACTITY=ACTIT(I)                                                          DDD02090
      WRITE(6,*)'ACTIT(I)',ACTIT(I)                                            DDD02100
  600 RETURN                                                                   DDD02110
      END                                                                      DDD02120
      SUBROUTINE ACTIV2(CONCEN,ACTITY)                                         DDD02130
      REAL CONCEN,ACTITY,B1,B2,B3                                              DDD02140
      COMMON /BAKE/X1,X2,EH,K,L,M,KK,N,NO,CONC,CONST2,                         DDD02150
     1CONST,RADIUS,PRESS,D00,D01,Q,CTOTAI(16),                                 DDD02160
     2CABAR,CBBAR,VISSOT,VISSOL,CONCET(16),CB(16),                             DDD02170
     3AM,ROHO,ROH1,CONACT,GASCOT,ACTIT(16),IMAX,IO,CONST3                      DDD02180
     4,CONCE2(16),ACTIT2(16)                                                   DDD02190
      DO 10 I=2,16                                                             DDD02200
```

```
FILE: DDD      FORTRAN  *   UNIV D'/OF OTTAWA CMS

      IF(CONCEN-CONCE2(I)) 20,50,10                                    DDD02210
   10 CONTINUE                                                         DDD02220
   20 IF(I-16)30,25,600                                                DDD02230
   25 IF(CONCEN-CONCE2(I)) 30,50,600                                   DDD02240
   30 B1=(ACTIT2(I)-ACTIT2(I-1))/(CONCE2(I)-CONCE2(I-1))               DDD02250
      B2=CONCEN-CONCE2(I-1)                                            DDD02260
      B3=ACTIT2(I-1)                                                   DDD02270
      ACTITY=B1*B2+B3                                                  DDD02280
      GO TO 600                                                        DDD02290
   50 ACTITY=ACTIT2(I)                                                 DDD02300
  600 RETURN                                                           DDD02310
      END                                                              DDD02320
      SUBROUTINE ACTINV(ACTITY,CONCEN)                                 DDD02330
      REAL CONCEN,ACTITY,B1,B2,B3                                      DDD02340
      COMMON /BAKE/X1,X2,EH,K,L,M,KK,N,NO,CONC,CONST2,                 DDD02350
     1CONST,RADIUS,PRESS,D00,D01,Q,CTOTAI(16),                         DDD02360
     2CABAR,CBBAR,VISSOT,VISSOL,CONCET(16),CB(16),                     DDD02370
     3AM,ROH0,ROH1,CONACT,GASCOT,ACTIT(16),IMAX,I0,CONST3              DDD02380
     4,CONCE2(16),ACTIT2(16)                                           DDD02390
      DO 10 I=2,16                                                     DDD02400
      IF(ACTITY-ACTIT(I)) 20,50,10                                     DDD02410
   10 CONTINUE                                                         DDD02420
   20 IF(I-16) 30,25,600                                               DDD02430
   25 IF(ACTITY-ACTIT(I)) 30,50,600                                    DDD02440
   30 B1=(CONCET(I)-CONCET(I-1))/(ACTIT(I)-ACTIT(I-1))                 DDD02450
      B2=ACTITY-ACTIT(I-1)                                             DDD02460
      B3=CONCET(I-1)                                                   DDD02470
      CONCEN=B1*B2+B3                                                  DDD02480
      GO TO 600                                                        DDD02490
   50 CONCEN=CONCET(I)                                                 DDD02500
  600 RETURN                                                           DDD02510
      END                                                              DDD02520
      SUBROUTINE TOTCON(CONCA,CTOTAL)                                  DDD02530
      REAL CONCA,CTOTAL,B1,B2,B3                                       DDD02540
      COMMON /BAKE/X1,X2,EH,K,L,M,KK,N,NO,CONC,CONST2,                 DDD02550
     1CONST,RADIUS,PRESS,D00,D01,Q,CTOTAI(16),                         DDD02560
     2CABAR,CBBAR,VISSOT,VISSOL,CONCET(16),CB(16),                     DDD02570
     3AM,ROH0,ROH1,CONACT,GASCOT,ACTIT(16),IMAX,I0,CONST3              DDD02580
     4,CONCE2(16),ACTIT2(16)                                           DDD02590
      DO 10 I=2,16                                                     DDD02600
      IF(CONCA-CONCET(I)) 20,50,10                                     DDD02610
   10 CONTINUE                                                         DDD02620
   20 IF(I-16)30,25,600                                                DDD02630
   25 IF(CONCA-CONCET(I)) 30,50,600                                    DDD02640
   30 B1=(CTOTAI(I)-CTOTAI(I-1))/(CONCET(I)-CONCET(I-1))               DDD02650
      B2=CONCA-CONCET(I-1)                                             DDD02660
      B3=CTOTAI(I-1)                                                   DDD02670
      CTOTAL=B1*B2+B3                                                  DDD02680
      GO TO 600                                                        DDD02690
   50 CTOTAL=CTOTAI(I)                                                 DDD02700
  600 RETURN                                                           DDD02710
      END                                                              DDD02720
      SUBROUTINE MOLFRS(MOLFR2,CA2)                                    DDD02730
      REAL MOLFR(16),B1,B2,B3,MOLFR2,CA2                               DDD02740
      COMMON /BAKE/X1,X2,EH,K,L,M,KK,N,NO,CONC,CONST2,                 DDD02750
```

```
FILE: DDD      FORTRAN  *   UNIV D'/OF OTTAWA CMS

     1CONST,RADIUS,PRESS,D00,D01,Q,CTOTAI(16),                          DDD02760
     2CABAR,CBBAR,VISSOT,VISSOL,CONCET(16),CB(16),                      DDD02770
     3AM,ROH0,ROH1,CONACT,GASCOT,ACTIT(16),IMAX,I0,CONST3               DDD02780
     4,CONCE2(16),ACTIT2(16)                                            DDD02790
      DO 10 I=2,16                                                      DDD02800
      MOLFR(I)=CONCET(I)/CTOTAI(I)                                      DDD02810
      IF(MOLFR2-MOLFR(I)) 20,50,10                                      DDD02820
   10 CONTINUE                                                          DDD02830
   20 IF(I-16) 30,25,600                                                DDD02840
   25 IF(MOLFR2-MOLFR(I)) 30,50,600                                     DDD02850
   30 B1=(CONCET(I)-CONCET(I-1))/(MOLFR(I)-MOLFR(I-1))                  DDD02860
      B2=MOLFR2-MOLFR(I-1)                                              DDD02870
      B3=CONCET(I-1)                                                    DDD02880
      CA2=B1*B2+B3                                                      DDD02890
      GO TO 600                                                         DDD02900
   50 CA2=CONCET(I)                                                     DDD02910
600   RETURN                                                           DDD02920
      END                                                               DDD02930
      SUBROUTINE POTEN1(CONCEN,ROH,FUNCK)                               DDD02940
      REAL FUNC,CONCEN,B1,B2,B3,C,ROH2                                  DDD02950
     1,FUNCK,ROH                                                        DDD02960
      COMMON /BAKE/X1,X2,EH,K,L,M,KK,N,N0,CONC,CONST2,                  DDD02970
     1CONST,RADIUS,PRESS,D00,D01,Q,CTOTAI(16),                          DDD02980
     2CABAR,CBBAR,VISSOT,VISSOL,CONCET(16),CB(16),                      DDD02990
     3AM,ROH0,ROH1,CONACT,GASCOT,ACTIT(16),IMAX,I0,CONST3               DDD03000
     4,CONCE2(16),ACTIT2(16)                                            DDD03010
      DO 10 I=2,16                                                      DDD03020
      IF(CONCEN-CONCET(I)) 20,50,10                                     DDD03030
   10 CONTINUE                                                          DDD03040
   20 IF(I-16) 30,25,13                                                 DDD03050
   25 IF(CONCEN-CONCET(I)) 30,50,600                                    DDD03060
   30 B1=(CB(I)-CB(I-1))/(CONCET(I)-CONCET(I-1))                        DDD03070
      B2=CONCEN-CONCET(I-1)                                             DDD03080
      B3=CB(I-1)                                                        DDD03090
      C=B1*B2+B3                                                        DDD03100
      GO TO 600                                                         DDD03110
   50 C=CB(I)                                                           DDD03120
  600 C=C/(RADIUS)**AM                                                  DDD03130
      ROH1=1.0E0+D00/RADIUS                                             DDD03140
      ROH0=1.0E0-D00/RADIUS+D00/RADIUS                                  DDD03150
      ROH2=1.0E0+D00/RADIUS-D01/RADIUS                                  DDD03160
      IF(ROH-ROH2) 11,11,12                                             DDD03170
   11 FUNC=-C/(ROH1-ROH)**AM                                            DDD03180
      IF(FUNC+13.0E0) 14,14,15                                          DDD03190
   15 FUNCK=EXP(-FUNC)                                                  DDD03200
      GO TO 13                                                          DDD03210
   14 FUNCK=EXP(13.0E+0)                                                DDD03220
      GO TO 13                                                          DDD03230
   12 IF(ROH-ROH0) 14,14,17                                             DDD03240
   17 FUNCK=EXP(-10.000)                                                DDD03250
   13 RETURN                                                            DDD03260
      END                                                               DDD03270
      SUBROUTINE FRIC1(ROH,FUNCB)                                       DDD03280
      REAL FUNC,RAMDA,FUNCB,ROH                                         DDD03290
      COMMON /BAKE/X1,X2,EH,K,L,M,KK,N,N0,CONC.CONST2,                  DDD03300
```

```
FILE: DDD      FORTRAN  *   UNIV D'/OF OTTAWA CMS

     1CONST,RADIUS,PRESS,D00,D01,Q,CTOTAI(16),                          DDD03310
     2CABAR,CBBAR,VISSOT,VISSOL,CONCET(16),CB(16),                      DDD03320
     3AM,ROH0,ROH1,CONACT,GASCOT,ACTIT(16),IMAX,I0,CONST3               DDD03330
     4,CONCE2(16),ACTIT2(16)                                            DDD03340
      RAMDA=1.0E+00-ROH0/ROH1                                           DDD03350
      IF(RAMDA-0.2E+00) 12,12,13                                        DDD03360
   13 FUNCB=44.57E+00-416.2E+0*RAMDA+934.9E0*RAMDA**2+302.4E+00*        DDD03370
     1RAMDA**3                                                          DDD03380
      GO TO 14                                                          DDD03390
   12 FUNCB=1.0E+0                                                      DDD03400
   14 RETURN                                                            DDD03410
      END                                                               DDD03420
      SUBROUTINE TRANS2(CA3GUE,ALPH0,CA3AVE,RATIO,VOLMOL)               DDD03430
      REAL ALPH1,DIFF,ALPH,SEP,RATIO,ROH,CTOTAL                         DDD03440
     1,RO(16),CA3GUE,ALPH0,CA3AVE,CB3GUE,CONCB                          DDD03450
     2,ALPH01,ALPH11,CA3TOT,CB3AVE,DENS                                 DDD03460
      COMMON /BAKE/X1,X2,EH,K,L,M,KK,N,N0,CONC,CONST2,                  DDD03470
     1CONST,RADIUS,PRESS,D00,D01,Q,CTOTAI(16),                          DDD03480
     2CABAR,CBBAR,VISSOT,VISSOL,CONCET(16),                             DDD03490
     3CB(16),AM,ROH0,ROH1,CONACT,GASCOT,ACTIT(16),IMAX,I0,CONST3        DDD03500
     4,CONCE2(16),ACTIT2(16)                                            DDD03510
      X1=(581.0E+02/1.61E+0)*Q/RADIUS**2/CONC*0.39E+0/0.8931E+0         DDD03520
      X2=686.0E+0/17.0E+05*PRESS/CONC                                   DDD03530
      CALL TOTCON(CA3GUE,CTOTAL)                                        DDD03540
   51 FORMAT(5E12.3)                                                    DDD03550
      CB3GUE=CTOTAL-CA3GUE                                              DDD03560
      CALL TOTCON(CONC,CTOTAL)                                          DDD03570
      CONCB=CTOTAL-CONC                                                 DDD03580
      CABAR=CA3GUE                                                      DDD03590
      CBBAR=CB3GUE                                                      DDD03600
      I=0                                                               DDD03610
      I=I+1                                                             DDD03620
      CALL FDELT1(ALPH0,ALPH1,VOLMOL,SEKI1,SEKI2)                       DDD03630
   25 ALPH01=ALPH0                                                      DDD03640
      ALPH11=ALPH1                                                      DDD03650
      ALPH0=ALPH0-CONST/2.0E+00**I                                      DDD03660
      CALL FDELT1(ALPH0,ALPH1,VOLMOL,SEKI1,SEKI2)                       DDD03670
      IF(ALPH1) 22,22,25                                                DDD03680
   22 ALPH0=(ALPH11*ALPH0-ALPH01*ALPH1)/(ALPH11-ALPH1)                  DDD03690
      CALL FDELT1(ALPH0,ALPH1,VOLMOL,SEKI1,SEKI2)                       DDD03700
           WRITE(6,*)' SEKI1',SEKI1,' SEKI2',SEKI2                      DDD03710
      CA3AVE=SEKI1/SEKI2                                                DDD03720
      CALL TOTCON(CA3AVE,CA3TOT)                                        DDD03730
      CB3AVE=CA3TOT-CA3AVE                                              DDD03740
      DENS=(CA3AVE*46.0E0+CB3AVE*100.0E0)/(682.3E01*100.E0)             DDD03750
      RATIO=2.00E00*SEKI2*8.0000*X1/X2*DENS                             DDD03760
           WRITE(6,*)' RATIO',RATIO                                     DDD03770
      RETURN                                                            DDD03780
      END                                                               DDD03790
      SUBROUTINE FDELT1(ALPH0,ALPH1,VOLMOL,SEKI1,SEKI2)                 DDD03800
      REAL ROH,BETA(16),STEP,ALPH,BET,FUNCG,CA1,CA2,CA3,CA4,            DDD03810
     1CB1,CB2,CB3,CB4,CA3RGE,ALPH0,ALPH1,SEKI1,SEKI2,AL,                DDD03820
     2ALP(17),CAR(16)                                                   DDD03830
      COMMON /BAKE/X1,X2,EH,K,L,M,KK,N,N0,CONC,CONST2,                  DDD03840
     1CONST,RADIUS,PRESS,D00,D01,Q,CTOTAI(16),                          DDD03850
```

```
     2CABAR,CBBAR,VISSOT,VISSOL,CONCET(16),CB(16),                    DDD03860
     3AM,ROH0,ROH1,CONACT,GASCOT,ACTIT(16),IMAX,IO,CONST3             DDD03870
     4,CONCE2(16),ACTIT2(16)                                          DDD03880
      STEP=1.E0/EH+0.1E0                                              DDD03890
      N=INT(STEP)                                                     DDD03900
      ALP(1)=ALPH0                                                    DDD03910
      BETA(1)=0.0000                                                  DDD03920
      ROH=0.000                                                       DDD03930
      SEKI1=0.000E0                                                   DDD03940
      SEKI2= 0.0000E0                                                 DDD03950
      DO 18 I=1,N                                                     DDD03960
      ALPH=ALP(I)                                                     DDD03970
      BET=BETA(I)                                                     DDD03980
      CA1=EH*BET                                                      DDD03990
      IF(I.GE.2) GO TO 14                                             DDD04000
      CB1=0.000                                                       DDD04010
      GO TO 15                                                        DDD04020
   14 CALL DERBE1(ROH,ALPH,BET,FUNCG,CA3RGE,VOLMOL)                   DDD04030
   51 FORMAT(5D12.3)                                                  DDD04040
      CAR(I)=CA3RGE                                                   DDD04050
      CB1=EH*FUNCG                                                    DDD04060
   15 ROH=ROH+EH*0.5000                                               DDD04070
      ALPH=ALP(I)+CA1*0.5000                                          DDD04080
      BET=BETA(I)+CB1*0.5000                                          DDD04090
      CA2=EH*BET                                                      DDD04100
      CALL DERBE1(ROH,ALPH,BET,FUNCG,CA3RGE,VOLMOL)                   DDD04110
      CB2=EH*FUNCG                                                    DDD04120
      ALPH=ALP(I)+CA2*0.5000                                          DDD04130
      BET=BETA(I)+CB2*0.5000                                          DDD04140
      CA3=EH*BET                                                      DDD04150
      CALL DERBE1(ROH,ALPH,BET,FUNCG,CA3RGE,VOLMOL)                   DDD04160
      CB3=EH*FUNCG                                                    DDD04170
      ROH=ROH+EH*0.500                                                DDD04180
      ALPH=ALP(I)+CA3                                                 DDD04190
      BET=BETA(I)+CB3                                                 DDD04200
      CA4=EH*BET                                                      DDD04210
      CALL DERBE1(ROH,ALPH,BET,FUNCG,CA3RGE,VOLMOL)                   DDD04220
      CB4=EH*FUNCG                                                    DDD04230
      ALP(I+1)=ALP(I)+(CA1+2.0000*CA2+                                DDD04240
     12.000000*CA3+CA4)/6.000                                         DDD04250
      BETA(I+1)=BETA(I)+(CB1+2.0E0*CB2+2.0E0*CB3+CB4)/6.0E0           DDD04260
18         CONTINUE                                                   DDD04270
      ROH=0.5E0*EH                                                    DDD04280
      DO 28 I=1,N                                                     DDD04290
      AL =(ALP(I)+ALP(I+1))/2.00E0                                    DDD04300
      SEKI1=SEKI1+CAR(I)*ROH*EH*AL                                    DDD04310
      SEKI2=SEKI2+AL*ROH*EH                                           DDD04320
      ROH=ROH+EH                                                      DDD04330
28       CONTINUE                                                     DDD04340
       ALPH1=ALP(N+1)                                                 DDD04350
600       RETURN                                                      DDD04360
      END                                                             DDD04370
      SUBROUTINE DERBE1(ROH,ALPH,BET,FUNCG,CA3RGE,VOLMOL)             DDD04380
      REAL FUNCK,FUNCB,ALPH,CA3RGE,CAR,DIFF,FRAMOL,                   DDD04390
     1VISCC,ACA2LN,ACCALN,ACTCAR,CONB,CBAR,ACB2LN,ACCBLN,             DDD04400
```

```
FILE: DDD      FORTRAN  *   UNIV D'/OF OTTAWA CMS

          IF(DIFF-10.0E+0) 17,17,18                                    DDD01110
 17       MOLFR3=MOLFR3                                                DDD01120
          SEP=1.00E+0-CONC/SEP                                         DDD01130
          WRITE(6,*) 'SEP',SEP,'RATIO',RATIO                           DDD01140
          WRITE(6,*)'MOLFR1',MOLFR1,'MOLFR3',MOLFR3                    DDD01150
 42     CONTINUE                                                      DDD01160
 41  CONTINUE                                                         DDD01170
     STOP                                                             DDD01180
     END                                                              DDD01190
*********************************************************************DDD01200
                                                                      DDD01210
  THIS PROGRAM CALCULATE SEPARATION AND FLUX WHEN POTEANTIAL AND      DDD01220
  FRICTION ARE GIVEN AS FUNCTIONS OF RADIUS                           DDD01230
-----------------------------------------------------------------     DDD01240
     SUBROUTINE GUESC3(CA3GUE,CA3AVE,RATIO,ALPH01,VOLMOL)             DDD01250
     REAL DIFF,CA3AVE,SEP,RATIO,ALPH0,CA3GUE,ALPH01                   DDD01260
     COMMON /BAKE/X1,X2,EH,K,L,M,KK,N,NO,CONC,CONST2,                 DDD01270
    1CONST,RADIUS,PRESS,D00,D01,Q,CTOTAI(16),                         DDD01280
    2CABAR,CBBAR,VISSOT,VISSOL,CONCET(16),CB(16),                     DDD01290
    3AM,ROH0,ROH1,CONACT,GASCOT,ACTIT(16),IMAX,IO,CONST3              DDD01300
    4,CONCE2(16),ACTIT2(16)                                           DDD01310
     I=0                                                              DDD01320
 22  I=I+1                                                            DDD01330
     ALPH0=ALPH01                                                     DDD01340
     CALL TRANS2(CA3GUE,ALPH0,CA3AVE,RATIO,VOLMOL)                    DDD01350
     WRITE(6,*) 'CA3GUE',CA3GUE,'CA3AVE',CA3AVE                       DDD01360
 51  FORMAT(5D12.3)                                                   DDD01370
     DIFF=ABS(CA3GUE-CA3AVE)                                          DDD01380
     IF(DIFF.LE.500.0E+0) GO TO 24                                    DDD01390
     IF(CA3GUE-CA3AVE) 25,25,26                                       DDD01400
 25  CA3GUE=CA3GUE+CONST2/2.0E0**I                                    DDD01410
     ALPH0=ALPH01                                                     DDD01420
     CALL TRANS2(CA3GUE,ALPH0,CA3AVE,RATIO,VOLMOL)                    DDD01430
     IF(CA3GUE-CA3AVE) 25,25,27                                       DDD01440
 27  I=I+1                                                            DDD01450
 26  CA3GUE=CA3GUE-CONST2/2.0E+0**I                                   DDD01460
     ALPH0=ALPH01                                                     DDD01470
     CALL TRANS2(CA3GUE,ALPH0,CA3AVE,RATIO,VOLMOL)                    DDD01480
     IF(CA3GUE-CA3AVE) 22,22,26                                       DDD01490
 24  SEP=1.0E0-CA3AVE/CONC                                            DDD01500
     RETURN                                                           DDD01510
     END                                                              DDD01520
     SUBROUTINE AXINTL(CA3RGE,CAR,ALPH,ROH,VOLMOL)                    DDD01530
     REAL ACTLN,CAR,ACTITY,FUNCB,CA3RGE,ALPH,ROH                      DDD01540
    1,CONBCT,CTOTA1,CTOTA2,CAR1,AA,BB                                 DDD01550
     COMMON /BAKE/X1,X2,EH,K,L,M,KK,N,NO,CONC,CONST2,                 DDD01560
    1CONST,RADIUS,PRESS,D00,D01,Q,CTOTAI(16),                         DDD01570
    2CABAR,CBBAR,VISSOT,VISSOL,CONCET(16),CB(16),                     DDD01580
    3AM,ROH0,ROH1,CONACT,GASCOT,ACTIT(16),IMAX,IO,CONST3              DDD01590
    4,CONCE2(16),ACTIT2(16)                                           DDD01600
 51  FORMAT(5E12.3)                                                   DDD01610
     CALL POTEN1(CONC,ROH,FUNCK)                                      DDD01620
     CAR=CONC*FUNCK                                                   DDD01630
     CALL ACTIV(CAR,CONBCT)                                           DDD01640
     ACTLN=ALOG(CONBCT)                                               DDD01650
```

```
FILE: DDD      FORTRAN  *   UNIV D'/OF OTTAWA CMS

     2CARCAL,ACTB2,ACTCBR,ROH,BET,FUNCG,CTOTAL                          DDD04410
     3,CONBCT,X11,CABAR1,CBBAR1                                         DDD04420
      COMMON /BAKE/X1,X2,EH,K,L,M,KK,N,NO,CONC,CONST2,                  DDD04430
     1CONST,RADIUS,PRESS,D00,D01,Q,CTOTAI(16),                          DDD04440
     2CABAR,CBBAR,VISSOT,VISSOL,CONCET(16),CB(16),                      DDD04450
     3AM,ROHO,ROH1,CONACT,GASCOT,ACTIT(16),IMAX,IO,CONST3               DDD04460
     4,CONCE2(16),ACTIT2(16)                                            DDD04470
      CA3RGE=CONC                                                       DDD04480
   51 FORMAT(5D12.3)                                                    DDD04490
      CALL POTEN1(CA3RGE,ROH,FUNCK)                                     DDD04500
      CAR=CA3RGE*FUNCK                                                  DDD04510
      I=0                                                               DDD04520
   22 I=I+1                                                             DDD04530
      CALL AXINTL(CA3RGE,CARCAL,ALPH,ROH,VOLMOL)                        DDD04540
      DIFF=ABS(CAR-CARCAL)                                              DDD04550
      IF (DIFF.LE.1000) GO TO 23                                        DDD04560
      IF (CAR-CARCAL) 24,24,25                                          DDD04570
   24 CA3RGE=CA3RGE+CONST3/2.0E0**I                                     DDD04580
      CALL POTEN1(CA3RGE,ROH,FUNCK)                                     DDD04590
      CAR=CA3RGE*FUNCK                                                  DDD04600
      CALL AXINTL(CA3RGE,CARCAL,ALPH,ROH,VOLMOL)                        DDD04610
      IF (CAR-CARCAL) 24,24,26                                          DDD04620
   26 I=I+1                                                             DDD04630
   25 CA3RGE=CA3RGE-CONST3/2.0E0**I                                     DDD04640
      CALL POTEN1(CA3RGE,ROH,FUNCK)                                     DDD04650
      CAR=CA3RGE*FUNCK                                                  DDD04660
      CALL AXINTL(CA3RGE,CARCAL,ALPH,ROH,VOLMOL)                        DDD04670
      IF(CAR-CARCAL) 22,22,25                                           DDD04680
   23 IF(CARCAL-1713.E01) 34,35,35                                      DDD04690
   34 IF(CARCAL) 37,37,38                                               DDD04700
   38 CA3RGE=CA3RGE                                                     DDD04710
      GO TO 36                                                          DDD04720
   37 CA3RGE=0.1E0*CONC                                                 DDD04730
      GO TO 36                                                          DDD04740
   35 CA3RGE=CARCAL*0.95E0                                              DDD04750
   36 CALL TOTCON(CABAR,CTOTAL)                                         DDD04760
      FRAMOL=CABAR/CTOTAL                                               DDD04770
      VISCC=VISSOT*FRAMOL+VISSOL*(1.0E0-FRAMOL)                         DDD04780
      X11=X1*(VISCC/VISSOL)                                             DDD04790
      CONBCT=CONACT                                                     DDD04800
      ACA2LN=ALOG(CONBCT)                                               DDD04810
      CALL ACTIV(CA3RGE,ACTCAR)                                         DDD04820
      ACCALN=ALOG(ACTCAR)                                               DDD04830
      CALL TOTCON(CONC,CTOTAL)                                          DDD04840
      CONB=CTOTAL-CONC                                                  DDD04850
      CALL TOTCON(CA3RGE,CTOTAL)                                        DDD04860
      CBAR=CTOTAL-CA3RGE                                                DDD04870
      CALL ACTIV2(CONB,ACTB2)                                           DDD04880
      ACB2LN=ALOG(ACTB2)                                                DDD04890
      CALL ACTIV2(CBAR,ACTCBR)                                          DDD04900
      ACCBLN=ALOG(ACTCBR)                                               DDD04910
      CABAR1=(4.0E0*CA3RGE+CONC)/5.0E0                                  DDD04920
      CBBAR1=(4.0E0*CBAR+CONB)/5.0E00                                   DDD04930
      FUNCG=-BET/ROH-X2/X11                                             DDD04940
     1-((CABAR1/CONB)*(ACA2LN-ACCALN)+(CBBAR1/CONB)                     DDD04950
     2*(ACB2LN                                                          DDD04960
     3-ACCBLN))/X11                                                     DDD04970
600   RETURN                                                            DDD04980
      END                                                               DDD04990
```

```
FILE: DDD       RESULT   *   UNIV D'/OF OTTAWA CMS

   ALPH01        EH         PRESS        D01        ROH00
 0.700E-01 0.100E+00 0.170E+07 0.256E+01 0.100E+00
  K   L   M KK MMM NNN NN
  0   0   3   1   1   1   1
   D00          Q           CONC1
 0.120E+01 0.265E+01 0.400E+04
   CONST     CONST2     CONST3     VISSOT     VISSOL
 0.600E-01 0.200E+04 0.500E+04 0.115E-02 0.390E-03
   VOLMOL     GASCOT     CA3GUE
 0.583E-04 0.240E+04 0.500E+04
 IMAX =            16
         CONCET(I),I=1,IMAX
 0.000E+00 0.686E+02 0.173E+03 0.351E+03 0.535E+03 0.725E+03 0.112E+04
 0.155E+04 0.249E+04 0.358E+04 0.486E+04 0.638E+04 0.821E+04 0.105E+05
 0.134E+05 0.171E+05
         CB(I),I=1,IMAX
 0.109E+02 0.112E+02 0.113E+02 0.113E+02 0.112E+02 0.107E+02 0.840E+01
 0.550E+01 0.280E+01 0.000E+00 0.000E+00-0.108E+02-0.119E+02 0.340E+01
 0.580E+01 0.000E+00
         CTOTAI(I),I=1,IMAX
 0.682E+04 0.686E+04 0.692E+04 0.703E+04 0.713E+04 0.725E+04 0.748E+04
 0.773E+04 0.830E+04 0.895E+04 0.971E+04 0.106E+05 0.117E+05 0.131E+05
 0.148E+05 0.171E+05
         ACTIT(I),I=1,IMAX
 0.000E+00 0.226E+00 0.562E+00 0.659E+00 0.708E+00 0.740E+00 0.776E+00
 0.812E+00 0.836E+00 0.848E+00 0.859E+00 0.860E+00 0.879E+00 0.902E+00
 0.934E+00 0.100E+01
         CONCE2(I),I=1,IMAX
 0.000E+00 0.148E+04 0.265E+04 0.352E+04 0.425E+04 0.486E+04 0.537E+04
 0.581E+04 0.619E+04 0.636E+04 0.652E+04 0.660E+04 0.668E+04 0.675E+04
 0.679E+04 0.682E+04
         ACTIT2(I),I=1,IMAX
 0.000E+00 0.661E+00 0.824E+00 0.892E+00 0.929E+00 0.930E+00 0.940E+00
 0.947E+00 0.956E+00 0.964E+00 0.971E+00 0.974E+00 0.979E+00 0.986E+00
 0.992E+00 0.100E+01
   RADIUS       PSP
 0.520E+01 0.200E+02
 CONC  4000.00000
 CONACT 0.851617813      VOLMOL 0.582999928E-04
 B1 0.000000000E+00 B2 0.000000000E+00 B3 0.000000000E+00
 CONC1  4000.00000      CA1TOT  9200.60156
 MOLFR1 0.434754133
  SEKI1  86.1417084       SEKI2 0.153342523E-01
  RATIO 0.577892661
 CA3GUE  5000.00000      CA3AVE  5617.59766
  SEKI1  80.8784637       SEKI2 0.143973343E-01
  RATIO 0.542583466
  SEKI1  83.3489838       SEKI2 0.148371123E-01
  RATIO 0.559157312
  SEKI1  83.3489838       SEKI2 0.148371123E-01
  RATIO 0.559157312
 CA3GUE  5500.00000      CA3AVE  5617.59766
 CONC  4023.43774       CA2  4023.43774
  SEKI1  172.126999       SEKI2 0.305308327E-01
  RATIO  1.15079784
```

```
FILE: DDD      RESULT   *   UNIV D'/OF OTTAWA CMS

 CA3GUE  7.19999981      CA3AVE  5637.80859
  SEKI1  136.375946       SEKI2 0.241895467E-01
  RATIO 0.911777079
  SEKI1  115.883194       SEKI2 0.205546543E-01
  RATIO 0.774766922
  SEKI1  102.611130       SEKI2 0.182005391E-01
  RATIO 0.686033070
  SEKI1  93.3166504       SEKI2 0.165519193E-01
  RATIO 0.623891592
  SEKI1  86.4470520       SEKI2 0.153334253E-01
  RATIO 0.577963173
  SEKI1  81.1719055       SEKI2 0.143977590E-01
  RATIO 0.542695045
  SEKI1  83.6479187       SEKI2 0.148369446E-01
  RATIO 0.559249043
  SEKI1  83.6479187       SEKI2 0.148369446E-01
  RATIO 0.559249043
 CA3GUE  5507.19922      CA3AVE  5637.81250
 CONC  4023.43774       CA2  4023.43774
  SEKI1  172.126999       SEKI2 0.305308327E-01
  RATIO  1.15079784
 CA3GUE  7.19999981      CA3AVE  5637.80859
  SEKI1  136.375946       SEKI2 0.241895467E-01
  RATIO 0.911777079
  SEKI1  115.883194       SEKI2 0.205546543E-01
  RATIO 0.774766922
  SEKI1  102.611130       SEKI2 0.182005391E-01
  RATIO 0.686033070
  SEKI1  93.3166504       SEKI2 0.165519193E-01
  RATIO 0.623891592
  SEKI1  86.4470520       SEKI2 0.153334253E-01
  RATIO 0.577963173
  SEKI1  81.1719055       SEKI2 0.143977590E-01
  RATIO 0.542695045
  SEKI1  83.6479187       SEKI2 0.148369446E-01
  RATIO 0.559249043
  SEKI1  83.6479187       SEKI2 0.148369446E-01
  RATIO 0.559249043
 CA3GUE  5507.19922      CA3AVE  5637.81250
 SEP 0.286347747      RATIO 0.559249043
 MOLFR1 0.434754133      MOLFR3 0.553582549


One Run
Time: 0.2 minute
```

```
FILE: FILE     DATA     *   UNIV D'/OF OTTAWA CMS

   0.07e0     0.10e0    17.0e05     2.560e0      0.1e0
 0  0  3  1  1  1  1
   1.2e0      2.65e0    400.e01
   0.06e0     2000.e0   5000.e0     1.15e-3     0.39e-3
 58.3e-06  2400.0e00    500.e01
16
   0.0e01    6.861e01  17.30e01    35.13e01    53.51e01    72.46e01    112.2e01
 154.7e01    249.0e01  358.0e01    485.7e01    637.8e01    821.1e01    1048.e01
 1335.e01    1713.e01
   10.9e0     11.2e0     11.3e0      11.3e0      11.2e0      10.7e0      8.4e0
    5.5e0      2.8e0      0.0e0       0.0e0     -10.8e0     -11.9e0      3.4e0
    5.8e0      0.0e0
 682.3e01    686.1e01  692.1e01    702.6e01    713.4e01    724.6e01    748.2e01
 773.4e01    829.7e01  894.9e01    971.4e01    1063.e01    1173.e01    1310.e01
 1483.e01    1713.e01
    0.0e0      0.226e0   0.562e0     0.659e0     0.708e0     0.740e0     0.776e0
  0.812e0      0.836e0   0.848e0     0.859e0     0.860e0     0.879e0     0.902e0
  0.934e0      1.000e0
    0.0e01     148.e01   265.e01     351.9e01    425.2e01    485.7e01    536.9e01
 580.7e01    618.7e01  636.0e01    652.1e01    659.9e01    667.5e01    674.8e01
 679.2e01    682.3e01
    0.0e0      0.661e0   0.824e0     0.892e0     0.929e0     0.930e0     0.940e0
  0.947e0      0.956e0   0.964e0     0.971e0     0.974e0     0.979e0     0.986e0
  0.992e0      1.000e0
    5.2e0      20.0e0
```